

MATHEMATISCHES FORSCHUNGSINSTITUT OBERWOLFACH

Report No. 39/2018

DOI: 10.4171/OWR/2018/39

Reactive Flows in Deformable, Complex Media

Organised by

Margot Gerritsen, Stanford
Iuliu Sorin Pop, Diepenbeek
Florin Adrian Radu, Bergen
Barbara Wohlmuth, Garching

26 August – 1 September 2018

ABSTRACT. Many processes of highest actuality in the real life are described through systems of equations posed in complex domains. Of particular interest is the situation when the domain is changing in time, undergoing deformations that depend on the unknown quantities of the model. Such kind of problems are encountered as mathematical models in the subsurface, material science, or biological systems. The emerging mathematical models account for various processes at different scales, and the key issue is to integrate the domain deformation in the multi-scale context. The focus in this workshop was on novel techniques and ideas in the mathematical modelling, analysis, the numerical discretization and the upscaling of problems as described above.

Mathematics Subject Classification (2010): 35 (Partial differential equations), 65 (Numerical analysis), 74 (Mechanics of deformable solids), 76 (Fluid mechanics).

Introduction by the Organisers

Problems involving flow, reactive transport and mechanical or bio-chemical deformations in complex media are encountered in fields of utmost societal relevance. Such aspects have been addressed during this meeting from a mathematical prospect: the mathematical modelling and analysis, the numerical discretization and simulation. The goal was to find major mathematical challenges connected with such issues and the underlying applications. This was facilitated by the active involvement of the participants, who were scientists with various expertise, sharing the interest and will to collaborate and exchange ideas.

The workshop was attended by 52 scientists from 9 countries, including 5 young scientists supported by the "Oberwolfach Leibniz Graduate Students" Programme

and two by US National Science Foundation. One of the participants, Prof. Ivan Yotov, was awarded the Simons Visiting Professorship. This supported his visits to the universities in Bergen (Norway) and Hasselt (Belgium). There were 30 presentations addressing the workshop theme from various prospects:

- Mathematical methods, including homogenization, multi-scale analysis, and model order reduction;
- Discretisation schemes, including (mixed and conformal) finite elements, finite volumes, enriched Galerkin or gradient discretisation methods, including multi-scale methods and mixed dimensional discretisations;
- Complex mathematical models, including coupled porous medium and free flow, or flow and mechanical deformation, diffuse interface and free boundary models, problems in fractured media, or sub-continuum scale models.

The organizers would like to acknowledge the involvement of Jan Nordbotten (Bergen), who was co-organiser of the first edition of this workshop and was also involved in the organisation of this workshop. The meeting took place in a friendly and inspiring atmosphere. The presentations of highest level were accompanied by fruitful discussions, which generated promising initiatives. As sustained unanimously by all participants, this would not have been possible without the support from the MFO. The hospitality and the wonderful conditions offered in Oberwolfach, thanks to the dedicated work of the MFO staff was gratefully acknowledged by all participants.

Acknowledgement: The MFO and the workshop organizers would like to thank the National Science Foundation for supporting the participation of junior researchers in the workshop by the grant DMS-1641185, “US Junior Oberwolfach Fellows”. Moreover, the MFO and the workshop organizers would like to thank the Simons Foundation for supporting Ivan Yotov in the “Simons Visiting Professors” program at the MFO.

Workshop: Reactive Flows in Deformable, Complex Media**Table of Contents**

Rainer Helmig (joint with Thomas Fetzner, Katharian Heck, Bernd Flemisch) <i>Coupling two-phase compositional porous-medium and free flow</i>	2391
Maria Neuss-Radu (joint with Markus Gahn and Peter Knabner) <i>Effective models for metabolic processes in living cells including substrate channeling</i>	2393
Robert Eymard (joint with J. Droniou, T. Gallouët, C. Guichard, R. Herbin, A. Prignet, K. Talbot) <i>Approximation of the miscible flow in porous media problem</i>	2396
Mario Putti (joint with Enrico Facca, Franco Cardin) <i>Complex patterns arising from Optimal Transportation Problems</i>	2398
Jakub W. Both (joint with Kundan Kumar, Jan M. Nordbotten, Florin A. Radu) <i>Linear Biot equations from a gradient flow perspective</i>	2400
Thomas Wick (joint with Stefan Frei and Thomas Richter) <i>Long-term simulation of large deformation, mechano-chemical FSI in ALE and fully Eulerian coordinates</i>	2403
Angela Stevens (joint with Martin Burger, Marco Di Francesco, Elio Espejo, Simone Fagioli, Juan J. L. Velázquez) <i>Sorting in two species aggregation and chemotaxis</i>	2405
Andro Mikelić (joint with C.J. van Duijn, Mary F. Wheeler, Thomas Wick) <i>Thermoporoelasticity via homogenization</i>	2410
Ben Schweizer (joint with E. El Behi-Gornostaeva, K. Mitra) <i>Traveling wave solutions for the Richards equation with hysteresis</i>	2412
Dmitri Kuzmin (joint with Christopher Kees, Christoph Lohmann, Manuel Quezada de Luna, Sibusiso Mabuza, John N. Shadid) <i>Algebraic limiting techniques and hp-adaptivity for continuous finite element discretizations</i>	2414
Mary F. Wheeler (joint with Sanjay Srinivasan, Sanghyun Lee, and Rencheng Dong) <i>Representation of Diffusive Fractures in a Fractured Porous Media and Carbonate Acidizing</i>	2417
Wietse M. Boon (joint with Jan M. Nordbotten and Jon E. Vatne) <i>Mixed-Dimensional Partial Differential Equations: applications to flow and mechanics in media with thin inclusions</i>	2420

Carmen Rodrigo (joint with Manuel Borregales, Francisco J. Gaspar, Kundan Kumar, Florin A. Radu) <i>New approaches to the fixed-stress split scheme for solving Biot's model</i>	2421
Todd Arbogast (joint with Marc A. Hesse and Abraham L. Taicher) <i>Mixed Methods for Two-Phase Darcy-Stokes Mixtures of Partially Melted Materials with Regions of Zero Porosity</i>	2424
G�eraldine Pichot (joint with Patrick Laug, Jocelyne Erhel, Romain Le Goc, Caroline Darcel, Philippe Davy, Jean-Raynald de Dreuzy) <i>Flow simulations in geology-based Discrete Fracture Networks</i>	2427
J.Tinsley Oden (joint with Faghihi, Daniel; Scarabosio, Laura; Wohlmuth, Barbara, and Lima, Ernesto) <i>Principles of Predictive Computational Science: Predictive Models of Random Heterogeneous Materials and Tumor Growth</i>	2431
Johannes Kraus (joint with Qingguo Hong, Maria Lymbery, Fadi Philo) <i>Parameter-robust stability and strongly mass-conservative discretization of multi-permeability poroelasticity model</i>	2432
Ivan Yotov <i>Biot-Stokes modeling of fluid-poroelastic structure interaction</i>	2435
Paolo Zunino <i>Computational models for the interaction of fractures and wells with poroelastic media</i>	2438
Nicola Castelletto (joint with Massimiliano Ferronato, Andrea Franceschini, Randolph R. Settghost, Joshua A. White) <i>Fully-implicit solvers for coupled poromechanics of fractured reservoirs</i>	2439
Markus Bause (joint with M. Anselmann, S. Becher, U. K�ocher, G. Matthies, F. A. Radu, F. Schieweck) <i>Towards the fully dynamic system of poroelasticity: Efficient variational space-time methods</i>	2441
Ulrich R�ude (joint with Dominik Bartuschat, Martin Bauer, Simon Bogner, Sebastian Eibl, Ehsan Fattahi, Christian Godenschwager, Harald K�ostler, Christoph Rettinger, Florian Schornbaum, Christoph Schwarzmeier) <i>Pore Scale Simulation — Potential and Limitations</i>	2444
Ehsan Fattahi (joint with Ivan Pribec, Thomas Becker) <i>Steps towards lattice Boltzmann methods for deformable media</i>	2448
Carina Bringedal (joint with Iuliu Sorin Pop) <i>Upscaling of a phase field formulation for reactive transport</i>	2451
Mario Ohlberger (joint with Stephan Rave, Felix Schindler, Tobias Wedemeier) <i>Model reduction for parameterized systems and inverse problems</i>	2454

Martin Vohralik (joint with Soleiman Yousef)	
<i>A simple a posteriori estimate on general polytopal meshes with applications to complex porous media flows</i>	2457
Markus Gahn (joint with Maria Neuss-Radu and Peter Knabner)	
<i>Effective interface transmission conditions for transport processes through thin heterogeneous membranes</i>	2460
Nadja Ray (joint with Jens Oberlander, Peter Frolkovic)	
<i>Upscaling reactive transport in an evolving porous medium</i>	2463
Luca Formaggia (joint with Anna Scotti)	
<i>Numerical models for fault reactivation based on Nitsche method and XFEM</i>	2464

Abstracts

Coupling two-phase compositional porous-medium and free flow

RAINER HELMIG

(joint work with Thomas Fetzer, Katharian Heck, Bernd Flemisch)

Understanding the coupled exchange processes between a free flow and flow through a porous medium is important for a wide spectrum of applications in many of research. Possible applications arise from environmental science, medical science, aerospace engineering, civil engineering, process engineering, energy supply, safety issues, and technical design problems. A common feature in all these applications is the interface between the free-flow and the porous-medium flow domain. In the vicinity of this interface, processes in both domains control the coupled exchange fluxes. Therefore, modeling the interface region is a key challenge and requires the consideration of various processes on different scales with varying physical complexity, and thus the application of adequate modeling strategies.

Evaporation from soil is a good example of the immense variety of challenges. The corresponding patterns and evaporation rates strongly influence the water and energy balance of terrestrial surfaces, driving a multitude of climatic processes. To predict evaporative drying rates from porous media remains a challenge for several reasons. First, there are complex ambient conditions at the interface, such as radiation, humidity, temperature, air velocity, turbulence and boundary-layer effects. Second, the small-scale internal porous-medium properties lead to abrupt transitions and complex fluid dynamics. Third, the processes involved are characterised by complex interactions between the porous medium and the free-flow system. Modelling such coupled systems while accounting for the respective processes in both domains is a challenging task, especially since many of these systems are dominated by multi-phase compositional flow processes on different scales in space and time.

Currently existing concepts for coupling free and porous-medium flow use relatively simple interface concepts ([1]). We will revise these concepts, aiming for a *complex* interface concept on the REV scale. This concept should adapt its own model complexity flexibly, depending on the changes in the relevant free-flow or boundary-layer processes and conditions ([2]).

What are the main steps:

First, understanding the relevant processes and the key properties in the free flow (e.g. turbulence, boundary layer formation), in the porous medium (e.g. capillary flow, thermal conduction), and at their common interface (e.g. roughness) is important for the analysis of resulting coupled exchange fluxes. Second, bridging scales by properly accounting for effects occurring on smaller spatial and temporal scales is important for an efficient simulation and accurate results. Third, for the numerical modeling, numerical stable and mass conservative schemes are required. In addition, inside the two domains the relevant scales and processes are different

and a sufficiently high resolution in interface-normal direction is required for a good approximation of the exchange fluxes. Fourth, comparing numerical simulations with laboratory experiments is difficult due the coupled interplay of mass, momentum, and energy transport composed of advective and diffusive transport mechanisms which occur in a small area around the interface.

The focus of this presentation was on the explanation of the new model concept for multi-phase porous-medium flow coupled to a turbulent free flow, both including multi-component and energy transport. It was aimed to show an REV-scale two-domain concept which can handle two models in two separated sub-domains and to couple them via appropriate coupling conditions at a sharp interface. One goal was to perform this coupling without introducing additional degrees of freedom on the interface. An existing porous-medium model, using the equations by Darcy or Forchheimer and discretized with the cell-centered finite volume method, was coupled to a (Reynolds-Averaged) Navier-Stokes model discretized with a marker-and-cell scheme (also known as staggered grid). In this framework, eddy-viscosity based turbulence models of different complexity were presented. In addition, simplifications of the coupling conditions were introduced and discussed.

Numerical results for the analysis of different model concepts, parameters, and setups were presented ([3], [2]). In the first part, the developed model concepts and coupling methods were compared to a previous work which uses the box method for spatial discretization. The investigated turbulence models produce differences in stage-I evaporation rates of about 12% compared to their mean rate. Under specific conditions, simpli

cations of the free-flow model concept can speed-up the simulations by preserving the quality of the results. The analyses of the turbulent Schmidt number, the turbulent Prandtl number, and the Beavers-Joseph coefficient showed an influence of up to +10% on stage-I evaporation rates when each value is varied from unity to other physical meaningful values. In a second study, the model results were compared to different evaporation experiments from the literature and showed a good qualitative and quantitative agreement. Most difficulties were observed in reproducing the temperature evolution over time, or the transition from stage-I to stage-II evaporation. The results showed that the model predictions are sensitive to the boundary conditions, the considered model dimension, and the porous-medium properties. Finally, the effect of three different kinds of roughness were analyzed: heterogeneities, roughness resulting from the sand-grains and from porous obstacles. The roughness of the porous medium has a strong influence on the entire evaporation process and may add additional stages to the typical evaporation stages known from at and homogeneous media.

REFERENCES

- [1] Vanderborght, J., Fetzer, T., Mosthaf, K., Smits, K. and Helmig, R., *Model concepts for heat and water transport in soils and across the soil-atmosphere interface Part 1: Theory*, Water Resources Research **53** (2017), 1057–1079.
- [2] Fetzer, T., Smits, K. M. and Helmig, R., *Effect of Turbulence and Roughness on Coupled Porous-Medium/Free-Flow Exchange Processes*, Transport in Porous Media **114** (2) (2016), 395–424.
- [3] Baber K., K. Mosthaf, Flemisch B., Helmig R., Müthing S. and Wohlmuth B., *Numerical scheme for coupling two-phase compositional porous-media flow and one-phase compositional free flow*, IMA J. Appl. Math. **114** (2) (2016), 395–424.

Effective models for metabolic processes in living cells including substrate channeling

MARIA NEUSS-RADU

(joint work with Markus Gahn and Peter Knabner)

The central metabolism in plant cells contains among others starch and sucrose synthesis, glycolysis and respiration, see also Figure 1. Enzymes of glycolysis are distributed in the cytosol or bound to the surface of mitochondria (metabolic channelling). The aim of our investigations is to quantify the impact of metabolic channeling on the carbon partitioning between starch, sucrose and respiration.

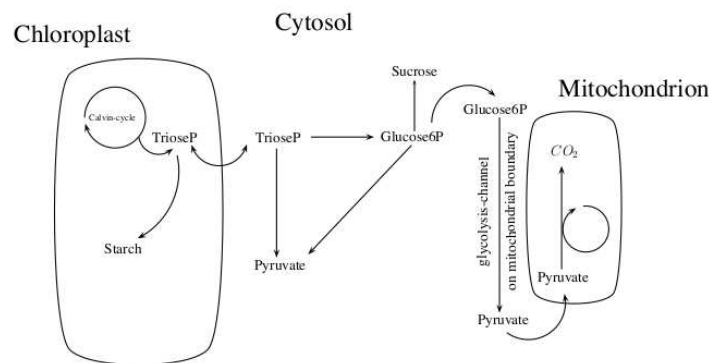


FIGURE 1. Schematic overview of the central carbon metabolism. At the mitochondrial membrane, the glycolytic channel is depicted.

The domain Ω (a plant cell) on which the mathematical model is formulated consists of the subdomains Ω_1^ϵ occupied by the cytosol and Ω_2^ϵ occupied by the organelles relevant for our applications (chloroplasts (also called plastids) and mitochondria), separated by the interface Γ_ϵ modelling the organellar membranes.

We consider a reaction-diffusion system for concentrations $u^{j,\epsilon} = (u_1^{j,\epsilon}, \dots, u_m^{j,\epsilon}) : (0, T) \times \Omega_j^\epsilon \rightarrow \mathbb{R}^m$ for $j = 1, 2$, and $u^{b,\epsilon} = (u_1^{b,\epsilon}, \dots, u_m^{b,\epsilon}) : (0, T) \times \Gamma^\epsilon \rightarrow \mathbb{R}^m$:

$$\begin{aligned} \partial_t u_i^{j,\epsilon} - \nabla \cdot (D_i^{j,\epsilon} \nabla u_i^{j,\epsilon}) &= f_i^{j,\epsilon}(u^{j,\epsilon}) && \text{in } (0, T) \times \Omega_j^\epsilon, \\ \partial_t u_i^{b,\epsilon} - \epsilon^2 \nabla^{\Gamma^\epsilon} \cdot (D_i^{b,\epsilon} \nabla^{\Gamma^\epsilon} u_i^{b,\epsilon}) &= f_i^{b,\epsilon}(u^{1,\epsilon}, u^{2,\epsilon}, u^{b,\epsilon}) && \text{on } (0, T) \times \Gamma^\epsilon, \\ -D_i^{j,\epsilon} \nabla u_i^{j,\epsilon} \cdot \nu_j^\epsilon &= -\epsilon h_i^{j,\epsilon}(u^{1,\epsilon}, u^{2,\epsilon}, u^{b,\epsilon}) && \text{on } (0, T) \times \Gamma^\epsilon, \\ -D_i^{1,\epsilon} \nabla u_i^{1,\epsilon} \cdot \nu_1^\epsilon &= 0 && \text{on } (0, T) \times \partial\Omega, \\ u_i^{j,\epsilon}(0) &= u_{i,0}^j && \text{in } \Omega_j^\epsilon, \\ u_i^{b,\epsilon}(0) &= u_{i,0}^b && \text{in } \Gamma^\epsilon. \end{aligned}$$

The structure of the subdomains Ω_1^ϵ and Ω_2^ϵ is periodic and is obtained by the repetition of a scaled standard cell $\epsilon Y = \epsilon(0, 1)^n$, where $Y = Y_1 \cup \Gamma \cup Y_2$, with open sets $Y_1, Y_2, Y_2 \subset \subset Y$. This leads to a connected subdomain Ω_1^ϵ and a disconnected Ω_2^ϵ . We observe that in both subdomains Ω_1^ϵ and Ω_2^ϵ the diffusion coefficients are of the same order with respect to the scale parameter ϵ . The nonlinear functions appearing in the right hand side of the equations and transmission/boundary conditions are the kinetics of multi-substrate enzymatic reactions and are given by rational functions of the solution components, see [2] for a detailed description.

Based on energy estimates and estimates for shifts of the solutions $u^{2,\epsilon}$ and $u^{b,\epsilon}$, the following convergence results are obtained in the limit $\epsilon \rightarrow 0$. The proof is based on a Kolmogorov-type compactness result by Simon, see [3], and its generalization form [1].

Theorem 1 (see [2]). *There exist $u^{1,0} \in L^2((0, T), H^1(\Omega))^m \cap H^1((0, T), H^1(\Omega)')^m$, and $u^{1,1} \in L^2((0, T) \times \Omega, H_{\text{per}}^1(Y)/\mathbb{R})^m$, such that up to a subsequence it holds*

$$\begin{aligned} \tilde{u}_i^{1,\epsilon} &\rightarrow u_i^{1,0} && \text{strongly in } L^2((0, T), L^2(\Omega)), \\ \nabla \tilde{u}_i^{1,\epsilon} &\rightarrow \nabla_x u_i^{1,0} + \nabla_y u_i^{1,1} && \text{in the two-scale sense,} \\ u_i^{1,\epsilon} &\rightarrow u_i^{1,0} && \text{strongly in the two-scale sense on } \Gamma^\epsilon, \\ \partial_t \bar{u}_i^{1,\epsilon} &\rightharpoonup |Y_1| \partial_t u_i^{1,0} && \text{weakly in } L^2((0, T), H^1(\Omega)'). \end{aligned}$$

There exists $u^{b,0} \in L^2((0, T) \times \Omega, H_{\text{per}}^1(\Gamma))^m$ with $\partial_t u^{b,0} \in L^2((0, T) \times \Omega \times \Gamma)^m$, such that up to a subsequence,

$$\begin{aligned} \mathcal{T}_\epsilon^b u_i^{b,\epsilon} &\rightarrow u_i^{b,0} && \text{strongly in } L^1((0, T) \times \Omega \times \Gamma), \\ \epsilon \nabla^{\Gamma^\epsilon} u_i^{b,\epsilon} &\rightarrow \nabla_y^\Gamma u_i^{b,0} && \text{in the two-scale sense on } \Gamma^\epsilon, \\ \partial_t u_i^{b,\epsilon} &\rightarrow \partial_t u_i^{b,0} && \text{in the two-scale sense on } \Gamma^\epsilon. \end{aligned}$$

There exists $u^{2,0} \in L^2((0, T) \times \Omega)^m$ with $\partial_t u^{2,0} \in L^2((0, T), H^1(\Omega)')^m$, such that up to a subsequence

$$\begin{aligned} \mathcal{T}_\epsilon \bar{u}_i^{2,\epsilon} &\rightarrow \chi_{Y_2} u_i^{2,0} && \text{strongly in } L^1((0, T) \times \Omega \times Y), \\ \overline{\nabla u_i^{2,\epsilon}} &\rightarrow 0 && \text{in the two-scale sense,} \\ \mathcal{T}_\epsilon^b u_i^{2,\epsilon} &\rightarrow u_i^{2,0} && \text{strongly in } L^1((0, T) \times \Omega \times \Gamma), \\ \partial_t \bar{u}_i^{2,\epsilon} &\rightarrow |Y_2| \partial_t u_i^{2,0} && \text{weakly in } L^2((0, T), H^1(\Omega)'). \end{aligned}$$

Passing to the limit in the microscopic equations, we obtain the following macroscopic model.

Theorem 2 (see [2]). *For the function $u^{1,\epsilon}$ on the connected domain Ω_1^ϵ we obtain:*

$$\begin{aligned} |Y_1| \partial_t u_i^{1,0} - \nabla \cdot (D_i^* \nabla u_i^{1,0}) &= \int_\Gamma h_i^1(t, y, u^{1,0}, u^{2,0}, u^{b,0}(y)) d\sigma_y \\ &+ \int_{Y_1} f_i^1(t, y, u^{1,0}) dy && \text{in } (0, T) \times \Omega, \\ -D_i^* \nabla u_i^{1,0} \cdot \nu &= 0 && \text{on } (0, T) \times \partial\Omega, \\ u_i^{1,0}(0) &= u_{i,0}^1 && \text{in } L^2(\Omega), \end{aligned}$$

with the homogenized diffusion-coefficient D_i^* given by

$$(D_i^*(x))_{kl} = \int_{Y_1} D_i^1(x, y) (\nabla w_k(x, y) + e_k) \cdot (\nabla w_l(x, y) + e_l) dy,$$

where w_k solves the cell-problem

$$\begin{aligned} -\nabla_y \cdot (D_i^1(x, y) (\nabla_y w_k(x, y) + e_k)) &= 0 && \text{in } \Omega \times Y_1, \\ -D_i^1(x, y) (\nabla_y w_k(x, y) + e_k) \cdot \nu &= 0 && \text{on } \Omega \times \Gamma, \end{aligned}$$

For the function $u^{2,\epsilon}$ on the disconnected domain Ω_2^ϵ the diffusion-term vanishes and we obtain the ODE:

$$\begin{aligned} |Y_2| \partial_t u_i^{2,0} &= \int_\Gamma h_i^2(t, y, u^{1,0}, u^{2,0}, u^{b,0}(y)) d\sigma_y \\ &+ \int_{Y_2} f_i^2(t, y, u^{2,0}) dy && \text{in } (0, T) \times \Omega, \\ u_i^{2,0}(0) &= u_{i,0}^2 && \text{in } \Omega. \end{aligned}$$

For the surface-concentration $u^{b,\epsilon}$ it holds:

$$\begin{aligned} \partial_t u_i^{b,0} - \nabla_y^\Gamma \cdot (D_i^b \nabla_y^\Gamma u_i^{b,0}) &= f_i^b(u^{1,0}, u^{2,0}, u^{b,0}) && \text{in } (0, T) \times \Omega \times \Gamma, \\ u_i^{b,0}(0) &= u_{i,0}^b && \text{in } \Omega \times \Gamma. \end{aligned}$$

All equations are coupled via the nonlinearities on the right-hand side.

Outlook: To give a quantitative answer to the biological question about the partition of carbohydrates, numerical simulations of the effective model are required. Furthermore, the model can be improved e.g., by including the dynamics

of the association of the enzymes with the mitochondrial membrane as well as the dynamics of the mitochondria themselves, like change of shape (e.g., by swelling) and location inside a living cell, fusion or division.

REFERENCES

- [1] M. Gahn, M. Neuss-Radu, *A characterization of relatively compact sets in $L^p(\Omega; B)$* , Stud. Univ. Babeş-Bolyai Math. **61** (2016), 279–290.
- [2] M. Gahn, M. Neuss-Radu, P. Knabner, *Derivation of an effective model for metabolic processes in living cells including substrate channeling*, Vietnam J. Math. **42** (2017), 265–293.
- [3] J. Simon, *Compact sets in the space $L^p((0, T); B)$* Ann. Mat. Pura Appl., **146** (1987), 65–96.

Approximation of the miscible flow in porous media problem

ROBERT EYMARD

(joint work with J. Droniou, T. Gallouët, C. Guichard,
R. Herbin, A. Prignet, K. Talbot)

The miscible flow in porous media problem.

Our aim is to approximate the miscible flow in porous media problem (improperly called “Peaceman’s model” [4] by myself during my talk), as defined by the following equations.

$$\left. \begin{aligned} \mathbf{u}(x, t) &= -\frac{\mathbf{K}(x)}{\mu(c(x, t))} \nabla p(x, t) \\ \operatorname{div} \mathbf{u}(x, t) &= (q^I - q^P)(x, t) \end{aligned} \right\}, \quad (x, t) \in \Omega \times (0, T);$$

$\Phi(x) \partial_t c(x, t) - \operatorname{div}(\mathbf{D}_x \mathbf{u}(x, t) \nabla c - c \mathbf{u})(x, t) = (\hat{c} q^I - c q^P)(x, t)$, $(x, t) \in \Omega \times (0, T)$, together with an initial value prescription for the concentration c . The reservoir-dependent quantities of porosity and absolute permeability are Φ and \mathbf{K} , respectively. The coefficient $\mathbf{D}_x \mathbf{u}$ is the diffusion-dispersion tensor, and the coefficient \hat{c} is the injected concentration. We assume no-flow boundary conditions, which imply compatibility conditions on the data, and we impose zero-average value for the pressure. Russell and Wheeler [5] give a complete derivation of this problem.

The numerical scheme obtained through the Gradient Discretisation method.

Our game was to approximate the previous problem only using the following tools:

- The set $X_{\mathcal{D}}$ of discrete unknowns is a finite-dimensional vector space over \mathbb{R} .
- $\Pi_{\mathcal{D}} : X_{\mathcal{D}} \rightarrow L^2(\Omega)$ is a linear mapping, called the function reconstruction operator.
- $\nabla_{\mathcal{D}} : X_{\mathcal{D}} \rightarrow L^2(\Omega)^d$ is a linear mapping called the gradient reconstruction operator.

These objects are extensively studied in [1]. Many schemes are included in this framework, such as:

- Finite-difference scheme on rectangular meshes,
- Mass-lumped P^1 conforming scheme, or Control-Volume Finite Element method,
- The discontinuous Galerkin SIPG method [3]...

An advantage of this framework is that the convergence properties and error estimates are proved only once (for linear elliptic or parabolic problems, and in the case of many other ones), and hold for all the methods which enter into the framework. For example, in the case of a linear elliptic problem, an error estimate is shown in terms of consistency and conformity of the function and gradient reconstructions.

In the case of the miscible flow in porous media problem, the numerical scheme is obtained too through the replacement, in the weak formulation of the problem, of the continuous unknowns by the discrete ones $\Pi_{\mathcal{D}}p$, $\nabla_{\mathcal{D}}p$, $\Pi_{\mathcal{D}}c$ and $\nabla_{\mathcal{D}}c$.

Mathematical and numerical results.

We proved the convergence of the scheme in [2], in the case where the continuous model is modified by bounding and truncating some terms involved in the problem. The convergence properties (obtained through estimates and compactness results) only hold for a subsequence and do not include L^∞ bounds on the unknown fields.

The scheme has been validated on two numerical examples.

- An analytical radial solution, given by $c(r, t) = \psi_N(\frac{N+1}{2} \frac{r^2}{t})$, where

$$\psi_N(z) = e^{-z} \sum_{k=0}^N \frac{z^k}{k!}$$

is solution to

$$\forall z > 0, \quad -z\psi'_N(z) + N\psi'_N(z) - z\psi''_N(z) = 0,$$

with $\psi_N(0) = 1$ and $\psi_N(+\infty) = 0$,

- The literature test provided in [4].

In the case where the physical diffusion is insufficient, we stabilize the method, thanks to the addition in the numerical scheme of isotropic numerical diffusion.

$$\begin{aligned} (\mathbf{D}_h(x, \mathbf{u}))_{i,i} &= \max \left((\mathbf{D}_x \mathbf{u})_{i,i}, |\mathbf{u}|h \right), \\ (\mathbf{D}_h(x, \mathbf{u}))_{i,j} &= (\mathbf{D}_x \mathbf{u})_{i,j} \text{ for } j \neq i, \end{aligned}$$

REFERENCES

- [1] J. Droniou, R. Eymard, T. Gallouët, C. Guichard, and R. Herbin. *The gradient discretisation method*. Mathematics & Applications (82). Springer, Heidelberg, 2018. <https://doi.org/10.1007/978-3-319-79042-8>.
- [2] J. Droniou, R. Eymard, A. Prignet and K. Talbot. Unified Convergence Analysis of Numerical Schemes for a Miscible Displacement Problem. *Found. Comput. Math.* (2018). <https://doi.org/10.1007/s10208-018-9387-y>.
- [3] R. Eymard and C. Guichard. Discontinuous Galerkin gradient discretisations for the approximation of second-order differential operators in divergence form. *C. Comp. Appl. Math.* (2018) 37: 4023. <https://doi.org/10.1007/s40314-017-0558-2>

- [4] D.W. Peaceman and H.H. Rachford Jr. Numerical calculation of multidimensional miscible displacement. *Soc. Pet. Eng. J.*, 2(4):327–339, 1962.
- [5] T.F. Russell and M.F. Wheeler. Finite element and finite difference methods for continuous flows in porous media. In *The mathematics of reservoir simulation*, volume 1 of *Frontiers in Applied Mathematics*, pages 35–106. SIAM, Philadelphia, 1983.

Complex patterns arising from Optimal Transportation Problems

MARIO PUTTI

(joint work with Enrico Facca, Franco Cardin)

We have recently developed an original dynamic formulation of the Monge-Kantorovich (MK) partial differential equations modeling L^1 Optimal Transport (OT) problems first proposed by [1]. Our formulation reads as follows [2]. Given an open bounded domain $\Omega \subset \mathbb{R}^n$ and two positive densities $f^+, f^- \in L^1(\Omega)$ such that $\int_{\Omega} f^+ dx = \int_{\Omega} f^- dx$, we want to find the pair of functions $(\mu, u) : [0, +\infty[\times \Omega \mapsto \mathbb{R}^+ \times \mathbb{R}^n$ that satisfies:

$$(1) \quad \begin{aligned} -\nabla \cdot (\mu(t, x) \nabla u(t, x)) &= f^+(x) - f^-(x) = f(x) && \text{in } \Omega \\ \mu'(t, x) &= \mu(t, x) (|\nabla u(t, x)| - 1) && \text{in } [0, +\infty) \\ \mu(0, x) &= \mu_0(x) > 0 \end{aligned}$$

complemented by zero Neumann boundary conditions on $\partial\Omega$. We conjectured in [2] that as $t \rightarrow +\infty$ the pair (μ, u) tends to the OT density and potential (μ^*, u^*) defined in [1] solution of the Monge-Kantorovich equations. Always in [2] local in time existence and uniqueness of the solution pair $(\mu(t), u(t))$ was proved under the assumption of $f \in L^\infty(\Omega)$ and $\mu_0 \in C^\delta(\Omega)$, where for simplicity we have dropped the dependence on x . The main difficulty in obtaining existence and uniqueness of the solution to (1) at large times is the absence of a uniform upper bound for $|\nabla u(t)|$ or $|\mu(t) \nabla u(t)|$. However, several numerical experiments shown also in [3] support the conjecture of the convergence of μ towards the solution of the MK equations.

Further support of the conjecture is given by the derivation of a candidate-Lyapunov function $\mathcal{L}(\mu)$ proposed in [3] given by the sum of an energy and a mass functional, \mathcal{E} and \mathcal{M} , respectively:

$$\mathcal{L}(\mu) := \mathcal{E}(\mu) + \mathcal{M}(\mu)$$

$$\mathcal{E}(\mu) := \sup_{\varphi \in \text{Lip}(\Omega)} \left\{ \int_{\Omega} \left(f\varphi - \mu \frac{|\nabla \varphi|^2}{2} \right) dx \right\} \quad \mathcal{M}(\mu) := \frac{1}{2} \int_{\Omega} \mu dx$$

where $\text{Lip}(\Omega)$ denotes the space of Lipschitz continuous functions in Ω . In the previous equation, the energy functional is written in variational form and represents the Dirichlet energy of the system. It can be show that \mathcal{L} has a negative Lie derivative along the μ -trajectories, its unique minimizer is μ^* , solution of the Monge-Kantorovich equations, and its unique minimum is the L^1 -Wasserstein distance between the two densities f^+ and f^- .

An extension to the above mentioned model is proposed in [4], whereby a power β is added to the flux term of the dynamic equation for the transport density. The model then becomes:

$$\begin{aligned} -\nabla \cdot (\mu(t)\nabla u(t)) &= f^+ - f^- = f, \\ \mu'(t) &= [\mu(t)|\nabla u(t)]^\beta - \mu(t), \\ \mu(0) &= \mu_0(x) > 0, \end{aligned}$$

again completed with zero Neumann boundary conditions. We conjecture that the solution pair $(\mu(t), u(t))$ of the above system converges toward an equilibrium configuration as $t \rightarrow \infty$ and that this equilibrium point is related to congested ($0 < \beta < 1$) and branched ($\beta > 1$) OT problems. Empirically, a sub-linear growth of the flux term ($0 < \beta < 1$) penalizes the flux intensity (i.e. the transport density) and promotes the spreading of transport paths over Ω . Correspondingly, the equilibrium solutions are reminiscent of Congested Transport (CT). On the other hand, a super-linear growth favors flux intensity and promotes concentrated transport, leading to the emergence of “singular” and “fractal-like” configurations that resemble the structures typical of Branched Transport (BT), as shown e.g. in [5, 6].

A candidate Lyapunov function can be identified also in this case and is given by a sum of the Dirichlet energy and a nonlinear mass functional:

$$\mathcal{L}_\beta(\mu) := \mathcal{E}(\mu) + \mathcal{M}_\beta(\mu),$$

$$\mathcal{E}(\mu) := \frac{1}{2} \int_\Omega \mu |\nabla u(\mu)|^2 dx; \quad \mathcal{M}_\beta(\mu) := \begin{cases} \frac{1}{2} \int_\Omega \ln(\mu) dx & \text{if } \beta = 2 \\ \frac{1}{2} \int_\Omega \frac{\mu^{\frac{2-\beta}{\beta}}}{\beta} dx & \text{otherwise} \end{cases}.$$

Also the case $\beta = 1$, \mathcal{L}_β decreases in along $\mu(t)$ -trajectories. While for the case $0 < \beta < 1$ we can prove the equivalence between the minimization of the Lyapunov candidate function and the CT problem, for $\beta > 1$ we are not able to characterize rigorously the minimizers of \mathcal{L} . Moreover, numerical simulations show that the final long-time solution depends upon the initial states, suggesting that the Lyapunov candidate functional is highly non-convex.

The numerical solution of our formulation for all $\beta > 0$ is easily obtained by means of Galerkin finite elements using piecewise constant basis functions for μ and piecewise linear basis functions on a uniformly refined triangulation for u . The time derivative can be discretized by forward Euler or by backward Euler with Picard approximation. Future work includes the development of Newton method.

For $\beta = 1$ the proposed numerical approach is fast, accurate, and robust, and provides an efficient tool for the solution of L^1 OT problems and the evaluation of L^1 Wasserstein distances. For $0 < \beta < 1$ the considered numerical method share the same efficiency. On the other hand, for $\beta > 1$, numerical approximations of μ

display the singular structures that, we conjecture, are related to local minima of \mathcal{L} .

Notwithstanding these difficulties, the numerical results we obtain are highly promising for the simulation of fractal-like structures commonly arising in nature, such as e.g., blood vessels, river networks, tree branches, plant roots, etc. An application to the dynamics of plant roots is under investigation.

REFERENCES

- [1] L. C. Evans and W. Gangbo, *Differential equations methods for the Monge-Kantorovich mass transfer problem*, Mem. Am. Math. Soc., **137** (1999), 1–66.
- [2] E. Facca, F. Cardin, and M. Putti, *Towards a stationary Monge-Kantorovich dynamics: The Physarum Polycephalum experience*, SIAM J. Appl. Math., **78** (2018), 651–676.
- [3] E. Facca, S. Daneri, F. Cardin, and M. Putti, *Numerical solution of Monge-Kantorovich equations via a dynamic formulation*, SIAM J. Sci. Comput., Submitted, (2018).
- [4] E. Facca, F. Cardin, and M. Putti, *Extended Dynamic-Monge-Kantorovich equations for Congested and Branched Optimal Transport Problems* SIAM J. Appl. Math., Submitted, (2018), 651–676.
- [5] F. Santambrogio, *Optimal transport for applied mathematicians*, Birkäuser, NY, (2015).
- [6] P. Pegon, F. Santambrogio, and Q. Xia, *A fractal shape optimization problem in branched transport*, J. Math. Pure Appl., In print, (2018).

Linear Biot equations from a gradient flow perspective

JAKUB W. BOTH

(joint work with Kundan Kumar, Jan M. Nordbotten, Florin A. Radu)

Linear poroelasticity is the simplest model describing flow in deformable porous media [2, 6]. However, it is the building block for various extensions and thus of interest. In this work, we approach linear poroelasticity from a new perspective. We model it as generalized gradient flow [10] and demonstrate that based on this approach, well-posedness and robust splitting schemes can be derived naturally. The final results are not necessarily new [9, 12], but their derivation is. Considering nonlinear extensions, this approach seems very promising.

1. CLASSICAL AND GENERALIZED GRADIENT FLOWS

In order to describe a classical gradient flow in a Hilbert space we need to:

- (i) Choose a state space \mathcal{X} (a Hilbert space with inner product $\langle \cdot, \cdot \rangle$ and induced norm $|\cdot|$).
- (ii) Define an energy $\mathcal{E}(x)$ for states $x \in \mathcal{X}$.

Then states change, minimizing the total energy locally as effectively as possible

$$(1) \quad \dot{x} = -\nabla \mathcal{E}(x),$$

which is equivalent with the minimization problem

$$(2) \quad \dot{x} = \operatorname{arginf}_q \left\{ \langle \nabla \mathcal{E}(x), q \rangle + \frac{1}{2} |q|^2 \right\}.$$

The framework can be generalized [10], incorporating dissipation and a characterization of changes of state via process vectors. In addition to (i)–(ii):

- (iii) Choose a process space $\mathcal{P}_{\dot{x}}$, and assign how states can change $\dot{x} = \mathcal{T}(x)p$, where $x \in \mathcal{X}$, $p \in \mathcal{P}_{\dot{x}}$, and $\mathcal{T}(x)$ is a transformation operator.
- (iv) Choose a dissipation potential $\mathcal{D}(p)$, defining the cost for changes of state.

Given the current state, the generalized gradient flow defines the change of state

$$(3) \quad \dot{x} = \mathcal{T}(x)p \quad \text{and} \quad p = \underset{q}{\operatorname{arginf}} \{ \langle \mathcal{E}'(x), \mathcal{T}(x)q \rangle + \mathcal{D}(x; q) \},$$

i.e., the loss of energy is maximized under minimal cost. Compared to classical gradient flows, zero or infinite cost is allowed.

2. LINEAR BIOT EQUATIONS AS GENERALIZED GRADIENT FLOW

We derive the quasi-static, linear Biot equations [2] as generalized gradient flow (3). Here, we consider a highly simplified setting, focusing on the essentials. In particular, we neglect any external impacts as volume or surface forces, and we consider solely homogeneous boundary conditions for normal fluxes and mechanical displacements. Furthermore, we consider isotropic, homogeneous materials. For generalizations the components (i)–(iv) have to be modified accordingly.

In the following, let $\langle \cdot, \cdot \rangle$ denote the $L^2(\Omega)$ -inner product with induced norm $\| \cdot \|$, where $\Omega \subset \mathbb{R}^d$, $d \in \{2, 3\}$, defines the porous material.

- (i) As state space, we choose $\mathcal{X} := \{(\mathbf{u}, m)\}$, where \mathbf{u} is the displacement, and m is the fluid mass scaled by the inverse of some reference fluid density.
- (ii) Displacements \mathbf{u} change with rate $\dot{\mathbf{u}}$. Masses m change via fluxes \mathbf{q} , conserving mass $\dot{m} + \nabla \cdot \mathbf{q} = 0$ on Ω . Let $\Gamma_{\mathbf{u}}, \Gamma_{\mathbf{q}} \subset \partial\Omega$ with positive measure, then we choose function spaces corresponding to the process vectors $(\dot{\mathbf{u}}, \mathbf{q})$

$$\begin{aligned} \mathcal{V} &:= \left\{ \mathbf{v} \in H^1(\Omega) \mid \mathbf{v} = \vec{0} \text{ on } \Gamma_{\mathbf{u}} \right\}, \\ \mathcal{Z} &:= \left\{ \mathbf{z} \in H(\operatorname{div}; \Omega) \mid \mathbf{z} \cdot \mathbf{n} = 0 \text{ on } \Gamma_{\mathbf{q}} \right\}. \end{aligned}$$

- (iii) The energy \mathcal{E} is given by the Helmholtz free energy of a linearly poroelastic system $\mathcal{E}(\mathbf{u}, m) := \frac{1}{2} \langle \mathbb{C}\boldsymbol{\varepsilon}(\mathbf{u}), \boldsymbol{\varepsilon}(\mathbf{u}) \rangle + \frac{M}{2} \|m - \alpha \nabla \cdot \mathbf{u}\|^2$, cf. e.g. [6], where \mathbb{C} is a fourth-order stiffness tensor, $\boldsymbol{\varepsilon}(\mathbf{u})$ is the linearized strain tensor, M is the inverse of the compressibility, α is the Biot coefficient.
- (iv) Accounting for viscous dissipation due to fluid flow, we choose the potential $\mathcal{D}(\mathbf{q}) := \frac{1}{2} \langle \kappa^{-1} \mathbf{q}, \mathbf{q} \rangle$, where κ is the mobility. Mechanical deformation comes at no cost.

The generalized gradient flow framework (3), defines the evolution of states $(\mathbf{u}, m) \in \mathcal{X}$. Given some initial condition $m(0) = m_0$, the changes of states satisfy

$$(4) \quad \dot{m} = -\nabla \cdot \mathbf{q},$$

$$(5) \quad (\dot{\mathbf{u}}, \mathbf{q}) = \underset{(\mathbf{v}, \mathbf{z}) \in \mathcal{V} \times \mathcal{Z}}{\operatorname{argmin}} \left\{ \langle \mathbb{C}\boldsymbol{\varepsilon}(\mathbf{u}), \boldsymbol{\varepsilon}(\mathbf{v}) \rangle + \langle M(m - \alpha \nabla \cdot \mathbf{u}), -\alpha \nabla \cdot \mathbf{v} \rangle \right. \\ \left. \langle M(m - \alpha \nabla \cdot \mathbf{u}), -\nabla \cdot \mathbf{q} \rangle + \frac{1}{2} \langle \kappa^{-1} \mathbf{z}, \mathbf{z} \rangle \right\},$$

similarly stated in [8]. Setting $m = \frac{1}{M}p + \alpha \nabla \cdot \mathbf{u}$, the corresponding, necessary optimality conditions are identical to the quasi-static, linear Biot equations [2].

3. WELL-POSEDNESS OF THE LINEAR BIOT EQUATIONS

Due to the lack of dissipation due to mechanical deformation, the generalized gradient flow (4)–(5) does not define a classical gradient flow. However, following ideas by [11], it can be reformulated as decoupled classical gradient flow for the reduced energy $\mathcal{E}_{\text{red}}(m) := \inf_{\mathbf{u}} \mathcal{E}(\mathbf{u}, m)$ and a minimization problem

$$(6) \quad \dot{m} - \nabla \cdot \kappa \nabla \partial_m \mathcal{E}_{\text{red}}(m) = 0, \quad m(0) = m_0,$$

$$(7) \quad \mathbf{u} = \underset{\mathbf{v}}{\operatorname{arginf}} \mathcal{E}(\mathbf{v}, m).$$

Lemma 1. *Assume $\mathcal{E}_{\text{red}}(m_0) < \infty$. Then (6)–(7) has a unique solution, satisfying $\mathbf{u} \in L^\infty(0, T; H^1(\Omega))$, $m \in H^1(0, T; H^{-1}(\Omega)) \cap L^\infty(0, T; L^2(\Omega))$.*

Proof. As \mathcal{E}_{red} is convex, (6) has a unique solution [1, 11]. As $\mathcal{E}(\mathbf{u}, m)$ is strictly convex in \mathbf{u} , (7) has a unique solution. The solution satisfies the energy identity [1]

$$\int_0^T \|\dot{m}\|_{-1, \kappa}^2 dt + \mathcal{E}(\mathbf{u}(T), m(T)) = \mathcal{E}_{\text{red}}(m(0)),$$

where $\|m\|_{-1, \kappa}^2 := \langle (-\nabla \cdot \kappa \nabla)^{-1} \dot{m}, \dot{m} \rangle$ with $(-\nabla \cdot \kappa \nabla)^{-1}$ being the inverse operator of $(-\nabla \cdot \kappa \nabla) : H_0^1(\Omega) \rightarrow H^{-1}(\Omega)$. The regularity results are a consequence. \square

4. UNDRAINED SPLITTING SCHEME DERIVED AS ALTERNATING MINIMIZATION

Let Δt denote a constant time step size. A natural implicit time discretization of (6)–(7) is given by the minimizing movement scheme

$$(8) \quad (\mathbf{u}^n, m^n) = \operatorname{arginf}_{(\mathbf{u}, m)} \mathcal{E}_{\Delta t}(m^{n-1}; \mathbf{u}, m),$$

$$\mathcal{E}_{\Delta t}(m^{n-1}; \mathbf{u}, m) := \frac{1}{2\Delta t} \|m - m^{n-1}\|_{-1, \kappa}^2 + \mathcal{E}(\mathbf{u}, m),$$

which is equivalent with the implicit Euler time discretization of the Biot equations. Considering the popularity of physical, sequential splitting schemes [3, 4, 5, 9], it is natural to apply an alternating minimization method for (8)

$$(9) \quad 1. \text{ Step : } \quad \mathbf{u}^{n,i} = \operatorname{arginf}_{\mathbf{u}} \mathcal{E}_{\Delta t}(m^{n-1}; \mathbf{u}, m^{n,i-1}),$$

$$(10) \quad 2. \text{ Step : } \quad m^{n,i} = \operatorname{arginf}_m \mathcal{E}_{\Delta t}(m^{n-1}; \mathbf{u}^{n,i}, m).$$

The scheme is identical with the undrained splitting scheme, which is known to have a contraction property [9]. Utilizing the above interpretation, and the fact that $\mathcal{E}_{\Delta t}$ is strictly convex, linear, global convergence follows directly, cf., e.g., [7].

5. CONCLUDING REMARKS AND OUTLOOK

The gradient flow framework has been demonstrated as powerful modelling tool for poroelasticity. Simple analysis and the derivation of a splitting scheme are more or less direct consequences. This perspective seems promising considering extensions as nonlinear compressibility of solid and fluid [3], non-Newtonian fluids, poroviscoelasticity, plasticity etc. Future work will be devoted to those topics.

REFERENCES

- [1] L. Ambrosio, N. Gigli, G. Savaré, *Gradient Flows: In Metric Spaces and in the Space of Probability Measures*, Birkhäuser (2005).
- [2] M.A. Biot, *General theory of three-dimensional consolidation*, J Appl Phys **12** (1941), 155–164.
- [3] M. Borregales, K. Kumar, J.M. Nordbotten, F.A. Radu, *Robust iterative schemes for non-linear poromechanics*, Computat Geosci **22** (2018), 1021–1038.
- [4] J.W. Both, M. Borregales, K. Kumar, J.M. Nordbotten, F.A. Radu, *Robust fixed stress splitting for Biot's equations in heterogeneous media*, Appl Math Lett **68** (2017), 101–108.
- [5] J.W. Both, K. Kumar, J.M. Nordbotten, F.A. Radu, *Anderson accelerated fixed-stress splitting schemes for consolidation of unsaturated porous media*, Comput Math Appl (2018).
- [6] O. Coussy, *Poromechanics*, Wiley (2004).
- [7] Z.Q. Luo, P. Tseng, *On the convergence of the coordinate descent method for convex differentiable minimization*, J Optimiz Theory App **72** (1992), 7–35.
- [8] C. Miehe, S. Mauthe, S. Teichtmeister, *Minimization principles for the coupled problem of Darcy-Biot-type fluid transport in porous media linked to phase field modeling of fracture*, J Mech Phys Solids **82** (2015), 186–217.
- [9] A. Mikelić, M.F. Wheeler, *Convergence of iterative coupling for coupled flow and geomechanics*, Computat Geosci **17** (2013), 455–461.
- [10] M.A. Peletier, *Variational modelling: energies, gradient flows, and large deviations*, Lecture Notes, Würzburg, Germany (2014).
- [11] R. Rossi, S. Savaré, *Gradient flows of non convex functionals in Hilbert spaces and applications*, ESAIM Contr Optim Ca **12** (2006), 564–614.
- [12] R. Showalter, *Diffusion in Poro-Elastic Media*, J Math Anal Appl **251** (2000), 310–340.

Long-term simulation of large deformation, mechano-chemical FSI in ALE and fully Eulerian coordinates

THOMAS WICK

(joint work with Stefan Frei and Thomas Richter)

In this presentation, we developed numerical schemes for mechano-chemical fluid-structure interactions with long-term effects using a two-scale algorithm [6]. A typical example for such a situation is the formation and growth of plaque in blood vessels. The key challenges in the model are as follows:

- Modeling of solid growth (plaque) in ALE (arbitrary Lagrangian Eulerian) and fully Eulerian coordinates;
- Coupling of the solid growth problem to the incompressible Navier-Stokes equations;
- ⇒ FSI (fluid-structure interaction);
- Coupling of FSI to biochemical processes modeled in terms of an ODE
- ⇒ Reactive flow in a deformable, thin channel
- Development of a numerical two-scale algorithm for handling multiple temporal scales: long-scale solid growth and short scale fluid dynamics.

Our model is inspired by the models considered in [10, 11, 12]. In [10, 11], a model for the formation and growth of plaques in blood vessels was derived. It consists of two main parts: a fluid structure-interaction problem describing the biomechanical interaction between the blood flow and the vessel wall, and a

system of transport equations describing the dynamics and biochemical reactions of monocytes, macrophages and foam cells in the lumen and in the vessel wall. These two problems are coupled with growth modeling. For the numerical computation of the solution, a monolithic approach based on an ALE scheme was employed. In [12], the model from [10, 11] was extended to include more general mechano-chemical-fluid-structure interaction problems. For the numerical treatment again an ALE approach was used and numerical tests were performed to analyze the convergence of the numerical scheme and the quality of the mesh transformation under large solid deformations.

In difference to [10, 11, 12], in [6], we derived a fully Eulerian framework (based on the PhD thesis of Stefan Frei [4], a recent overview article [5], and older preliminary experiences published in [7]). The fully Eulerian technique is capable to compute very large deformations up to contact. In plaque growth applications, it remains, however, the question, whether full contact is of relevance since plaque will often rupture before it completely closes the channel [8]; an overview of vulnerable plaque and its rupture can be found in [3].

In order to concentrate on a fully Eulerian FSI model towards clogging, the biochemical reactions were reduced to an ODE in [6], which is, obviously, open to discussions whether such a reduced model still can adequately model the major chemical effects. To drive the solid growth, we developed an approach to calculate effective wall stresses with the goal to design a two-scale algorithm. This algorithm is motivated by the fact that dynamics of the fluid demand to resolve a scale of seconds, growth typically takes place in a range of months.

While [10, 11, 12] showed detailed numerical simulations, including computational convergence results, using the previously mentioned ALE technique, in [6], we further compared ALE to the fully Eulerian framework. Not only did we develop two numerical approaches, but we also did implement them in different open-source software packages (employing the FSI-template [9] based on deal.II [1] and, on the other hand, Gascoigne3D [2]). During these implementations, we found several inconsistencies (and also bugs) in both frameworks and both codes. This shows once more that a robust numerical framework for simulating multi-physics problems is very difficult and needs careful verifications.

At the Oberwolfach meeting in August 2018, it was agreed upon that the problem is very complex and needs further investigations into several directions of mathematical and numerical nature. Some open future questions are:

- Extending in [6] to the full PDE chemical model proposed in [10, 11];
- Further investigations of the validity of the two-scale algorithm;
- Further numerical tests in particular with respect to larger inflow conditions;
- Careful investigations whether non-symmetric solid growth can be modeled;
- Local mesh and time step adaptivity and parallel computing to reduce the computational cost;
- 3D simulations.

REFERENCES

- [1] W. Bangerth, T. Heister, L. Heltai, G. Kanschat, M. Kronbichler, M. Maier, B. Turcksin, *The deal.II Library, Version 8.3*, Archive of Numerical Software, **4** (2016), 1-11.
- [2] R. Becker and M. Braack and D. Meidner and T. Richter and B. Vexler, *The finite element toolkit GASCOIGNE*, [HTTP://WWW.GASCOIGNE.UNI-HD.DE](http://www.gascoigne.uni-hd.de)
- [3] A. V. Finn, M. Nakano, J. Narula, F.D. Kolodgie, R. Virmani, *Concept of vulnerable/unstable plaque*, *Arterioscler. Thromb. Vasc. Biol.* **30** (2010), 1282 - 1292.
- [4] S. Frei, *Eulerian finite element methods for interface problems and fluid-structure interactions*, Heidelberg University, Dissertation (2016).
- [5] S. Frei, T. Richter, *An accurate Eulerian approach for fluid-structure interactions*. In *Fluid-Structure Interaction: Modeling, Adaptive Discretization and Solvers* (eds. S. Frei and B. Holm and T. Richter and T. Wick and H. Yang), Radon Series on Computational and Applied Mathematics (2017).
- [6] S. Frei and T. Richter and T. Wick, *Long-term simulation of large deformation, mechano-chemical fluid-structure interactions in {ALE} and fully Eulerian coordinates*, *Journal of Computational Physics* **321** (2016), 874 - 891.
- [7] T. Richter and T. Wick, *Finite elements for fluid-structure interaction in ALE and fully Eulerian coordinates*, *Comp. Methods Appl. Mech. Engrg.* **199** (2010), 2633-2642.
- [8] Texas Heart Institute, *Vulnerable Plaque*, <https://www.texasheart.org/heart-health/heart-information-center/topics/vulnerable-plaque/>, accessed on Sep 20, 2018.
- [9] T. Wick, *Solving Monolithic Fluid-Structure Interaction Problems in Arbitrary Lagrangian Eulerian Coordinates with the deal.II Library*, Archive of Numerical Software, **1** (2013), 1-19.
- [10] Y. Yang, *Mathematical Modeling and Simulation of the Evolution of Plaques in Blood Vessels*, Heidelberg University, Dissertation (2014).
- [11] Y. Yang, W. Jaeger, M. Neuss-Radu, T. Richter, *Mathematical modeling and simulation of the evolution of plaques in blood vessels*, *Journal of Mathematical Biology* **72** (2015), 973-996.
- [12] Y. Yang, T. Richter, W. Jaeger, M. Neuss-Radu, *An ALE approach to mechano-chemical processes in fluid-structure interaction*, *International Journal for Numerical Methods in Fluids* **84** (2016), 199-220.

Sorting in two species aggregation and chemotaxis

ANGELA STEVENS

(joint work with Martin Burger, Marco Di Francesco, Elio Espejo, Simone Fagioli, Juan J. L. Velázquez)

One biological model-system for development is the cellular slime mold *Dictyostelium discoideum*, *Dd*. Under starvation conditions the amoebae produce an attractive signal, namely cAMP. The amoebae sense this signal and move towards higher concentrations. After aggregation and mound formation in *Dd*, the amoebae start to pre-differentiate into pre-stalk and pre-spore cells. In the mound these amoebae vary w.r.t. their chemotactic sensitivity. Amoebae with stronger chemotactic abilities can be found at the top of the mound. Amoebae which are weaker w.r.t. to chemotaxis can be found closer to the bottom of the mound. Later, these differently sorted amoebae differentiate into two cell types. The amoebae from the top of mound form the stalk of the fruiting body. The amoebae from the bottom

of the mound become surviving spores. The outcome of cell sorting seems to be a pre-stage for cell differentiation.

Jäger and Luckhaus [4] showed, that chemotaxis can serve as the main mechanism for self-organization of Dd . This means, that a 2-dimensional chemotaxis model must exhibit blow-up of solutions. A simplified version of the classical Keller-Segel model reads as follows. Let u be the density of the amoebae, and v be the concentration of the chemo-attractant in Ω . Then

$$\partial_t u = \Delta u - \chi \nabla \cdot (u \nabla v) \quad , \quad \partial_t v = \eta \Delta v + \alpha u - \beta v$$

with Neumann boundary conditions on $\partial\Omega$, models chemotactic motion of the amoebae due to a self-produced chemo-attractant, where $\chi > 0$ is the chemotactic sensitivity. Define $\bar{w} = \frac{1}{|\Omega|} \int_{\Omega} w \, dx$. Then $\bar{u}(t) = \bar{u}_0$ and $\frac{1}{\eta}(\partial_t + \beta)\bar{v} = \frac{\alpha}{\eta}\bar{u} = \frac{\alpha}{\eta}\bar{u}_0$. Consider $\tilde{v} := v - \bar{v}$, then $\frac{1}{\eta}(\partial_t + \beta)\tilde{v} = \Delta \tilde{v} + \frac{\alpha}{\eta}(u - \bar{u}_0)$.

For fast diffusion of chemical molecules we obtain

$$\partial_t u = \Delta u - \chi \nabla \cdot (u \nabla v) \quad , \quad 0 = \Delta \tilde{v} + \frac{\alpha}{\eta} u - \frac{\alpha}{\eta} \bar{u}_0 .$$

The last equation can be further rescaled to $0 = \Delta v + u - 1$.

For the radial symmetric situation it was proved in [4], that there exist parameter regimes for which global solutions exist. Further, there exist parameter regimes for which blow-up happens in finite time. The explicit critical value for this switch of behavior can be read of the estimates in the proof. Among others, a strong chemotactic sensitivity χ gives rise to self-organization.

Can chemotaxis also serve as the main mechanism for cell sorting?

A suitable model for chemotactic cell sorting in the mound would be spatially 3-dimensional and show spatial ordering of the cells in correlation to their chemotactic sensitivity. As a first test-problem we considered a mathematical model with two chemotactic species in two spatial dimensions and asked if it is possible to obtain blow-up for one species, whereas the solution for the other species still exists, see [3]. Let u_1, u_2 be the densities of two cell types, and v the concentration of the chemo-attractant. Consider

$$\begin{aligned} \partial_t u_1 &= \Delta u_1 - \chi_1 \nabla \cdot (u_1 \nabla v) & , & \quad \partial_t u_2 = \mu_2 \Delta u_2 - \chi_2 \nabla \cdot (u_2 \nabla v) \\ \partial_t v &= \Delta v + u_1 + u_2 - 1 \end{aligned}$$

in $B_R(0), t > 0$, with Neumann boundary conditions. Here $\chi_1, \chi_2 > 0$ are the different chemotactic sensitivities, and μ_2 describes the strength of random motion of species u_2 . For $\chi_2 = 0$, the system is decoupled. Then u_1 can - 'just' - blow up, whereas u_2 does not. What happens for $\chi_2 \ll 1$?

Existence of classical solutions have been proved in [2]. Global existence for general multi-component chemotaxis systems with Dirichlet boundary conditions has been shown in [5]. Consider radial symmetric solutions and rewrite the system in terms of the rescaled mass functions

$$M_i(t, r) = \int_0^r u_i(t, \xi) \xi \, d\xi \quad , \quad i = 1, 2,$$

with $r = |x|$. Then $\partial_r v = \frac{M_1+M_2}{r} - \frac{r}{2}$ and

$$\begin{aligned} \partial_t M_1 &= r \partial_r \left(\frac{1}{r} \partial_r M_1 \right) - \chi_1 \left(\frac{r}{2} - \frac{M_1+M_2}{r} \right) \partial_r M_1 \\ \partial_t M_2 &= \mu_2 r \partial_r \left(\frac{1}{r} \partial_r M_2 \right) - \chi_2 \left(\frac{r}{2} - \frac{M_1+M_2}{r} \right) \partial_r M_2 \end{aligned}$$

with boundary condition $M_1(t, 1) = m_1, M_2(t, 1) = m_2$. Global solutions exist, if

$$m_1 < \min \left\{ \frac{\mu_2}{\chi_2}, \frac{2(2 - \chi_1 m_2)}{\chi_1} \right\} \quad \text{and} \quad m_2 < \min \left\{ \frac{1}{\chi_1}, \frac{2(2\mu_2 - \chi_2 m_1)}{\chi_2} \right\} .$$

Blow-up in finite time happens if

$$m_1 > \frac{2}{\chi_1} \quad \text{and} \quad \int_{B_1(0)} |x|^2 u_1(t, x) dx \ll 1 .$$

If u_1 blows up in finite time, then also u_2 blows up at the same time.

Formally, the asymptotics for parameters χ_1, χ_2, μ_2 could be calculated, for which $M_2 \ll M_1$ near the blow-up point. In such cases singularity formation for u_2 without mass aggregation is possible, whereas u_1 shows mass aggregation.

Can differential attraction, repulsion, and diffusion lead to sorting and segregation?

Again, we consider two cell-types and now the following energy functional

$$\mathcal{E}[\rho_1, \rho_2] = \int f(\rho_1, \rho_2) dx - \frac{1}{2} \int \rho_1 S_1 * \rho_1 dx - \frac{1}{2} \int \rho_2 S_2 * \rho_2 dx - \int \rho_1 K * \rho_2 dx .$$

The f -term represents repulsive effects, and S_1, S_2, K are non-negative, smooth, radially decreasing, attractive potentials with finite mass. Here S_1, S_2 model self-attraction, whereas K models cross attraction. Specifically we use $f(\rho_1, \rho_2) = \frac{\varepsilon}{2}(\rho_1 + \rho_2)^2$. Formally, the related gradient flow of $\mathcal{E}[\rho_1, \rho_2]$ then reads

$$\begin{aligned} \partial_t \rho_1 &= \nabla \cdot (\varepsilon \rho_1 \nabla(\rho_1 + \rho_2) - \rho_1 \nabla S_1 * \rho_1 - \rho_1 \nabla K * \rho_2) \\ \partial_t \rho_2 &= \nabla \cdot (\varepsilon \rho_2 \nabla(\rho_1 + \rho_2) - \rho_2 \nabla S_2 * \rho_2 - \rho_2 \nabla K * \rho_1) \end{aligned}$$

Here we focus on the one-dimensional case. We proved in [1] that discontinuous stationary patterns can arise, and that ρ_1, ρ_2 can separate completely in the stationary state, i.e. both cell densities feature a jump discontinuity at exactly the same point, with $w = \rho_1 + \rho_2$ remaining smooth at that point.

In order to get some intuitive insight, consider the following canonical model.

$$\partial_t \rho_1 = \nabla \cdot (\varepsilon \rho_1 \nabla(\rho_1 + \rho_2) - \rho_1 \nabla V_1), \quad \partial_t \rho_2 = \nabla \cdot (\varepsilon \rho_2 \nabla(\rho_1 + \rho_2) - \rho_2 \nabla V_2)$$

Here V_1, V_2 are smooth and given potentials.

Proposition: If $(\rho_1^\infty, \rho_2^\infty)$ is a (weak) stationary solution of (1), then

$$\text{supp}(\rho_1^\infty) \cap \text{supp}(\rho_2^\infty) \subset \{\nabla V_1 = \nabla V_2\} .$$

Theorem: Let K be the fundamental solution of the Laplace equation on \mathbb{R}^d . Let $S_1 = \sigma_1 K, S_2 = \sigma_2 K$ with $\sigma_1 \leq 1 \leq \sigma_2$ and $\sigma_1 \neq \sigma_2$.

Then every stationary solution (ρ_1, ρ_2) of (1) is fully segregated,

i.e. $\text{supp}(\rho_1) \cap \text{supp}(\rho_2)$ has zero Lebesgue measure.

Segregation Dynamics: Consider $w := \rho_1 + \rho_2$ and $\zeta := (\rho_1 - \rho_2)/w$. Then

$$\partial_t w = \nabla \cdot \left(\varepsilon w \nabla w - w \frac{1 + \zeta}{2} \nabla V_1 - w \frac{1 - \zeta}{2} \nabla V_2 \right)$$

Thus the dynamics of the total density w are governed by a porous medium equation with additional convective terms. Further

$$w \partial_t \zeta = \left(\varepsilon w \nabla w - w \frac{1 + \zeta}{2} \nabla V_1 - w \frac{1 - \zeta}{2} \nabla V_2 \right) \cdot \nabla \zeta - \frac{1 - \zeta^2}{2} \nabla \cdot (w \nabla (V_1 - V_2)) .$$

The first term on the right hand side is along the flux of w , which determines the spatial position and shape of the solution. The crucial part for the segregation dynamics is the second term, which has two fixed points $\zeta = \pm 1$, corresponding to segregation. Depending on the sign of $\nabla \cdot (w \nabla (V_1 - V_2))$ one of them is stable. Thus there is always dynamics towards a segregated state, driven by the differences in the attractive forces. We consider one-dimensional steady states

$$(\varepsilon \rho_1 [\rho_1 + \rho_2]_x - \rho_1 S'_1 * \rho_1 - \rho_1 K' * \rho_2)_x = (\varepsilon \rho_2 [\rho_1 + \rho_2]_x - \rho_2 S'_2 * \rho_2 - \rho_2 K' * \rho_1)_x = 0,$$

and minimizers of the energy functional

$$\mathcal{F}[\rho_1, \rho_2] = \frac{\varepsilon}{2} \int (\rho_1 + \rho_2)^2 dx - \frac{1}{2} \int \rho_1 S_1 * \rho_1 dx - \frac{1}{2} \int \rho_2 S_2 * \rho_2 dx - \int \rho_1 K * \rho_2 dx$$

on $\mathcal{M} = \{(\rho_1, \rho_2) \in (L^2(\mathbb{R}) \cup L^1(\mathbb{R}))^2 \mid \rho_i \geq 0, \int_{\mathbb{R}} \rho_i dx = m_i\}$, for given m_1, m_2 .

Proposition: Let $(\rho_1, \rho_2) \in \mathcal{M} \cap BV(\mathbb{R})^2$ be a minimizer for the energy functional $\mathcal{F}[\rho_1, \rho_2]$ such that $w = \rho_1 + \rho_2$ is Lipschitz continuous. Then (ρ_1, ρ_2) is a weak solution of our steady state system, and every weak solution of this PDE-system is a critical point of \mathcal{F} .

Lemma: (Coercivity)

Assume that the Fourier transforms of the interaction kernels for all $\xi \in \mathbb{R}$ satisfy

$$\varepsilon > \min\{\hat{S}_1(\xi), \hat{S}_2(\xi)\} \text{ and } (\varepsilon - \hat{S}_1(\xi))(\varepsilon - \hat{S}_2(\xi)) > (\varepsilon - \hat{K}(\xi))^2 .$$

Then there exists no global minimizer $(\rho_1, \rho_2) \in \mathcal{M}$.

Theorem: Assume the conditions of the above Lemma, then there exists no nonzero stationary solution of our stationary PDE.

Example: For three Gaussian kernels the second condition in our Lemma is satisfied, if $\|K\|_{L^1} > \max\{\|S_1\|_{L^1}, \|S_2\|_{L^1}\}$ and if the variance of K is small compared to that of S_1, S_2 . Then cross attraction is relevant only at very small distances between particles of different species, and dominates self interaction.

Intuitive interpretation: Two - possibly separated - patterns for ρ_1 and ρ_2 (attained at a steady state) tend to glue together at the closest points of their boundaries.

Example:

$$S_1(x) = \frac{A_1}{\sigma_1\sqrt{\pi}} \exp(-x^2/(2\sigma_1^2)), \quad S_2(x) = \frac{A_2}{\sigma_2\sqrt{\pi}} \exp(-x^2/(2\sigma_2^2))$$

$$K(x) = \frac{B}{\lambda\sqrt{\pi}} \exp(-x^2/(2\lambda^2)).$$

The conditions of our Lemma are met, if $B > \max\{A_1, A_2\}$ and $\lambda < \min\{\sigma_1, \sigma_2\}$. Similar conditions can be achieved for other specific interaction kernels.

Theorem: (For any dimension)

Let $K \in C^2(\mathbb{R})$ have a unique maximum at zero. Let $S_i = \sigma_i K$ for some $\sigma_1, \sigma_2 > 0$ with $\sigma_1 + \sigma_2 > 2$. Let $(\rho_1^\infty, \rho_2^\infty)$ be a local minimizer of \mathcal{F} on \mathcal{M} . Define $\mathcal{S} := \text{supp}(\rho_1^\infty) \cap \text{supp}(\rho_2^\infty)$. Then \mathcal{S} has zero Lebesgue measure.

Proposition: Let $(\rho_1^\infty, \rho_2^\infty) \in \mathcal{M} \cup BV(\mathbb{R})^2$ be a weak solution to our stationary PDE-system. Then $\text{supp}(\rho_1^\infty + \rho_2^\infty)$ is simply connected.

Definition: A stationary solution (ρ_1, ρ_2) of our steady state system is called a symmetric segregated steady state, if there exist $L_1, L_2 > 0$ such that

$$\text{supp}(\rho_1) = [-L_1, L_1] =: I_1, \quad \text{supp}(\rho_2) = [-L_2, -L_1] \cup [L_1, L_2] =: I_2,$$

where ρ_1, ρ_2 are regular even functions with $w = \rho_1 + \rho_2$ being monotone decreasing on $[0, L_2]$ and $w(L_2) = 0$.

Let S_1, S_2, K be symmetric and strictly decreasing on $[0, +\infty]$. Let e.g. $S_i = \sigma_i K$, $\sigma_1 > 1 > \sigma_2$ and $S_1'(L_1) \leq K'(L_1)$, then

Proposition: Under the above assumptions and for fixed $0 < L_1 < L_2$, there exists a unique (up to mass normalisation) symmetric segregated steady state (ρ_1, ρ_2) to our stationary PDE with $\varepsilon = \varepsilon(L_1, L_2) > 0$.

Theorem: There exists a constant ε_0 such that for all $\varepsilon \in (0, \varepsilon_0)$ the stationary PDE admits a unique segregated steady state solution with fixed mass.

REFERENCES

- [1] M. Burger, M. Di Francesco, S. Fagioli, and A. Stevens, *Sorting phenomena in a mathematical model for two mutually attracting/repelling species*, SIAM J. Math. Analysis **50** (2018), 3210–3250.
- [2] E. Espejo, *Global solutions and finite time blow up in a two species model for chemotaxis* PhD-thesis, University of Leipzig (2008).
- [3] E. Espejo, A. Stevens, and J.J.L. Velázquez, *Simultaneous finite time blow-up in a two-species model for chemotaxis*, Analysis, **29** (2009), 317–338.
- [4] W. Jäger and S. Luckhaus, *On explosions of solutions to a system of partial differential equations modelling chemotaxis*, Trans. Amer. Math. Soc., **329** (1992), 819–824.
- [5] G. Wolansky, *Multi-components chemotactic system in the absence of conflicts*, European J. of Appl. Math., **13** (2002), 641–661.

Thermoporoelasticity via homogenization

ANDRO MIKELIĆ

(joint work with C.J. van Duijn, Mary F. Wheeler, Thomas Wick)

In the talk a derivation of a macroscopic model for thermoporoelasticity from the pore scale linearized fluid-structure and energy equations was presented. Our starting point are the continuum mechanics thermodynamically compatible pore scale equations corresponding to realistic rock mechanics parameters. They are upscaled using two-scale asymptotic expansions and the following dimensional equations of the semi-linear thermoporoelasticity are obtained:

$$\begin{aligned}
 (1) \quad & \frac{\partial}{\partial t} \left\{ \frac{P}{\Lambda M} - \frac{4-2\nu}{(1+\nu)(1-2\nu)} \frac{\beta_s T}{M} + \operatorname{div}_x ((\Phi I - \mathcal{B}^H) \mathbf{U}) \right\} + \operatorname{div}_x \mathbf{V}^D = 0, \\
 (2) \quad & \mathbf{V}^D = \frac{\mathcal{K} \ell^2}{\eta(T)} \left(\rho_f^0 \beta_f g(T - T_0 - \frac{1}{\beta_f}) \mathbf{e}_3 - \nabla_x P \right), \\
 (3) \quad & \left(\tilde{\rho}c + \frac{\beta_s^2 \Lambda T_0}{M} \right) \frac{\partial T}{\partial t} + \Lambda \beta_s T_0 \frac{\partial}{\partial t} \left(-\frac{P}{\Lambda M} - (\Phi I - \mathcal{B}^H) : e_x(\mathbf{U}) \right) - \\
 & \operatorname{div}_x (\mathcal{B}^{term} \nabla_x T) + \rho_f^0 c_f \mathbf{V}^D \cdot \nabla_x T = h_f \Phi + h_s (1 - \Phi), \\
 (4) \quad & - \operatorname{div}_x \left(\mathcal{G} \Lambda e_x(\mathbf{U}) - (\Phi I - \mathcal{B}^H) P - ((1 - \Phi) I + \mathcal{B}^H) (3\lambda + 2\nu) \beta_s (T - T_0) \right) = \\
 & \rho_f^0 \beta_f \Phi g(T - T_0) \mathbf{e}_3 - (\rho_f^0 \Phi + \rho_s (1 - \Phi)) g \mathbf{e}_3,
 \end{aligned}$$

where

$$\begin{aligned}
 \tilde{\rho}c &= \Phi \rho_f^0 c_f + (1 - \Phi) \rho_s c_s; \\
 \mathcal{B}^{therm} &= \frac{\tilde{\rho}c}{\rho_f^0 c_f} \kappa_f \operatorname{Pe} \mathcal{B} \quad (\text{the homogenized thermal dispersion coefficient}).
 \end{aligned}$$

All coefficients and variables appearing in (1)-(4) are defined in Table 1.

We also provide details when comparing our results to those obtained by Coussy et al [2] and Lee and Mei [5], [6]. The choice of the characteristic time scale was presented in detail and based on realistic data. It determinates whether the homogenized system will be fully coupled (see e.g. [4]) or decoupled (see e.g. [1])

For the upscaled equations (1)-(4) a Lyapunov functional (a generalization of Biot's free energy) is constructed and the well-posedness of the model is discussed. Possible applications to large time numerical simulations are pointed out.

Details are in the preprint [3].

	QUANTITY	UNIT
u_c	characteristic solid state displacement ($\leq 5\% L$)	m (meter)
$\mathbf{U} = u_c \mathbf{u}^0$	solid phase displacement	m (meter)
L	domain size	m (meter)
ν	Poisson's ratio	dimensionless
μ	Lamé's parameter	Pa (Pascal)
Λ	characteristic value of Young's moduli	Pa (Pascal)
$\Lambda \mathcal{G}$	Gassmann's 4th order positive definite symmetric tensor	Pa (Pascal)
$p_h p_c = \rho_f^0 g L$	hydrostatic pressure	Pa (Pascal)
$P = p_c(p^0 - p_h x_3)$	fluid phase pressure	Pa (Pascal)
$T = \Delta T \vartheta^0 + T_0$	temperature	K (Kelvin)
$\eta = \eta(T) = \eta_c \eta(\vartheta^0)$	dynamic viscosity	$kg/(m s)$
ℓ	pore size	m (meter)
\mathcal{B}^H	part of Biot's parameter	a constant dimensionless matrix
$\mathcal{K}^{phys} = \ell^2 \mathcal{K}$	permeability	m^2
Φ	porosity	dimensionless with values in $(0, 1)$
β	coefficient of thermal expansion	$1/K$
$\rho_f^0 c_f$	fluid heat capacity	Pa/K
$h_f \Phi + h_s(1 - \Phi)$	effective heat source	Pa/s
$K_g = \frac{L^2 \rho_s g}{\Lambda u_c}$	Bousinessq force	dimensionless
$K_B = C_0 K_S = K_S \frac{K_g \rho_f^0 \beta_f \Delta T}{K_S \rho_s}$	buoyancy	$O(K_S)$
$\Lambda M > 0$	compressibility	Pa

TABLE 1. Description of parameters and unknowns.

REFERENCES

[1] G. Allaire, O. Bernard, J.-F. Duf r che, A. Mikeli c, *Ion transport through deformable porous media: derivation of the macroscopic equations using upscaling*, Comp. Appl. Math., Vol. **36** (2017), 1431– 1462.

[2] O. Coussy, L. Dormieux, E. Detournay, *From mixture theory to Biot's approach for porous media*, International Journal of Solids and Structures, **35(34)** (1998), 4619-4635.

[3] C.J. van Duijn, A. Mikeli c, M. F. Wheeler, T. Wick, *Thermoporoelasticity via homogenization I. Modeling and formal two-scale expansions*, preprint < hal-01650194 >, November 2017, hal-udl.archives-ouvertes.fr

[4] W. J ger, A. Mikeli c, M. Neuss-Radu, *Homogenization-limit of a model system for interaction of flow, chemical reactions and mechanics in cell tissues*, SIAM J. Math. Anal., Vol. **43** (2011), p. 1390–1435.

- [5] C. K. Lee, C. C. Mei, *Thermal consolidation in porous media by homogenization theory-I. Derivation of macroscale equations*, Advances in Water Resources, Vol. **20** (1997), p. 127-144.
- [6] C. K. Lee, C. C. Mei, *Thermal consolidation in porous media by homogenization theory-II. Calculation of effective coefficients*, Advances in Water Resources, Vol. **20** (1997), p. 145-156.

Traveling wave solutions for the Richards equation with hysteresis

BEN SCHWEIZER

(joint work with E. El Behi-Gornostaeva, K. Mitra)

Our analysis is motivated by a physical process in porous media: We assume that, initially, a porous medium is highly saturated in a top layer and has low saturation below that top layer. In two and more dimensions, the liquid can move downwards in two different ways: it can form a homogeneous saturation front or it can form gravity fingers; in the latter case, water enters preferentially along thin channels of high water saturation. We study a mathematical model for unsaturated flow in porous media that allows the formation of fingers [1, 2, 4, 5, 7].

In order to study saturation profiles, we search for traveling wave solutions for the system. We restrict here to one space dimension, the case that was also treated, e.g., in [8, 9]. If we find a traveling wave solution, we can predict qualitative properties of solutions and we have a method of calculating the speed of propagation. The one-dimensional results can also be interpreted in the higher dimensional setting: Considering a vertical slice of the domain, the one-dimensional saturation profile in the single finger can be expected to be an (approximate) traveling wave solution to the one-dimensional equations.

Let us describe the system of equations. We denote by $x \in \mathbb{R}$ the space variable, $t \in [0, \infty)$ is the time variable. The physical state in (x, t) is described by the saturation \tilde{s} and the pressure \tilde{p} , we consider $\tilde{s}, \tilde{p} : \mathbb{R} \times [0, \infty) \rightarrow \mathbb{R}$. Combining Darcy's law with mass conservation yields the unsaturated media flow equation

$$(1) \quad \partial_t \tilde{s} = \partial_x [k(\tilde{s})(\partial_x \tilde{p} + 1)],$$

where we have normalized the porosity of the medium and the gravity, which points in negative x -direction. The conductivity k is given, it is a nonnegative and nondecreasing coefficient function $s \mapsto k(s)$.

Equation (1) must be complemented with a constitutional law that relates pressure and saturation. We want to include hysteresis (the drainage and the imbibition curve are different and scanning curves can be explored by the system). For a capillary pressure function $[0, 1] \ni s \mapsto p_c(s) \in \mathbb{R}$ we consider play-type hysteresis ($\gamma > 0$) and non-equilibrium effects ($\tau > 0$) and demand

$$(2) \quad \tilde{p} \in p_c(\tilde{s}) + \gamma(\tilde{s}) H(\partial_t \tilde{s}) + \tau \partial_t \tilde{s}.$$

We use here the multivalued function

$$H(\zeta) := \begin{cases} 0 & \text{for } \zeta > 0, \\ [-1, 0] & \text{for } \zeta = 0, \\ -1 & \text{for } \zeta < 0. \end{cases}$$

Loosely speaking, our results treat the case $\gamma(s) = +\infty$, i.e., negative arguments of H do not occur.

It is known that regularized versions of the above equations permit traveling wave solutions. Furthermore, the regularized versions show oscillations and, in particular, the physically relevant effect of a saturation overshoot [3, 6]. Our result for the non-regularized hysteresis operator is that, despite the positive τ -term, the system permits the existence of monotone traveling wave profiles. These traveling waves describe the behavior of fronts in a bounded domain. The main result is that, when only imbibition and scanning curves can be reached by the system, monotone traveling wave profiles exist. In particular, we have a method to calculate the speed of fronts and/or fingers.

For our results, it is important that the non-equilibrium parameter exceeds a critical threshold, $\tau > \tau_*$. The proofs are based on a re-formulation of the equations and a careful phase-plane analysis.

REFERENCES

- [1] A. Y. Beliaev and S. M. Hassanizadeh. A theoretical model of hysteresis and dynamic effects in the capillary relation for two-phase flow in porous media. *Transp. Porous Media*, 43(3):487–510, 2001.
- [2] S. M. Hassanizadeh and W. G. Gray. Thermodynamic basis of capillary pressure in porous media. *Water Resour. Res.*, 29(10):3389–3405, 1993.
- [3] R. Hilfer and R. Steinle. Saturation overshoot and hysteresis for twophase flow in porous media. *The European Physical Journal Special Topics*, 223(11):2323–2338, 2014.
- [4] A. Lamacz, A. Rätz, and B. Schweizer. A well-posed hysteresis model for flows in porous media and applications to fingering effects. *Adv. Math. Sci. Appl.*, 21(1):33–64, 2011.
- [5] A. Rätz and B. Schweizer. Hysteresis models and gravity fingering in porous media. *ZAMM Z. Angew. Math. Mech.*, 94(7-8):645–654, 2014.
- [6] M. Schneider, T. Köppl, R. Helmig, R. Steinle, and R. Hilfer. Stable propagation of saturation overshoots for two-phase flow in porous media. *Transp. Porous Media*, 121(3):621–641, 2018.
- [7] B. Schweizer. Hysteresis in porous media: modelling and analysis. *Interfaces Free Bound.*, 19(3):417–447, 2017.
- [8] C. J. van Duijn, Y. Fan, L. A. Peletier, and I. S. Pop. Travelling wave solutions for degenerate pseudo-parabolic equations modelling two-phase flow in porous media. *Nonlinear Anal. Real World Appl.*, 14(3):1361–1383, 2013.
- [9] C. J. van Duijn, K. Mitra, and I. S. Pop. Travelling wave solutions for the Richards equation incorporating non-equilibrium effects in the capillarity pressure. *Nonlinear Anal. Real World Appl.*, 41:232–268, 2018.

Algebraic limiting techniques and hp -adaptivity for continuous finite element discretizations

DMITRI KUZMIN

(joint work with Christopher Kees, Christoph Lohmann, Manuel Quezada de Luna, Sibusiso Mabuza, John N. Shadid)

In this note, we review some new approaches to enforcing discrete maximum principles in continuous high-order finite element discretizations of hyperbolic conservation laws. As a model problem, we consider the linear advection equation

$$(1) \quad \frac{\partial u}{\partial t} + \nabla \cdot (\mathbf{v}u) = 0 \quad \text{in } \Omega,$$

where \mathbf{v} is a given velocity field and Ω is the domain of interest. A homogeneous flux boundary condition is imposed weakly on the inflow boundary of Ω . The standard Galerkin discretization leads to the semi-discrete system [5, 6]

$$(2) \quad M_C \frac{du}{dt} + Au = 0,$$

where $M_C = \{m_{ij}\}$ is the consistent mass matrix, $A = \{a_{ij}\}$ is the discrete transport operator, and $u = \{u_i\}$ is the vector of time-dependent nodal values associated with globally continuous Lagrange or Bernstein basis functions $\varphi_1, \dots, \varphi_{N_{\text{dof}}}$.

Following the derivation of *algebraic flux correction* (AFC) schemes [5] for \mathbb{P}_1 and \mathbb{Q}_1 finite element discretizations, we write system (2) in the form

$$(3) \quad M_L \frac{du}{dt} + (A - D)u = f \left(u, \frac{du}{dt} \right),$$

where $M_L = \{\delta_{ij} \sum_j m_{ij}\}$ is the lumped mass matrix and $D = \{d_{ij}\}$ is a symmetric perturbation matrix defined in terms of the artificial diffusion coefficients

$$(4) \quad d_{ij} = \begin{cases} \max\{a_{ij}, 0, a_{ji}\} & \text{if } j \neq i, \\ -\sum_{k \neq i} d_{ik} & \text{if } j = i. \end{cases}$$

By definition of M_L and D , the low-order *discrete upwind* approximation

$$(5) \quad M_L \frac{du}{dt} + (A - D)u = 0$$

is bound-preserving [5, 8]. Hence, any violations of discrete maximum principles are caused by the antidiffusive term $f(u, \dot{u}) = (M_L - M_C)\dot{u} - Du$. To suppress undershoots and overshoots, we decompose $f_i = \sum_e f_i^e$ into edge or element contributions f_i^e and apply adaptively chosen correction factors $\alpha^e \in [0, 1]$.

The simplest algebraic limiting techniques enforce local maximum principles via postprocessing based on the following predictor-corrector strategy [4, 5, 8]:

1. Calculate a bound-preserving low-order approximation \bar{u}^{n+1} using (5).
2. Add a sum of limited antidiffusive edge/element contributions to obtain

$$(6) \quad u_i^{n+1} = \bar{u}_i^{n+1} + \frac{\Delta t}{m_i} \sum_e \alpha^e f_i^e,$$

where Δt is the time step and m_i is the i -th diagonal entry of M_L . Adopting the design philosophy of *flux-corrected transport* (FCT) algorithms, the correction factors α^e are chosen so as to guarantee that $\bar{u}_i^{\min} \leq u_i^{n+1} \leq \bar{u}_i^{\max}$, where the bounds \bar{u}_i^{\max} and \bar{u}_i^{\min} are defined as local maxima and minima of \bar{u}^{n+1} [8]. Hence, the limited antidiffusive correction is *local extremum diminishing* (LED).

The predictor-corrector limiting strategy is ideally suited for numerical solution of evolutionary problems using small time steps. However, it is not to be recommended for steady-state computations since direct manipulation of the degrees of freedom at the antidiffusive correction stage prevents convergence to stationary solutions and the levels of numerical diffusion depend on the (pseudo-)time step. Instead of calculating and correcting a low-order predictor, a limited antidiffusive term \bar{f} can be incorporated into the residual of the nonlinear system

$$(7) \quad \bar{M} \frac{du}{dt} + \bar{A}u = \bar{f} \left(u, \frac{du}{dt} \right).$$

The solution-dependent correction factors α^e for the edge/element contributions $f_i^e(u, \dot{u})$ to $\bar{f}_i = \sum_e \alpha^e f_i^e$ are defined so that $\bar{f}_i = 0$ whenever u_i is a local maximum or minimum. In contrast to predictor-corrector approaches, monolithic limiting techniques of this kind constrain the perturbation of the Galerkin system (2) in an iterative manner [2, 5]. The recently developed theory of algebraic flux correction schemes [3] provides a set of sufficient conditions for well-posedness of nonlinear discrete problems and convergence of iterative solvers in the steady state limit. Limiter functions that possess all desired theoretical properties in the context of \mathbb{P}_1 and \mathbb{Q}_1 finite element approximations can be found in [6].

The extension of algebraic limiting to high-order piecewise-polynomial approximations calls for the use of finite element basis functions φ_i which guarantee that the numerical solution $u_h = \sum_i u_i \varphi_i$ is bounded by the maxima and minima of its coefficients u_i not only at the nodal points but also in-between. In contrast to high-order Lagrange elements, the Bernstein basis representation of u_h does provide this property. As shown in [1, 8], FCT-like limiting techniques are applicable to arbitrary-order Bernstein-Bézier elements but require careful localization to preserve the high-order accuracy of the target scheme for smooth data.

Another promising approach to constraining high-order continuous Galerkin discretizations is the use of limiters in the basis functions of *partitioned* finite element spaces, as proposed in [7]. Let $V_{ph,p} = \text{span}\{\varphi_1^H, \dots, \varphi_{N_{\text{dof}}}^H\}$ denote the space of continuous piecewise-polynomial functions such that $u_h|_K \in \mathbb{P}_p(K)$ or $u_h|_K \in \mathbb{Q}_p(K)$ for each $u_h \in V_{ph,p}$, $p \in \mathbb{N}$ and each element $K \in \mathcal{T}_{ph}$ of a conforming finite element mesh \mathcal{T}_{ph} . Using a $\mathbb{P}_1/\mathbb{Q}_1$ approximation on elements of the embedded *submesh* \mathcal{T}_h , we define the space $V_{h,1} = \text{span}\{\varphi_1^L, \dots, \varphi_{N_{\text{dof}}}^L\}$. To design an adaptive finite element scheme which employs the high-order approximation u_h^H in ‘smooth’ cells and the low-order approximation u_h^L in ‘troubled’ cells, we define the partitioned space $V_h(\alpha_h) := \text{span}\{\varphi_1, \dots, \varphi_{N_{\text{dof}}}\} \subset V_{h,p+1}$ in terms of

$$(8) \quad \varphi_i(\mathbf{x}) = \alpha_h(\mathbf{x})\varphi_i^H(\mathbf{x}) + (1 - \alpha_h(\mathbf{x}))\varphi_i^L(\mathbf{x}), \quad \mathbf{x} \in \bar{\Omega}, \quad i = 1, \dots, N_{\text{dof}},$$

where α_h is a blending function which yields a convex average of φ_i^H and φ_i^L . The traditional approach to hp -adaptivity in finite element methods is to use piecewise-constant basis selectors ($\alpha_h|_K \equiv 1$ or $\alpha_h|_K \equiv 0$ for $K \in \mathcal{T}_{ph}$). To ensure continuity of traces at common boundaries of adjacent mesh cells, this adaptation strategy requires special treatment of ‘hanging’ nodes and is difficult to implement. Moreover, the outcome depends on many binary decisions and small changes of the data may produce entirely different finite element spaces. To avoid the theoretical and practical difficulties associated with this methodology, the use of continuous blending functions $\alpha_h = \sum_i \alpha_i \varphi_i^L$ was proposed in [7]. The partition of unity (PU) parameters $\alpha_i \in [0, 1]$ may be defined using error indicators, smoothness criteria, and/or a priori information about location of internal/boundary layers. Moreover, the use of artificial diffusion operators and limiters can be restricted to troubled cells where the blending function α_h is set to zero by a smoothness indicator. Numerical examples illustrating the potential of using continuous blending functions in partitioned space and time discretizations can be found in [7].

In summary, a finite element approximation can be constrained to satisfy discrete maximum principles by using limiters to combine the degrees of freedom, edge/element contributions, and/or basis functions corresponding to a high-order target scheme and its bound-preserving low-order counterpart. The combination of limiting techniques with hp -adaptivity based on the PU approach provides a very general framework for robust, accurate, and physics-compatible discretization of conservation laws on general meshes. Further efforts are currently required to extend the theoretical foundations of algebraic limiting [3] to high-order / partitioned FEM and develop more efficient iterative solvers for nonlinear systems.

REFERENCES

- [1] R. Anderson, V. Dobrev, Tz. Kolev, D. Kuzmin, M. Quezada de Luna, R. Rieben, V. Tomov, High-order local maximum principle preserving (MPP) discontinuous Galerkin finite element method for the transport equation. *J. Comput. Phys.* **334** (2017), 102–124.
- [2] S. Badia and J. Bonilla, Monotonicity-preserving finite element schemes based on differentiable nonlinear stabilization. *Computer Methods Appl. Mech. Engrg.* **313** (2017), 133–158.
- [3] G. Barrenechea, V. John, and P. Knobloch, Analysis of algebraic flux correction schemes. *SIAM J. Numer. Anal.* **54** (2016), 2427–2451.
- [4] J.-L. Guermond, M. Nazarov, B. Popov, Y. Yang, A second-order maximum principle preserving Lagrange finite element technique for nonlinear scalar conservation equations. *SIAM J. Numer. Anal.* **52** (2014), 2163–2182.
- [5] D. Kuzmin, Algebraic flux correction I. Scalar conservation laws. In: D. Kuzmin, R. Löhner and S. Turek (eds.) *Flux-Corrected Transport: Principles, Algorithms, and Applications*. Springer, 2nd edition: 145–192 (2012).
- [6] D. Kuzmin, Gradient-based limiting and stabilization of continuous Galerkin methods. *Ergebnisber. Angew. Math.* **589**, TU Dortmund University, 2018.
- [7] D. Kuzmin, M. Quezada de Luna, C. Kees, A partition of unity approach to adaptivity and limiting in continuous finite element methods. *Ergebnisber. Angew. Math.* **590**, TU Dortmund University, 2018.
- [8] C. Lohmann, D. Kuzmin, J.N. Shadid, S. Mabuza, Flux-corrected transport algorithms for continuous Galerkin methods based on high order Bernstein finite elements. *J. Comput. Phys.* **344** (2017), 151–186.

Representation of Diffusive Fractures in a Fractured Porous Media and Carbonate Acidizing

MARY F. WHEELER

(joint work with Sanjay Srinivasan, Sanghyun Lee, and Rencheng Dong)

Optimal design of hydraulic fractures is controlled by the distribution of natural fractures in the reservoir. Due to sparse information, there is uncertainty associated with the prediction of the natural fracture system. Our objective here is to:

- Quantify uncertainty associated with prediction of natural fractures using micro-seismic data and a Bayesian model selection approach
- Use fracture probability maps to implement a finite element phase-field approach for modeling interactions of propagating fracture with natural fractures

The proposed approach employs state-of-the-art numerical modeling of natural and hydraulic fractures using a diffusive adaptive finite element phase-field approach [1]. The diffusive phase field is defined using the probability map describing the uncertainty in the spatial distribution of natural fractures [2]. One example of the diffusive natural fracture network is shown in Fig. 1. That probability map is computed using a model selection procedure that utilizes a suite of prior models for the natural fracture network and a fast proxy to quickly evaluate the forward seismic response corresponding to slip events along fractures. Employing indicator functions, diffusive fracture networks are generated utilizing accurate computational adaptive mesh schemes based on a posteriori error estimators.

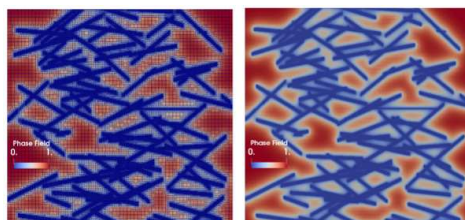


FIGURE 1. Initialization of phase field for complicated natural fracture network

The coupled algorithm was validated with existing benchmark problems which include prototype computations with fracture propagation and reservoir flows in a highly heterogeneous reservoir with natural fractures. Implementation of algorithm for computing fracture probability map based on the micro-seismic data for a Fort Worth basin data set reveals consistency between those results and the interpretation based on time lapse seismic information. Convergence of iterative solvers and numerical efficiencies of the methods were tested against different examples including field-scale problems. Results reveal that the interpretation of

uncertainty pertaining to the presence of fractures and utilizing that uncertainty within the phase field approach to simulate the interactions between induced and natural fracture yields complex structures that include fracture branching, fracture hooking, etc.

The novelty of this work lies in the efficient integration of the phase-field fracture propagation models to diffusive natural fracture networks with stochastic representation of uncertainty associated with the prediction of natural fractures in a reservoir. The presented method enables practicing engineers to simulate multiphysical problems in a reservoir with fractures efficiently and accurately. Together with efficient parallel implementation, our approach allows for cost-efficient approach to optimizing production processes in the field.

This work is being done in collaboration with Professor Sanjay Srinivasan at Pennsylvania State University and Professor Sanghyun Lee at Florida State University.

Our next topic is collaboration with Rencheng Dong, a graduate student at The University of Texas and Professor Sanghyun Lee at Florida State University.

Acidizing in unfractured carbonate reservoirs has been well studied through modeling and simulation. Since carbonate reservoirs are often naturally fractured, fractures should be modeled for realistic acidizing operations. Acidizing usually leads to large contrast in permeability between wormholes and rock matrix. The fracture system will further increase the complexity of the reactive flow. We present a pressure diffusion formulation with adaptive enriched Galerkin (EG) methods [3, 4] to handle these challenges for simulating acidizing in fractured carbonate reservoirs.

The fracture is treated as a diffusive zone [1]. A phase-field variable is defined as an indicator to distinguish fractures and unfractured rock matrix. The phase field varies from 0 (fracture) to 1 (unfractured matrix). A weighted pressure diffusion equation is derived to model the flow in both fractures and matrix through phase field. We adopt a two-scale continuum model for the acid transport. The coupled flow and reactive transport system is spatially discretized by enriched Galerkin methods. The entropy residual stabilization technique is used to avoid non-physical oscillations. Computational mesh is adaptively refined to track and resolve fine-scale wormholes.

To validate our generalized formulation, matrix acidizing in the unfractured carbonate reservoir is simulated [5]. Our two-dimensional simulation results can reproduce different dissolution patterns observed from laboratory core flooding experiments under different injection rates, including uniform dissolution, wormhole and face dissolution. Simulation is also done for acidizing in radial flow to mimic realistic near wellbore scenario. The porosity profiles for radial flow acidizing are shown in Fig. 2. Simulation results show that mesh size needs to be small enough to capture fine-scale wormhole growth. The adaptively refined mesh can produce comparable wormholes with the globally refined mesh. while the runtime of the adaptively refined mesh is just one quarter of the runtime for globally refined mesh

in our numerical tests. Since wormholes only occupy very small portion of computational domain, the adaptive mesh refinement is very useful to enhance the computational efficiency. When the formulation is applied in fractured carbonate reservoirs, the linear system to solve is better conditioned compared with the formulation where the fracture is treated as a sharp interface. Simulation results show that the fracture system controls the dissolution pattern since the wormhole growth is a self-feeding process. The generalized pressure diffraction formulation allows interactions of complicated natural fracture network.

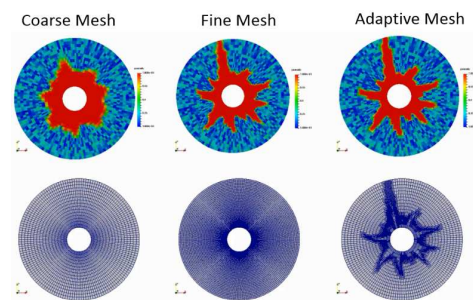


FIGURE 2. Porosity solutions after acidizing in radial unfractured carbonate reservoirs

We propose a novel pressure diffraction formulation for acidizing in fractured carbonate reservoirs. This diffusive approach can circumvent substantial permeability contrasts between fractures and unfractured matrix and allow complicated fracture network. The phase field can be initialized by the probability distribution of fractures, which connects the geology data and simulation naturally. Enriched Galerkin methods has less numerical dispersion and grid orientation effects than standard finite difference method.

REFERENCES

- [1] S. Lee, M. Wheeler, and T. Wick, *Pressure and fluid-driven fracture propagation in porous media using an adaptive finite element phase field model*, *Computer Methods in Applied Mechanics and Engineering* **305** (2016), 111-132.
- [2] S. Lee, M. Wheeler, T. Wick, and S. Srinivasan, *Initialization of phase-field fracture propagation in porous media using probability maps of fracture networks*, *Mechanics Research Communications* **80** (2017), 16-23.
- [3] S. Sun and J. Liu, *A locally conservative finite element method based on piecewise constant enrichment of the continuous Galerkin method*, *SIAM Journal on Scientific Computing* **31.4** (2009), 2528-2548.
- [4] S. Lee, Y. Lee, and M. Wheeler, *A locally conservative enriched Galerkin approximation and efficient solver for elliptic and parabolic problems*, *SIAM Journal on Scientific Computing* **38.3** (2016), A1404-A1429.
- [5] R. Dong, S. Lee, G. Pencheva, and M. Wheeler, *Numerical Simulation of Carbonate Matrix Acidizing Using Adaptive Enriched Galerkin Method*, In *InterPore 10th Annual Meeting* (2018).

Mixed-Dimensional Partial Differential Equations: applications to flow and mechanics in media with thin inclusions

WIETSE M. BOON

(joint work with Jan M. Nordbotten and Jon E. Vatne)

Mixed-dimensional partial differential equations are fully-coupled equations defined on manifolds of different dimensions. These equations typically arise in the modeling of physical processes in media containing thin inclusions. In this context, features with extreme aspect ratios are modeled as lower-dimensional manifolds, included within a surrounding medium. Examples are fractured and composite materials, but also wells (in geological applications), plant roots, or arteries and veins.

We limit the exposition to the context where the sub-manifolds are a single dimension lower than the full domain. Dimensional reduction is then repeated, by introducing lower-dimensional sub-manifolds at all intersections of existing manifolds. This leads to a hierarchy of sub-manifolds of codimension one, successively, which typically ranges from a three-dimensional bulk medium to zero-dimensional intersection points. Next, we note how the reduction of dimensionality leads to a mixed-dimensional differential geometry.

The connectivity between these manifolds is described with the use of directed graphs, referred to as trees. Assigning a tree to each manifold, a structure is introduced upon which functions and their appropriate traces can be defined. In the case of flow modeling, we define a pressure and flux variable as in [1]. The pressure is defined on manifolds of all dimensions whereas the flux is defined only on manifolds of dimension one and higher. Moreover, the normal trace of the flux variable in d dimensions is defined on all boundaries coinciding with $(d - 1)$ -manifolds, which are easily identified using the introduced trees.

We continue by considering differential operators. We are particularly interested in partial differential equations arising from conservation laws, such as flow in fractured media or mechanics of composite materials. After identifying the mixed-dimensional geometry, conservation of mass or linear momentum can be described using the mixed-dimensional divergence operator. This operator coincides with the conventional divergence in the surrounding medium, while on the lower-dimensional manifolds, it is supplemented by jump terms to incorporate contributions from higher-dimensional manifolds.

The mixed-dimensional divergence, together with its dual, are sufficient to define a mixed-dimensional Poisson equation. In terms of applications, this equation corresponds to modeling single-phase flow through a fractured medium. With this observation in mind, we note that any discretization scheme suitable for the conventional Poisson equation can be extended to solve the mixed-dimensional fracture flow problem [2].

Next, a generalization of the above concepts is presented in terms of exterior calculus, thereby introducing mixed-dimensional differential forms and the exterior

derivative. Together, a cochain complex is created, referred to as the mixed-dimensional De Rham complex. Analysis of this complex shows that it possesses the same cohomology structure as the full domain [3].

In the context of fracture flow, three numerical methods follow naturally [4] by identifying the appropriate differential forms and using results from finite element exterior calculus. However, in order to model more complex physical processes in the mixed-dimensional setting, the mixed-dimensional De Rham complex becomes a practical tool. In recent work [5], for example, the mixed formulation for linear elasticity is considered in which the symmetry of the stress tensor is imposed in a weak sense. In the analysis of the problem, it proves convenient to have access to the mixed-dimensional curl, which maps to the kernel of the divergence.

The general theory introduced herein forms a basis to analyze more complex, mixed-dimensional partial differential equations. The defined curl operator, for example, may be suited for modeling electromagnetism in media containing thin, embedded structures. Our aim in terms of future research includes the coupling flow and mechanics in terms of Biot equations in the mixed-dimensional setting. This is of particular interest in the modeling of subsurface applications such as CO₂ storage in which the storage site is considered a thin, poroelastic medium.

REFERENCES

- [1] W.M. Boon, J.M. Nordbotten, I. Yotov, *Robust discretization of flow in fractured porous media*, SIAM Journal on Numerical Analysis, **56**(4) (2018), 2203-2233
- [2] J.M. Nordbotten, W.M. Boon, A. Fumagalli, E. Keilegavlen, *Unified approach to discretization of flow in fractured porous media*, arXiv preprint arXiv:1802.05961 (2018).
- [3] W.M. Boon, J.M. Nordbotten, J. E. Vatne, *Mixed-dimensional partial differential equations*, arXiv preprint arXiv:1710.00556 (2017)
- [4] J.M. Nordbotten, W.M. Boon, *Modeling, structure and discretization of mixed-dimensional partial differential equations*, Domain Decomposition Methods in Science and Engineering XXIV, Lecture Notes in Computational Science and Engineering, arXiv preprint arXiv:1705.06876 (2018)
- [5] W.M. Boon, J.M. Nordbotten, *Stable Mixed Finite Elements for Linear Elasticity with Thin Inclusions*, in preparation.

New approaches to the fixed-stress split scheme for solving Biot's model

CARMEN RODRIGO

(joint work with Manuel Borregales, Francisco J. Gaspar, Kundan Kumar, Florin A. Radu)

Biot's equations [1] model the time dependent interaction between the deformation of an elastic porous material and the fluid flow inside of its pore network. If considering the displacements of the solid matrix \mathbf{u} and the pressure of the fluid p as primary variables, we obtain the so-called two-field formulation of the Biot's

consolidation model,

$$(1) \quad -\operatorname{div} \boldsymbol{\sigma}' + \alpha \nabla p = \rho \mathbf{g}, \quad \boldsymbol{\sigma}' = 2\mu \boldsymbol{\varepsilon}(\mathbf{u}) + \lambda \operatorname{div}(\mathbf{u}) \mathbf{I},$$

$$(2) \quad \frac{\partial}{\partial t} \left(\frac{1}{\beta} p + \alpha \nabla \cdot \mathbf{u} \right) - \nabla \cdot \left(\frac{1}{\mu_f} \mathbf{K} (\nabla p - \rho_f \mathbf{g}) \right) = f,$$

where λ and μ are the Lamé coefficients, \mathbf{I} is the identity tensor, $\boldsymbol{\sigma}'$ and $\boldsymbol{\varepsilon}$ are the effective stress and strain tensors for the porous medium, \mathbf{g} is the gravity vector, μ_f is the fluid viscosity and \mathbf{K} is the absolute permeability tensor, and ρ is the bulk density. β is the Biot modulus and α is the Biot coefficient.

There is a vast number of applications of this model, making very important its numerical simulation. In particular, the solution of the large linear systems of equations arising from the discretization of Biot's model is the most consuming part when real simulations are performed. For this reason, a lot of effort has been made in the last years to design efficient solution methods for these problems. There are two main approaches to deal with this problem, the monolithic or fully coupled methods, which solve the linear system simultaneously for all the unknowns, and the iterative coupling schemes, which solve sequentially the equations for fluid flow and geomechanics, at each time step, until a converged solution within a prescribed tolerance is achieved. The most used iterative coupling method is the fixed stress split scheme [2, 3, 4]. This sequential-implicit method basically consists in solving the flow equation by adding the stabilization term $L \frac{\partial p}{\partial t}$ in both sides of the equation:

$$(3) \quad \left(\frac{1}{\beta} + L \right) \frac{\partial p}{\partial t} - \nabla \cdot \left(\frac{1}{\mu_f} \mathbf{K} (\nabla p - \rho_f \mathbf{g}) \right) = f - \alpha \frac{\partial}{\partial t} (\nabla \cdot \mathbf{u}) + L \frac{\partial p}{\partial t},$$

where L is a parameter to fix, and then, the mechanics part is solved from the values obtained at the previous flow step. In this work, we present two new approaches to the fixed-stress split algorithm.

First, we propose a new version which forgets about the sequential nature of the temporal variable and considers the time direction as a further direction for parallelization, giving rise to a parallel-in-time iterative solution method. This type of methods are receiving a lot of interest nowadays because of the advent of massively parallel systems with thousands of threads, permitting to reduce drastically the computing time. The classical implementation of the fixed-stress split scheme (FS) is based on a time stepping approach for which at each time step one iterates between the solution of the flow and mechanics problems until reaching a converged global solution. More concretely, by using the backward Euler method on a uniform partition of the time interval $(0, T]$ with constant time-step size τ , $N\tau = T$, and denoting $\bar{\partial}_t \mathbf{u}_h^n := (\mathbf{u}_h^n - \mathbf{u}_h^{n-1})/\tau$ and $\bar{\partial}_t p_h^n := (p_h^n - p_h^{n-1})/\tau$, the algorithm is given as follows,

For $n = 1, 2, \dots, N$

For $i = 1, 2, \dots$

Step 1: Given $(\mathbf{u}_h^{n,i-1}, p_h^{n,i-1}) \in \mathbf{V}_h \times Q_h$, find $p_h^{n,i} \in Q_h$ such that

$$\left(\frac{1}{\beta} + L\right) (\bar{\partial}_t p_h^{n,i}, q_h) + b(p_h^{n,i}, q_h) = -\alpha(\operatorname{div} \bar{\partial}_t \mathbf{u}_h^{n,i-1}, q_h) + L(\bar{\partial}_t p_h^{n,i-1}, q_h) + (\tilde{f}, q_h) \quad \forall q_h \in Q_h.$$

Step 2: Given $p_h^{n,i} \in Q_h$, find $\mathbf{u}_h^{n,i} \in \mathbf{V}_h$ such that

$$2\mu(\varepsilon(\mathbf{u}_h^{n,i}), \varepsilon(\mathbf{v}_h)) + \lambda(\operatorname{div} \mathbf{u}_h^{n,i}, \operatorname{div} \mathbf{v}_h) = \alpha(p_h^{n,i}, \operatorname{div} \mathbf{v}_h) + (\rho \mathbf{g}, \mathbf{v}_h), \forall \mathbf{v}_h \in \mathbf{V}_h.$$

Here, V_h and Q_h are appropriate finite element spaces.

The proposed parallel-in-time fixed stress split method (PFS), however, iterates between the solution of the flow problem in the whole space-time grid, and the simultaneous solution of the mechanics problems at all time levels in a parallel-in-time way. Thus, given an initial guess $\{(\mathbf{u}_h^{n,0}, p_h^{n,0}), n = 0, 1, \dots, N\}$, this results in the following algorithm, which gives us a sequence of approximations $\{(\mathbf{u}_h^{n,i}, p_h^{n,i}), n = 0, 1, \dots, N\}, i \geq 1$,

Step 1: Given $\{(\mathbf{u}_h^{n,i-1}, p_h^{n,i-1}), n = 0, \dots, N\}$ find $\{p_h^{n,i} \in Q_h, n = 1, \dots, N\}$, such that

$$\left(\frac{1}{\beta} + L\right) \left(\frac{p_h^{n,i} - p_h^{n-1,i}}{\tau}, q_h\right) + b(p_h^{n,i}, q_h) = \alpha \left(\operatorname{div} \frac{\mathbf{u}_h^{n,i-1} - \mathbf{u}_h^{n-1,i-1}}{\tau}, q_h\right) + L \left(\frac{p_h^{n,i-1} - p_h^{n-1,i-1}}{\tau}, q_h\right) + (\tilde{f}, q_h), \quad \forall q_h \in Q_h,$$

$$p_h^{0,i} = p_0.$$

Step 2: Given $\{p_h^{n,i} \in Q_h, n = 1, \dots, N\}$, find $\{\mathbf{u}_h^{n,i} \in \mathbf{V}_h, n = 1, \dots, N\}$, such that

$$2\mu(\varepsilon(\mathbf{u}_h^{n,i}), \varepsilon(\mathbf{v}_h)) + \lambda(\operatorname{div} \mathbf{u}_h^{n,i}, \operatorname{div} \mathbf{v}_h) = \alpha(p_h^{n,i}, \operatorname{div} \mathbf{v}_h) + (\rho \mathbf{g}, \mathbf{v}_h), \quad \forall \mathbf{v}_h \in \mathbf{V}_h.$$

The convergence of the proposed approach is rigorously proved. Moreover, different numerical experiments show that the number of iterations required by the PFS is very similar to the iterations that the classical fixed-stress needs for convergence, so that we obtain a very similar behavior of the two methods. PFS, however, consumes around 20% of the wall time of FS, making this approach very appealing. More details about this new version of the fixed-stress split scheme can be found in [5].

Second, we consider an inexact version of the fixed-stress split scheme as smoother in a geometric multigrid framework, giving rise to a very efficient monolithic solver for Biot’s problem. The fixed-stress split scheme is equivalent to an iterative method based on the splitting of the system matrix $\mathcal{A} = \mathcal{M}_A - \mathcal{N}_A$ as,

$$\begin{bmatrix} A & B^T \\ B & -C \end{bmatrix} = \begin{bmatrix} A & B^T \\ 0 & -C + LM_p \end{bmatrix} - \begin{bmatrix} 0 & 0 \\ -B & LM_p \end{bmatrix},$$

where M_p is the mass matrix. In the multigrid context, it seems natural to consider as relaxation procedure an operator based on \mathcal{M}_A replacing the two diagonal block matrices by suitable smoothers. This means to consider relaxations as

$$\widetilde{\mathcal{M}}_A = \begin{bmatrix} M_A & B^T \\ 0 & M_S \end{bmatrix}, \quad \text{or} \quad \widetilde{\mathcal{M}}_A = \begin{bmatrix} M_A & 0 \\ 0 & M_S \end{bmatrix},$$

with M_A and M_S suitable smoothers for operators A and $S = -C + LM_p$, respectively. In particular, we consider symmetric Gauss-Seidel iterations for both A and S . This solver combines the advantages of being a fully coupled method, with the benefit of decoupling the flow and the mechanics part in the smoothing algorithm. Moreover, it deals with complex domains by using semi-structured grids, and it shows a very efficient behavior independently of the values of the physical parameters, even for heterogeneous materials. Furthermore, the fixed-stress split smoother is based on the physics of the problem, and therefore all parameters involved in the relaxation are based on the physical properties of the medium and are given a priori. More details about the monolithic multigrid method based on the fixed-stress split smoother are given in [6].

REFERENCES

- [1] M.A. Biot, *General theory of three-dimensional consolidation*, Journal of Applied Physics **12** (1941) 155–164.
- [2] J. Kim, H. Tchelepi, R. Juanes, *Stability and convergence of sequential methods for coupled flow and geomechanics: Fixed-stress and fixed-strain splits*, Comput. Methods. Appl. Mech. Eng., **200** (2011) 1591–1606.
- [3] A. Mikelic, M.F. Wheeler, *Convergence of iterative coupling for coupled flow and geomechanics*, Comput. Geosci., **17** (2013) 455–461.
- [4] J. Both, M. Borregales, F.A. Radu, K. Kumar, J.M. Nordbotten, *Robust fixed stress splitting for Biot's equations in heterogeneous media*, Applied Mathematics Letters, **68** (2017) 101–108.
- [5] M. Borregales, K. Kumar, F.A. Radu, C. Rodrigo, F.J. Gaspar, *About a parallel-in-time fixed-stress split method for the Biot's consolidation model*, Computers & Mathematics with Applications, in press.
- [6] F. J. Gaspar, C. Rodrigo, *On the fixed-stress split scheme as smoother in multigrid methods for coupling flow and geomechanics*, Comput. Methods Appl. Mech. Engrg., **326** (2017) 526–540.

Mixed Methods for Two-Phase Darcy-Stokes Mixtures of Partially Melted Materials with Regions of Zero Porosity

TODD ARBOGAST

(joint work with Marc A. Hesse and Abraham L. Taicher)

The Earth's mantle, or an ice sheet, is a deformable solid matrix phase within which a second phase, a fluid, may form due to melting processes. According to McKenzie [4], the mechanics of this system can be modeled using mixture theory as a dual-continuum. At each point of space, the solid matrix is governed by a highly viscous Stokes system, and the fluid melt, if it exists, is governed by a Darcy law. The mixing parameter is the porosity ϕ , which is the volume fraction of fluid

melt. It is assumed to be much smaller than one, but it may be zero in parts of the (bounded) domain $\Omega \subset \mathbb{R}^d$ where there is no fluid melt.

We can describe the mechanics using the subscripts f , s , and r to refer to a quantity associated with the fluid melt, the matrix solid, or the relative fluid minus solid, respectively. For simplicity, we set all constants to unity and apply a Boussinesq approximation (constant and equal densities for non-buoyancy terms). Fluid melt forms at the boundaries of rock crystals and so obeys a Darcy's law for fluid flow around solid matrix "grains", which is

$$\mathbf{u} = -\phi^2 \nabla q_f,$$

where \mathbf{u} is the Darcy velocity, q_f is the fluid pressure potential, and ϕ^2 is the porosity dependent relative permeability (more general forms may be treated—the important point is that it vanishes when $\phi = 0$). Mass conservation is expressed

$$\nabla \cdot (\mathbf{u} + \mathbf{v}_s) = 0,$$

where \mathbf{v}_s is the matrix solid velocity of the Earth. Conservation of momentum obeys the Stokes equation. In terms of the deviatoric stress of the mixture

$$\hat{\boldsymbol{\sigma}} = \hat{\boldsymbol{\sigma}}(\mathbf{v}_s) = 2(1 - \phi)(\mathcal{D}\mathbf{v}_s - \frac{1}{3}\nabla \cdot \mathbf{v}_s \mathbf{I}),$$

wherein $\mathcal{D}\mathbf{v}_s = \frac{1}{2}(\nabla\mathbf{v}_s + \nabla\mathbf{v}_s^T)$ is the symmetric gradient, we have that

$$-\nabla q + \nabla \cdot \hat{\boldsymbol{\sigma}}(\mathbf{v}_s) = \mathbf{G},$$

where $q = \bar{q} = \phi q_f + (1 - \phi)q_s = q_s + \phi q_r$ is the mixture pressure potential and \mathbf{G} is related to the gravitational body force. Finally, the solid and fluid pressures are related through a compaction relation

$$q_s - q_f = -\frac{1}{\phi} \nabla \cdot \mathbf{v}_s,$$

where $1/\phi$ is the solid matrix bulk viscosity.

When coupled with solute transport and thermal evolution, the model transitions dynamically in time from a non-porous single phase Stokes solid to a two-phase porous medium. The free boundary between the one and two-phase regions need *not* be determined explicitly; rather, the model equations based on mixture theory describe both phases over the entire domain Ω . Unfortunately, the Darcy part of the equations is mathematically degenerate in regions where the porosity is zero, since then there is only the one solid phase.

In the work [1], we assume that $\phi(\mathbf{x})$ is given at some instant of time, and we discuss only the mechanics part of the full model. With an eye to future use in a full, dynamic simulation, our goal is to find a well-posed variational framework of the problem and a (mixed) finite element approximation that manages the zero porosity case.

To handle the possible degeneracy, we define the *scaled relative velocity* and *scaled fluid potential* [2]

$$\tilde{\mathbf{v}}_r = \phi^{-1} \mathbf{u} \quad \text{and} \quad \tilde{q}_f = \phi^{1/2} q_f,$$

respectively, and we reformulate the problem as

$$\begin{aligned} \tilde{\mathbf{v}}_r + \phi \nabla(\phi^{-1/2} \tilde{q}_f) &= 0, \\ \phi^{-1/2} \nabla \cdot (\phi \tilde{\mathbf{v}}_r) + \frac{1}{1-\phi} (\tilde{q}_f - \phi^{1/2} q) &= 0, \\ -\nabla q + \nabla \cdot \hat{\boldsymbol{\sigma}}(\mathbf{v}_s) &= \mathbf{G}, \\ \nabla \cdot \mathbf{v}_s - \frac{\phi^{1/2}}{1-\phi} (\tilde{q}_f - \phi^{1/2} q) &= 0. \end{aligned}$$

These equations make sense if the gradient and divergence terms, which are duals of each other, are well-defined when $\phi = 0$. But

$$\phi^{-1/2} \nabla \cdot (\phi \tilde{\mathbf{v}}_r) = \phi^{1/2} \nabla \cdot \tilde{\mathbf{v}}_r + \phi^{-1/2} \nabla \phi \cdot \tilde{\mathbf{v}}_r$$

is well defined under the assumption

$$\phi \in L^\infty(\Omega) \quad \text{and} \quad \phi^{-1/2} \nabla \phi \in (L^\infty(\Omega))^d.$$

The scaled velocity $\tilde{\mathbf{v}}_r$ should be expected to lie in the space

$$H_\phi(\text{div}; \Omega) = \{ \mathbf{v} \in (L^2(\Omega))^d : \phi^{-1/2} \nabla \cdot (\phi \mathbf{v}) \in L^2(\Omega) \},$$

which is a Hilbert space with the inner product

$$(\mathbf{u}, \mathbf{v})_{H_\phi(\text{div}; \Omega)} = (\mathbf{u}, \mathbf{v}) + (\phi^{-1/2} \nabla \cdot (\phi \mathbf{u}), \phi^{-1/2} \nabla \cdot (\phi \mathbf{v})).$$

Moreover, these vector functions have a well-defined normal trace $\gamma(\mathbf{v}) = \phi^{1/2} \mathbf{v} \cdot \nu$ on $\partial\Omega$, where $\gamma : H(\text{div}; \Omega) \rightarrow H^{-1/2}(\partial\Omega)$ is bounded. For homogeneous Neumann boundary conditions, the problem can be recast in variational form: Find $\tilde{\mathbf{v}}_r \in H_{\phi,0}(\text{div}) = \{ \mathbf{v} \in H_\phi(\text{div}; \Omega) : \phi^{1/2} \mathbf{v} \cdot \nu = 0 \text{ on } \partial\Omega \}$, $\tilde{q}_f \in L^2$, $\mathbf{v}_s \in (H_0^1)^d$, and $q \in L^2/\mathbb{R}$ such that

$$\begin{aligned} (\tilde{\mathbf{v}}_r, \boldsymbol{\psi}_r) - (\tilde{q}_f, \phi^{-1/2} \nabla \cdot (\phi \boldsymbol{\psi}_r)) &= 0 & \forall \boldsymbol{\psi}_r \in H_{\phi,0}(\text{div}), \\ (\phi^{-1/2} \nabla \cdot (\phi \tilde{\mathbf{v}}_r), w_f) + \left(\frac{1}{1-\phi} (\tilde{q}_f - \phi^{1/2} q), w_f \right) &= 0 & \forall w_f \in L^2, \\ -(q, \nabla \cdot \boldsymbol{\psi}_s) + (\hat{\boldsymbol{\sigma}}(\mathbf{v}_s), \nabla \boldsymbol{\psi}_s) &= (\mathbf{G}, \boldsymbol{\psi}_s) & \forall \boldsymbol{\psi}_s \in (H_0^1)^d, \\ (\nabla \cdot \mathbf{v}_s, w) - \left(\frac{\phi^{1/2}}{1-\phi} (\tilde{q}_f - \phi^{1/2} q), w \right) &= 0 & \forall w \in L^2/\mathbb{R}. \end{aligned}$$

There exists a unique solution to this problem, and

$$\|\tilde{\mathbf{v}}_r\| + \|\phi^{-1/2} \nabla \cdot (\phi \tilde{\mathbf{v}}_r)\| + \|\tilde{q}_f\| + \|\mathbf{v}_s\|_1 + \|q\| \leq C.$$

A mixed finite element method can be defined based on the variational formulation. The lowest order Raviart-Thomas spaces can be used to approximate $(\tilde{\mathbf{v}}_r, \tilde{q}_f)$ by $(\tilde{\mathbf{v}}_{r,h}, \tilde{q}_{f,h})$, and any reasonable Stokes elements, such as Bernardi-Raugel or Taylor Hood elements, can be used to approximate (\mathbf{v}_s, q) by $(\mathbf{v}_{s,h}, q_h)$.

In terms of the Raviart-Thomas and L^2 projection $(\pi_{\text{RT}}, \mathcal{P}_{\text{RT}})$ and the Stokes H^1 and L^2 projections $(\pi_{\text{S}}, \mathcal{P}_{\text{S}})$, if the computational mesh is quasi-uniform,

$$\begin{aligned} & \|\tilde{\mathbf{v}}_r - \tilde{\mathbf{v}}_{r,h}\|_{L^2} + \|\mathcal{P}_{\text{RT}}[\phi^{-1/2}\nabla \cdot (\phi(\tilde{\mathbf{v}}_r - \tilde{\mathbf{v}}_{r,h}))]\|_{L^2} + \|\mathbf{v}_s - \mathbf{v}_{s,h}\|_{H^1} \\ & \quad + \|\tilde{q}_f - \tilde{q}_{f,h}\|_{L^2} + \|q - q_h\|_{L^2} \\ & \leq C\{\|\tilde{\mathbf{v}}_r - \pi_{\text{RT}}\tilde{\mathbf{v}}_r\|_{L^2} + \|\mathcal{P}_{\text{RT}}[\phi^{-1/2}\nabla \cdot (\phi(\tilde{\mathbf{v}}_r - \pi_{\text{RT}}\tilde{\mathbf{v}}_r))]\|_{L^2} \\ & \quad + \|q - \mathcal{P}_{\text{S}}q\|_{L^2} + \|\mathbf{v}_s - \pi_{\text{S}}\mathbf{v}_s\|_{H^1} + \|\tilde{q}_f - \mathcal{P}_{\text{RT}}\tilde{q}_f\|_{L^2}\}. \end{aligned}$$

That is, if the solution is sufficiently regular, the approximation error is $\mathcal{O}(h)$. The method as stated is locally non-conservative, but it can be modified to obtain a locally conservative method. On rectangular meshes, the method can also be implemented by an efficient cell-centered finite difference approximation of the first equation [3]. In this case, $\tilde{\mathbf{v}}_r$ can be eliminated locally, and a Stokes system with not one but *two* pressures results. Moreover, superconvergence is sometimes observed by this modified method.

Numerical results illustrate the performance of the mixed finite element method. They also verify the convergence of the method up to the regularity of the solution. If one replaces ϕ by, say $\max(\phi, \epsilon)$ to avoid any degeneracy, the condition number of the linear system remains bounded as $\epsilon \rightarrow 0^+$, unlike competing approaches that require nonzero ϕ .

REFERENCES

- [1] T. Arbogast, M. A. Hesse, and A. L. Taicher, *Mixed Methods for Two-Phase Darcy-Stokes Mixtures of Partially Melted Materials with Regions of Zero Porosity*, SIAM J. Sci. Comput., **39:2** (2017), B375–B402, DOI 10.1137/16M1091095.
- [2] T. Arbogast and A. L. Taicher, *A linear degenerate elliptic equation arising from two-phase mixtures*, SIAM J. Numer. Anal., **54:5** (2016), 3105–3122, DOI 10.1137/16M1067846.
- [3] T. Arbogast and A. L. Taicher, *A Cell-Centered Finite Difference Method for a Degenerate Elliptic Equation Arising from Two-Phase Mixtures*, Computational Geosciences, **21:4** (2017), 701–712, DOI 10.1007/s10596-017-9649-9.
- [4] D. McKenzie, *The Generation and Compaction of Partially Molten Rock*, J. Petrology, **25:3** (1984), 713–765.

Flow simulations in geology-based Discrete Fracture Networks

GÉRALDINE PICHOT

(joint work with Patrick Laug, Jocelyne Erhel, Romain Le Goc, Caroline Darcel, Philippe Davy, Jean-Raynald de Dreuzy)

1. MOTIVATION

The underground is a reservoir of natural resources (water, oil and gas, heat,...) and a potential warehouse storage solution. Using these resources and storage facilities in a sustainable way requires a good understanding of the physical, chemical and biological processes happening there. Also, the geometry of the subsurface

couples these processes together. Here, numerical models are very useful: they reduce the costs and risks of *in situ* experiments and allow long-term predictions.

2. GEOMETRIC MODEL

At first, we need to build a geometric model of the subsurface. Observations and experiments (investigations of drill cores and drill cuttings, lineament characterization, measurements of reflection seismics, transient electromagnetic soundings, ... [1]) give data for soil characterization and fracture locations. Fractures cannot be neglected as they critically impact the response of subsurface systems through their complex organisation over a broad range of scales. However, the information collected via the measurements are local. To derive an image of the full geometry, numerical models come into play. It is quite challenging to process tremendous amounts of noisy data, scattered and at different scales. Nevertheless, hydrogeologists are able to derive models for the subsurface, and especially for fracture systems [2]. The one we rely on is based on a spatial organization of fractures satisfying two main regimes: a dilute regime for the smallest fractures, where they can grow independently of each other, and a dense regime for which the density distribution is controlled by the mechanical interactions between fractures [3, 4]. In these models, called UFM (likely Universal Fracture Model), the fracture size distribution matches the observations and large fractures inhibit the smaller ones, creating T-termination configurations. Models mix spatial dimensions as fracture networks consist in a large number of 2D fractures interconnected in the 3D space [5]. These models are implemented in a dedicated software, called UFMLab. UFM networks may contain millions of fractures.

3. FLOW PROBLEM

Let us focus on a simple process, which is the flow of water within the fractures. The surrounding rock matrix is assumed impervious. The associated problem is governed by the Poiseuille's law and the mass conservation equation in each fracture combined with continuity conditions at the intersections between fractures. The transmissivity within the fractures is assumed heterogeneous and modeled by random fields whose parameters are given by the experiments.

4. MESH GENERATION

The next step is to build a mesh of the domain. To easily enforce the continuity conditions at the intersections, we request a mesh which takes the intersections into account, either with matching or non-matching grids at the intersections. However, even in the non-matching cases, the intricate configurations of the fracture systems make it difficult for standard planar meshers to generate a mesh of the geometry. The idea is then to discretize first the border and intersections to build a geometric model, valid for the planar mesher. It implies automatic corrections to build valid curve discretizations. These corrections are implemented in the

software `BLSURF_FRAC`¹. Then a planar mesher is called, for example, `BL2D` [6] or `BAMG` [7]. Up to now, the largest network successfully meshed with this technique contains 508,339 fractures which generate 1,031,231 intersections. It is meshed in 15 minutes using the combination of `BLSURF_FRAC` and `BL2D`, with 4 threads on a PC Intel Core i7 4 cores CPU @ 2.90 GHz, 32GB RAM memory. The final mesh contains 8,112,299 of triangles and 1,630,682 of intersection edges. Notice that the computational time can be improved on a computer with more RAM memory as memory swapping was detected during this numerical experiment. Also, we identified some sequential parts of `BLSURF_FRAC` that can be parallelized.

5. NUMERICAL METHODS AND IMPLEMENTATION

The next step is to solve the flow problem efficiently. We propose to solve this problem using a Mixed Hybrid Finite Elements Method (MHFEM) [8, 9, 10]. Possible non-matching grids at the intersections between fractures are handled by using suitable Mortar conditions [11, 12, 13, 14, 15]. In both, the matching and non-matching grids cases, we end up with a linear system whose matrix is symmetric positive definite. It is a sparse matrix with a L-shape structure. The linear system can be solved either with a direct solver (Cholesky factorization) or with an iterative solver (preconditioned conjugate gradient or multigrid). A way to improve the computational time of iterative solvers is to use domain decomposition techniques [16, 17]. We developed a Matlab code, called `NEF-Flow`, which implements the MHFEM either for matching or non-matching meshes, with sink/source terms and contrasts in transmissivities. Efficiency is obtained using Matlab vectorization. For example, we solved the flow problem in the largest network described above in 21 minutes on a PC Intel Core i7 4 cores CPU @ 2.90 GHz, 32GB RAM memory with a direct solver. Here again memory swapping was detected. Further numerical experiments are now performed with iterative solvers to reduce memory requirements. Also to keep an accurate solution with less triangles, we are investigating the use of a higher order hybridizable discontinuous Galerkin technique, the HHO method [18], combined with *a posteriori* error estimates [19] in order to refine only the fractures that carry most of the flow.

Acknowledgments. The author thanks the organizers of the workshop for their kind invitation. The author thanks the MFO and all its staff for the extremely good working and living conditions provided at Oberwolfach.

REFERENCES

- [1] Svensk Kärnbränslehantering AB (SKB), Site description of Forsmark at completion of the site investigation phase. SDM-Site Forsmark, *TR-08-05*, Stockholm (2008).
- [2] J. Maillot, P. Davy, R. Le Goc, C. Darcel and J.-R. de Dreuzy. Connectivity, permeability, and channeling in randomly distributed and kinematically defined discrete fracture network models. *Water Resources Research*, 52 (11), 8526–8545, (2016).

¹<http://pages.saclay.inria.fr/patrick.laug/logiciels/logiciels.html>

-
- [3] P. Davy, R. Le Goc, C. Darcel, O. Bour, J.-R. de Dreuzy and R. Munier. A likely universal model of fracture scaling and its consequence for crustal hydromechanics. *Journal of Geophysical Research: Solid Earth*, 115 (B10) (2010).
- [4] P. Davy, R. Le Goc and C. Darcel. A model of fracture nucleation, growth and arrest, and consequences for fracture density and scaling. *Journal of Geophysical Research: Solid Earth*, 118 (4), 1393–1407 (2013).
- [5] V. Martin, J. Jaffré and J. E. Roberts. Modeling fractures and barriers as interfaces for flow in porous media, *SIAM J. Sci. Comput.*, 26 (5), pp. 1667–1691 (2005).
- [6] H. Borouchaki, P. Laug and P. L. George. Parametric surface meshing using a combined advancing-front – generalized-Delaunay approach. *International Journal for Numerical Methods in Engineering*, 49 (1-2), 233–259 (2000).
- [7] F. Hecht, BAMG: Bidimensional Anisotropic Mesh Generator (2006).
- [8] D. N. Arnold and F. Brezzi. *Mixed and nonconforming finite element methods: postprocessing, and error estimates*, RAIRO M2AN, vol. 19, 732 (1985).
- [9] F. Brezzi and M. Fortin. *Mixed and Hybrid Finite Element Methods*, Springer-Verlag, New York, 1991.
- [10] J. E. Roberts and J. M. Thomas. *Mixed and hybrid methods*, *Handbook of numerical analysis*, Vol. 2, P.G. Ciarlet and J.L. Lions Ed., North Holland, p. 523 (1991).
- [11] T. Arbogast and Z. Chen, On the Implementation of Mixed Methods as Nonconforming Methods for Second-Order Elliptic Problems, *Mathematics of Computation*, 211-64, pp. 943–972 (1995).
- [12] T. Arbogast, L. C. Cowsar, M. F. Wheeler and I. Yotov, *Mixed finite element methods on non-matching multiblock grids*, *SIAM J. Numer. Anal.*, 37(4), pp. 1295-1315 (2000).
- [13] J. Maryška, O. Severýn and M. Vohralík. *Numerical simulation of fracture flow with a mixed-hybrid FEM stochastic discrete fracture network model*, *Computational Geosciences*, 8, pp. 217-234 (2004).
- [14] G. Pichot, J. Erhel and J.-R. de Dreuzy. A mixed hybrid Mortar method for solving flow in discrete fracture networks, *Applicable Analysis*, 89-10, pp. 1629-1643 (2010).
- [15] G. Pichot, J. Erhel, and J.-R. de Dreuzy. A generalized mixed hybrid mortar method for solving flow in stochastic discrete fracture networks. *SIAM J. Sci. Comput.*, 34(1):B86–B105 (2012).
- [16] B. Poirriez. Study and implementation of a domain decomposition method for the modelisation of flow in 3D fracture networks, PhD Thesis, University of Rennes 1 (2011).
- [17] G. Pichot, B. Poirriez, J. Erhel, and J.-R. De Dreuzy. A Mortar BDD method for solving flow in stochastic discrete fracture networks. *Domain Decomposition Methods in Science and Engineering XXI, Lecture Notes in Computational Science and Engineering (LNCSE)*, 98 (2014).
- [18] D. A. Di Pietro and A. Ern. A Hybrid High-Order locking-free method for linear elasticity on general meshes. *Comput. Meth. Appl. Mech. Engrg.*, 283:1–21 (2015).
- [19] A. Ern and M. Vohralík. Polynomial-degree-robust a posteriori estimates in a unified setting for conforming, nonconforming, discontinuous Galerkin, and mixed discretizations. *SIAM J. Numer. Anal.*, 53, pp. 1058–1081 (2015).

Principles of Predictive Computational Science: Predictive Models of Random Heterogeneous Materials and Tumor Growth

J. TINSLEY ODEN

(joint work with Faghihi, Daniel; Scarabosio, Laura; Wohlmuth, Barbara, and Lima, Ernesto)

To set stage for specific developments and applications, this presentation begins with an overview of the mathematical and philosophical foundations of predictive computational science, the discipline concerned with the use of mathematical and computational models to predict events in the physical universe in the presence of uncertainties. It is argued that the principal sources of uncertainty are: the system of reasoning (epistemology) selected to communicate logically notions of uncertainty, the uncertainties in observational data, model selection, model parameters, and uncertainties due to discretization errors. The Cox-Jaynes theory of logical probability is advocated as a comprehensive framework for representing uncertainty, it establishes that every extension of Aristotelian logic within uncertainties is Bayesian, and that the logical theory, based on propositional Boolean algebra, is isomorphic to the measure-based Kolmogorov theory of probability. Thereafter, Bayesian inferences are used to quantify uncertainties in data, models, and parameters. Model selection using Bayesian arguments is taken up later. Discretization error is quantified using a posteriori error estimation. Bayesian-based methods for model calibration, selection, and then prediction of quantities of interest are then described.

The discussion then proceeds to the development of predictive models of random heterogeneous media. The notion of optimal control of modeling error as a framework for generating sequences of surrogate models of lower dimension and complexity than a ground-truth model of high fidelity is described. Applications to problems in nano-manufacturing of semiconductors, random two-phase elastic materials, and heat conduction in random two-phase materials are described. There a greedy algorithm is developed whereby the domain of a stochastic model of the random material is partitioned into subdomains and a sequence of surrogate models of increasing accuracy in approximation of local quantities of interest (QoIs) is generated by successively adding fine-scale information until tolerances in estimates of error in the QoIs are met. The method generalizes the approach described in [1] to stochastic models. It is shown that the generation of sequences of surrogate models of increasing accuracy provides a setting for implementing a model-based version of the Multilevel Monte Carlo (MLMC) method for solving the stochastic system. Examples are cited in which this adaptive model based MLMC is substantially more efficient than the traditional MC method.

The presentation concludes with a discussion of OPAL, the Occam Plausibility Algorithm, which is presented as general framework for selection, calibration, and validation of computational models based, in part, on the idea of posterior Bayesian plausibilities. This methodology is applied to the selection of predictive models of tumor growth, selected from sets of models based on continuum mixture

theory, and well-known hallmarks of cancer. In particular experiments with laboratory animals injected with brain cancer cells (glioma) and then radiotherapy are presented in which plausible and valid models are selected from sets of up to 39 models, some involving many parameters. Very accurate predictions of the observed tumor mass, as approximated via MRI images, are obtained. Further details on the work described in his presentation can be found in references [2, 3].

REFERENCES

- [1] J.T. Oden, K.S. Vemagnati, *Estimation of local modeling error and goal-oriented modeling of heterogeneous materials: I. Error estimates and adaptive algorithms*, Journal of Computational Physics **164** (1) (2000), 22–47.
- [2] J.T. Oden, *Adaptive multiscale predictive modeling*, Acta Numerica (2018), 353–450.
- [3] E.A.B.F. Lima, J.T. Oden, B. Wohlmuth, AL. Shahmoradi, P.A. Hormuth II, T.E. Yankeelov, L. Scarabosio, and T. Horger, *Selection and validation of predictive models of radiation effects on tumor growth based on noninvasive imaging data*, Computer Methods in Applied Mechanics and Engineering **327** (2017), 277–305.

Parameter-robust stability and strongly mass-conservative discretization of multi-permeability poroelasticity model

JOHANNES KRAUS

(joint work with Qingguo Hong, Maria Lymbery, Fadi Philo)

Multiple-network poroelastic theory (MPET) has been introduced into geomechanics [1, 2] to describe mechanical deformation and fluid flow in porous media as a generalization of Biot’s theory [3, 4]. The deformable elastic matrix is assumed to be permeated by multiple fluid networks of pores and fissures with differing porosity and permeability. The biological MPET model captures flow across scales and networks in soft tissue and can be used as an embedding platform for more specific models, e.g. to describe water transport in the cerebral environment [8].

In an open domain $\Omega \subset \mathbb{R}^d$, $d = 2, 3$, the unknown physical variables in the MPET flux based model are the displacement \mathbf{u} , fluxes \mathbf{v}_i and corresponding pressures p_i $i = 1, \dots, n$. Imposing proper boundary and initial conditions and using the backward Euler method for time discretization one has to solve a static problem in each time step, which after rescaling and proper variable substitutions can be represented as an equation of the form

$$(1) \quad \mathcal{A} [\mathbf{u}^T, \mathbf{v}_1^T, \dots, \mathbf{v}_n^T, p_1, \dots, p_n]^T = [\mathbf{f}^T, \mathbf{0}^T, \dots, \mathbf{0}^T, g_1, \dots, g_n]^T \quad \text{where}$$

$$\mathcal{A} := \begin{bmatrix}
 -\operatorname{div} \epsilon - \lambda \nabla \operatorname{div} & 0 & \dots & \dots & 0 & \nabla & \dots & \dots & \nabla \\
 0 & R_1^{-1} I & 0 & \dots & 0 & \nabla & 0 & \dots & 0 \\
 \vdots & 0 & \ddots & & \vdots & 0 & \ddots & & \vdots \\
 \vdots & \vdots & & \ddots & 0 & \vdots & & \ddots & 0 \\
 0 & 0 & \dots & 0 & R_n^{-1} I & 0 & \dots & 0 & \nabla \\
 -\operatorname{div} & -\operatorname{div} & 0 & \dots & 0 & \tilde{\alpha}_{11} I & \alpha_{12} I & \dots & \alpha_{1n} I \\
 \vdots & 0 & \ddots & & \vdots & \alpha_{21} I & \ddots & & \alpha_{2n} I \\
 \vdots & \vdots & & \ddots & 0 & \vdots & & \ddots & \vdots \\
 -\operatorname{div} & 0 & \dots & 0 & -\operatorname{div} & \alpha_{n1} I & \alpha_{n2} I & \dots & \tilde{\alpha}_{nn} I
 \end{bmatrix}$$

is a scaled operator, $R_i^{-1} := \tau^{-1} K_i^{-1} \alpha_i^2$, $\alpha_{p_i} := \frac{c_{p_i}}{\alpha_i^2}$, $\beta_{ii} := \sum_{j=1, j \neq i}^n \beta_{ij}$, $\alpha_{ij} := \frac{\tau \beta_{ij}}{\alpha_i \alpha_j}$, $\tilde{\alpha}_{ii} := -\alpha_{p_i} - \alpha_{ii}$, $i, j = 1, \dots, n$.

The constants α_i are known in the literature as Biot-Willis parameters, c_{p_i} are referred to as the constrained specific storage coefficients, $\beta_{ij} = \beta_{ji}$ are the network transfer coefficients coupling the different networks [8]. Moreover, K_i denotes the hydraulic conductivity of the i th network and τ the time step size.

We make the rather general and reasonable assumptions that

$$(2) \quad \lambda > 0, \quad R_1^{-1}, \dots, R_n^{-1} > 0, \quad \alpha_{p_1}, \dots, \alpha_{p_n} \geq 0, \quad \alpha_{ij} \geq 0, \quad i, j = 1, \dots, n.$$

For convenience, let $\mathbf{v}^T = (\mathbf{v}_1^T, \dots, \mathbf{v}_n^T)$, $\mathbf{p}^T = (p_1, \dots, p_n)$, $\mathbf{z}^T = (\mathbf{z}_1^T, \dots, \mathbf{z}_n^T)$, $\mathbf{q}^T = (q_1, \dots, q_n)$ and $\mathbf{v}, \mathbf{z} \in \mathbf{V} = \mathbf{V}_1 \times \dots \times \mathbf{V}_n$, $\mathbf{p}, \mathbf{q} \in \mathbf{P} = P_1 \times \dots \times P_n$. Under proper boundary and initial conditions, system (1) has the following weak formulation: Find $(\mathbf{u}; \mathbf{v}; \mathbf{p}) \in \mathbf{U} \times \mathbf{V} \times \mathbf{P}$, such that for any $(\mathbf{w}; \mathbf{z}; \mathbf{q}) \in \mathbf{U} \times \mathbf{V} \times \mathbf{P}$ there holds

$$\begin{aligned}
 (\epsilon(\mathbf{u}), \epsilon(\mathbf{w})) + \lambda(\operatorname{div} \mathbf{u}, \operatorname{div} \mathbf{w}) - \sum_{i=1}^n (p_i, \operatorname{div} \mathbf{w}) &= (\mathbf{f}, \mathbf{w}) \\
 (R_i^{-1} \mathbf{v}_i, \mathbf{z}_i) - (p_i, \operatorname{div} \mathbf{z}_i) &= 0, \quad i = 1, \dots, n, \\
 -(\operatorname{div} \mathbf{u}, q_i) - (\operatorname{div} \mathbf{v}_i, q_i) + \tilde{\alpha}_{ii}(p_i, q_i) + \sum_{\substack{j=1 \\ j \neq i}}^n \alpha_{ij}(p_j, q_i) &= (g_i, q_i), \quad i = 1, \dots, n,
 \end{aligned}$$

or, equivalently, $\mathcal{A}((\mathbf{u}; \mathbf{v}; \mathbf{p}), (\mathbf{w}; \mathbf{z}; \mathbf{q})) = F(\mathbf{w}; \mathbf{z}; \mathbf{q})$ for all $(\mathbf{w}; \mathbf{z}; \mathbf{q}) \in \mathbf{U} \times \mathbf{V} \times \mathbf{P}$, $\mathbf{U} = \{\mathbf{u} \in H^1(\Omega)^d : \mathbf{u} = \mathbf{0} \text{ on } \Gamma_{\mathbf{u}, D}\}$, $\mathbf{V}_i = \{\mathbf{v}_i \in H(\operatorname{div}, \Omega) : \mathbf{v}_i \cdot \mathbf{n} = 0 \text{ on } \Gamma_{p_i, N}\}$, $P_i = L^2(\Omega)$, and $P_i = L_0^2(\Omega)$ if $\Gamma_{\mathbf{u}, D} = \Gamma = \partial\Omega$.

We define $R^{-1} := \max\{R_1^{-1}, \dots, R_n^{-1}\}$, $\lambda_0 := \max\{1, \lambda\}$, and the following $n \times n$ matrices

$$\Lambda_1 := \begin{bmatrix} \alpha_{11} & -\alpha_{12} & \dots & -\alpha_{1n} \\ -\alpha_{21} & \alpha_{22} & \dots & -\alpha_{2n} \\ \vdots & \vdots & \ddots & \vdots \\ -\alpha_{n1} & -\alpha_{n2} & \dots & \alpha_{nn} \end{bmatrix}, \quad \Lambda_2 := \begin{bmatrix} \alpha_{p_1} & 0 & \dots & 0 \\ 0 & \alpha_{p_2} & \dots & 0 \\ \vdots & \vdots & \ddots & \vdots \\ 0 & 0 & \dots & \alpha_{p_n} \end{bmatrix},$$

$$\Lambda_3 := \begin{bmatrix} R & 0 & \dots & 0 \\ 0 & R & \dots & 0 \\ \vdots & \vdots & \ddots & \vdots \\ 0 & 0 & \dots & R \end{bmatrix}, \quad \Lambda_4 := \begin{bmatrix} \frac{1}{\lambda_0} & \dots & \dots & \frac{1}{\lambda_0} \\ \vdots & & & \vdots \\ \vdots & & & \vdots \\ \frac{1}{\lambda_0} & \dots & \dots & \frac{1}{\lambda_0} \end{bmatrix}, \quad \Lambda := \sum_{i=1}^4 \Lambda_i.$$

From the above definitions of α_{ij} , β_{ii} and $\beta_{ij} = \beta_{ji}$, it is obvious that Λ_i are symmetric positive semidefinite (SPSD) for all $i = 1, 2, 3, 4$, and Λ_3 is symmetric positive definite (SPD). Hence, Λ and Λ^{-1} are SPD and can therefore be used to define norms.

The crucial idea is to equip the Hilbert spaces $\mathbf{U}, \mathbf{V}, \mathbf{P}$ with parameter-matrix-dependent norms $\|\cdot\|_{\mathbf{U}}, \|\cdot\|_{\mathbf{V}}, \|\cdot\|_{\mathbf{P}}$ induced by the following *inner products*:

(3a) $(\mathbf{u}, \mathbf{w})_{\mathbf{U}} = (\epsilon(\mathbf{u}), \epsilon(\mathbf{w})) + \lambda(\operatorname{div} \mathbf{u}, \operatorname{div} \mathbf{w}),$

(3b) $(\mathbf{v}, \mathbf{z})_{\mathbf{V}} = \sum_{i=1}^n (R_i^{-1} \mathbf{v}_i, \mathbf{z}_i) + (\Lambda^{-1} \operatorname{Div} \mathbf{v}, \operatorname{Div} \mathbf{z}),$

(3c) $(\mathbf{p}, \mathbf{q})_{\mathbf{P}} = (\Lambda \mathbf{p}, \mathbf{q}),$

where $\mathbf{p}^T = (p_1, \dots, p_n)$, $\mathbf{v}^T = (v_1^T, \dots, v_n^T)$, $(\operatorname{Div} \mathbf{v})^T = (\operatorname{div} \mathbf{v}_1, \dots, \operatorname{div} \mathbf{v}_n)$.

Then the bilinearform $\mathcal{A}((\cdot; \cdot; \cdot), (\cdot; \cdot; \cdot))$ related to the weak formulation of (1) is bounded with respect to the norms induced by (3), see [7].

Moreover, if for the spaces $\mathbf{U}, \mathbf{V}, \mathbf{P}$ there hold the inf-sup conditions

(4) $\inf_{q \in P_i} \sup_{\mathbf{v} \in \mathbf{V}_i} \frac{(\operatorname{div} \mathbf{v}, q)}{\|\mathbf{v}\|_{\operatorname{div}} \|q\|} \geq \beta_d, \quad i = 1, \dots, n,$

(5) $\inf_{(q_1, \dots, q_n) \in P_1 \times \dots \times P_n} \sup_{\mathbf{u} \in \mathbf{U}} \frac{(\operatorname{div} \mathbf{u}, \sum_{i=1}^n q_i)}{\|\mathbf{u}\|_1 \|\sum_{i=1}^n q_i\|} \geq \beta_s$

for some constants $\beta_d > 0$ and $\beta_s > 0$ then the considered MPET model is uniformly stable, see [7]. This means that there exists a constant $\omega > 0$ independent of the parameters $\lambda, R_i^{-1}, \alpha_{p_i}, \alpha_{ij}$ for all $i, j = 1, \dots, n$ and independent of the number of networks n , such that for $\mathbf{W} := \mathbf{U} \times \mathbf{V} \times \mathbf{P}$ we have

$$\inf_{(\mathbf{u}; \mathbf{v}; \mathbf{p}) \in \mathbf{W}} \sup_{(\mathbf{w}; \mathbf{z}; \mathbf{q}) \in \mathbf{W}} \frac{\mathcal{A}((\mathbf{u}; \mathbf{v}; \mathbf{p}), (\mathbf{w}; \mathbf{z}; \mathbf{q}))}{(\|\mathbf{u}\|_{\mathbf{U}} + \|\mathbf{v}\|_{\mathbf{V}} + \|\mathbf{p}\|_{\mathbf{P}})(\|\mathbf{w}\|_{\mathbf{U}} + \|\mathbf{z}\|_{\mathbf{V}} + \|\mathbf{q}\|_{\mathbf{P}})} \geq \omega.$$

The above stability result has first been proven in [5] for Biot's model of consolidation and generalized in [7] for the multi-permeability flux-based poroelasticity model. It induces (norm-equivalent) block-diagonal operator preconditioners that can be transferred to the discrete level subject to the existence of discrete inf-sup conditions analogous to (4) and (5), which can be verified for several well-known combinations of finite element spaces. In [7] a family of strongly mass-conservative discretizations has been analyzed in this context using an $H(\text{div})$ -conforming SIPG method to discretize the elastic subproblem. The authors establish discrete inf-sup stability for the multi-permeability flux-based poroelasticity model and prove optimal error estimates. A comparison with the mixed formulation introducing a total pressure unknown, as proposed in [6], is subject of ongoing research.

REFERENCES

- [1] M. Bai, D. Elsworth, J.-C. Roegiers, *Multiporosity/multipermeability approach to the simulation of naturally fractured reservoirs*, Water Resources Research **29(6)** (1993), 1621–1633.
- [2] G.I. Barenblatt, I.P. Zheltov, I.N. Kochina, *Basic concepts in the theory of seepage of homogeneous liquids in fissured rocks [strata]*, Journal of Applied Mathematics and Mechanics **24(5)** (1960), 1286–1303.
- [3] M.A. Biot, *General theory of three-dimensional consolidation*, J. Appl. Phys. **12(2)** (1941), 155–164.
- [4] M.A. Biot, *Theory of elasticity and consolidation for a porous anisotropic solid*, J. Appl. Phys. **26(2)** (1955), 182–185.
- [5] Q. Hong, J. Kraus, *Parameter-robust stability of classical three-field formulation of Biot's consolidation model*, Electronic Transactions on Numerical Analysis **48** (2018), 202–226.
- [6] J.J. Lee, E. Piersanti, K.-A. Mardal, M.E. Rognes, *A mixed finite element method for nearly incompressible multiple-network poroelasticity*, Preprint arXiv:1804.07568, April 20, 2018.
- [7] Q. Hong, J. Kraus, M. Lymbery, F. Philo, *Conservative discretizations and parameter-robust preconditioners for Biot and multiple-network flux-based poroelastic models*, Preprint arXiv:1806.00353, June 9, 2018.
- [8] B. Tully, Y. Ventikos, *Cerebral water transport using multiple-network poroelastic theory: application to normal pressure hydrocephalus*, Journal of Fluid Mechanics **667**, Cambridge University Press (2011), 188–215.

Biot-Stokes modeling of fluid-poroelastic structure interaction

IVAN YOTOV

Fluid-poroelastic structure interaction refers to the coupling of a free incompressible viscous fluid with a fluid within a poroelastic medium. Applications include groundwater flow in fractured aquifers, subsidence and compaction in oil and gas extraction, arterial flows, and industrial filters. In these applications, it is important to model properly the interaction between the free fluid with the fluid within the porous medium, and to take into account the effect of the deformation of the medium. The mathematical models are systems of PDEs that couple through physically meaningful interface conditions free fluid models such as Stokes or Navier-Stokes equations with Darcy flow. In regions involving deformable porous media the Darcy flow is coupled with elasticity and modeled by the Biot system of poroelasticity. Let $\Omega \subset \mathbf{R}^d$, $d = 2, 3$, be a union of non-overlapping regions Ω_f and Ω_p .

Here Ω_f is a free fluid region with flow governed by the Stokes equations and Ω_p is a poroelastic material governed by the Biot system. Let $\Gamma_{fp} = \partial\Omega_f \cap \partial\Omega_p$. Let $(\mathbf{u}_\star, p_\star)$ be the velocity-pressure pair in Ω_\star , $\star = f, p$, and let $\boldsymbol{\eta}_p$ be the displacement in Ω_p . Let $\mu > 0$ be the fluid viscosity, let \mathbf{f}_\star be the body force terms, and let q_\star be external source or sink terms. Let $\mathbf{D}(\mathbf{u}_f)$ and $\boldsymbol{\sigma}_f(\mathbf{u}_f, p_f)$ denote, respectively, the deformation rate tensor and the stress tensor:

$$(1) \quad \mathbf{D}(\mathbf{u}_f) = \frac{1}{2}(\nabla\mathbf{u}_f + \nabla\mathbf{u}_f^T), \quad \boldsymbol{\sigma}_f(\mathbf{u}_f, p_f) = -p_f\mathbf{I} + 2\mu\mathbf{D}(\mathbf{u}_f).$$

In the free fluid region Ω_f , (\mathbf{u}_f, p_f) satisfy the Stokes equations

$$(2) \quad -\nabla \cdot \boldsymbol{\sigma}_f(\mathbf{u}_f, p_f) = \mathbf{f}_f \quad \text{in } \Omega_f \times (0, T]$$

$$(3) \quad \nabla \cdot \mathbf{u}_f = q_f \quad \text{in } \Omega_f \times (0, T],$$

where $T > 0$ is the final time. Let $\boldsymbol{\sigma}_e(\boldsymbol{\eta}_p)$ and $\boldsymbol{\sigma}_p(\boldsymbol{\eta}_p, p_p)$ be the elastic and poroelastic stress tensors, respectively:

$$\boldsymbol{\sigma}_e(\boldsymbol{\eta}_p) = \lambda_p(\nabla \cdot \boldsymbol{\eta}_p)\mathbf{I} + 2\mu_p\mathbf{D}(\boldsymbol{\eta}_p), \quad \boldsymbol{\sigma}_p(\boldsymbol{\eta}_p, p_p) = \boldsymbol{\sigma}_e(\boldsymbol{\eta}_p) - \alpha p_p\mathbf{I},$$

where $0 < \lambda_{min} \leq \lambda_p(\mathbf{x}) \leq \lambda_{max}$ and $0 < \mu_{min} \leq \mu_p(\mathbf{x}) \leq \mu_{max}$ are the Lamé parameters and $0 \leq \alpha \leq 1$ is the Biot-Willis constant. The poroelasticity region Ω_p is governed by the quasi-static Biot system

$$\begin{aligned} -\nabla \cdot \boldsymbol{\sigma}_p(\boldsymbol{\eta}_p, p_p) &= \mathbf{f}_p, \quad \mu K^{-1}\mathbf{u}_p + \nabla p_p = 0, & \text{in } \Omega_p \times (0, T], \\ \frac{\partial}{\partial t}(s_0 p_p + \alpha \nabla \cdot \boldsymbol{\eta}_p) + \nabla \cdot \mathbf{u}_p &= q_p & \text{in } \Omega_p \times (0, T], \end{aligned}$$

where $s_0 \geq 0$ is a storage coefficient and K the symmetric and uniformly positive definite rock permeability tensor.

Previous work has involved developing and analysis of variational formulations, robust, stable, and accurate discretization techniques, and efficient coupling and time-splitting algorithms.

A non-iterative time-partitioned scheme with applications to blood flow is developed in [7]. The arterial wall is modeled with a thin permeable elastic lamina and a poroelastic structure, leading to a coupled Navier-Stokes and Biot system with an elastic interface. This work includes the development of a mathematical model with physically justifiable interface conditions, deriving an energy estimate of the fully coupled weak formulation, and analyzing the stability and approximation error of an efficient time-partitioned scheme. The effect of poroelasticity is studied in [5].

A Nitsche's coupling approach for coupled fluid flow with poroelastic media based on the Stokes-Biot problem is developed in [6], which allows for non-matching grids and time-partitioning for the mixed Darcy formulation. The continuity of normal flux condition, which is essential for the mixed Darcy problem, is imposed weakly using a penalty term. In addition to a complete stability and error analysis of the time-partitioned scheme, it is shown that it provides an optimal preconditioner for the monolithic scheme.

An alternative formulation using a Lagrange multiplier to impose weakly the normal flux interface condition is developed in [4, 3]. The advantage of this approach is improved accuracy of the interface coupling, ability to handle non-matching grids through mortar finite elements, and the suitability of the formulation for multiprocessor parallel implementation via non-overlapping domain decomposition. The well-posedness of the semidiscrete formulation is established using tools from differential algebraic equations. Stability and finite element error analysis is also performed.

In [8] we develop a reduced model for the Stokes-Biot system for flow in fractured media using a lower dimensional model in the fracture by averaging the Stokes equation in the transverse direction and deriving appropriate interface conditions between the fracture and the reservoir. This approach has improved efficiency and similar accuracy when compared to the full-dimensional model. We analyze the stability and temporal and spatial accuracy of the discrete formulation.

In [2] we study flow and transport in fractured poroelastic media using Stokes flow in the fractures and the Biot model in the porous media. The Stokes-Biot model is coupled with an advection-diffusion equation for modeling transport of chemical species within the fluid. The stability and convergence of the coupled finite element scheme are analyzed.

In [1] we propose and analyze a nonlinear model for fluid-poroelastic structure interaction with quasi-Newtonian fluids that exhibit a shear-thinning property. We establish existence and uniqueness of the solution for two alternative formulations of the proposed model. The analysis is performed in non-Hilbert spaces.

REFERENCES

- [1] I. Ambartsumyan, V. J. Ervin, T. Nguyen, and I. Yotov. A nonlinear Stokes-Biot model for the interaction of a non-Newtonian fluid with poroelastic media I: well-posedness of the model. arXiv:1803.00947, 2018.
- [2] I. Ambartsumyan, E. Khattatov, T. Nguyen, and I. Yotov. Flow and transport in fractured poroelastic media. Submitted to International Journal on Geomathematics.
- [3] I. Ambartsumyan, E. Khattatov, I. Yotov, and P. Zunino. Simulation of flow in fractured poroelastic media: a comparison of different discretization approaches. In *Finite difference methods, theory and applications*, volume 9045 of *Lecture Notes in Comput. Sci.*, pages 3–14. Springer, Cham, 2015.
- [4] I. Ambartsumyan, E. Khattatov, I. Yotov, and P. Zunino. A Lagrange multiplier method for a Stokes-Biot fluid-poroelastic structure interaction model. *Numer. Math.*, 140(2):513–553, 2018.
- [5] M. Bukac, I. Yotov, R. Zakerzadeh, and P. Zunino. Effects of poroelasticity on fluid-structure interaction in arteries: a computational sensitivity study. volume 14 of *MS&A. Model. Simul. Appl.*, pages 197–220. 2015.
- [6] M. Bukac, I. Yotov, R. Zakerzadeh, and P. Zunino. Partitioning strategies for the interaction of a fluid with a poroelastic material based on a Nitsche’s coupling approach. *Comput. Methods Appl. Mech. Engrg.*, 292:138–170, 2015.

- [7] M. Bukac, I. Yotov, and P. Zunino. An operator splitting approach for the interaction between a fluid and a multilayered poroelastic structure. *Numer. Methods Partial Differential Equations*, 31(4):1054–1100, 2015.
- [8] M. Bukac, I. Yotov, and P. Zunino. Dimensional model reduction for flow through fractures in poroelastic media. *ESAIM Math. Model. Numer. Anal.*, 51(4):1429–1471, 2017.

Computational models for the interaction of fractures and wells with poroelastic media

PAOLO ZUNINO

The simulation of multiscale, multiphysics, multimodel systems is among the grand challenges in Computational Science & Engineering. In this context, the application of topological (or geometrical) model reduction techniques plays an essential role. For example, small inclusions of a continuum can be described as zero-dimensional (0D) or one-dimensional (1D) concentrated sources in order to reduce the computational cost of simulations. However, concentrated sources lead to singular solutions that still require computationally expensive graded meshes to guarantee accurate approximation. Many problems in this area are not well investigated yet, such as the coupling of three-dimensional (3D) continua with embedded (1D) networks, although it arises in applications of paramount importance such as microcirculation, flow through perforated media and the study of reinforced materials. We will shed light on these unexplored mathematical problems by casting them in a new unified framework to formulate and approximate coupled partial differential equations (PDEs) on manifolds with heterogeneous dimensionality arising from topological model reduction. The main computational barrier consists in the ill-posedness of restriction operators (such as the trace operator) applied on manifolds with co-dimension larger than one.

Our ultimate objective is to exploit topological model reduction to perform large scale simulations of biomechanics of tumor micro-environment and geomechanics of fractured reservoirs. In this way, we will help the constantly growing effort to create a cyber-infrastructure among quantitative sciences and medicine. Similar considerations apply to geomechanics, where we will enable to combine state of art fracture propagation models with large scale reservoir simulation, for a better exploitation of the geological resources and safer control of the environmental impact.

We will overcome the computational challenges of approximating PDEs on manifolds with high dimensionality gap by means of nonlocal restriction operators that combine standard traces with mean values of the solution on low dimensional manifolds. This approach was originally proposed in [3, 4]. It has recently attracted the attention of several researchers from the perspective of theory and applications. On one hand, it requires particular attention to prove existence of a solution in the weak (or variational) sense [6, 5, 7, 10]. On the other hand, it is relevant for applications to microcirculation [1, 2, 8, 9]. This new approach has the fundamental advantage to enable the approximation of the problem using Galerkin projections on Hilbert spaces, which can not be otherwise applied because of regularity issues. The corresponding error analysis will naturally inform about the

concurrent modeling and discretization errors in the approximation of the original fully dimensional problem. In the case of problems with many inclusions organized in complex geometrical structures (such as networks), we will avoid excessively refined computational meshes exploiting finite element approximations enriched with specific non polynomial basis functions (XFEM) that depend on the proposed model reduction strategy and on the dimensionality of the problem. We call this new computational approach the *geometric embedded multiscale method* (GEMME).

REFERENCES

- [1] Cattaneo, L., Zunino, P.: A computational model of drug delivery through microcirculation to compare different tumor treatments. *International Journal for Numerical Methods in Biomedical Engineering* **30**(11), 1347–1371 (2014).
- [2] Cattaneo, L., Zunino, P.: Computational models for fluid exchange between microcirculation and tissue interstitium. *Networks and Heterogeneous Media* **9**(1), 135–159 (2014).
- [3] C. D’Angelo, *Finite element approximation of elliptic problems with Dirac measure terms in weighted spaces: Applications to one- and three-dimensional coupled problems*, SIAM Journal on Numerical Analysis, 50 (2012), pp. 194–215.
- [4] C. D’Angelo and A. Quarteroni, *On the coupling of 1d and 3d diffusion-reaction equations. application to tissue perfusion problems*, *Mathematical Models and Methods in Applied Sciences*, 18 (2008), pp. 1481–1504.
- [5] Koepl, T., Vidotto, E., Wohlmuth, B., Zunino, P.: Mathematical modelling, analysis and numerical approximation of second order elliptic problems with inclusions. *Mathematical Models and Methods in Applied Sciences* **28**(05) (2018)
- [6] Köppl, T., Wohlmuth, B.: Optimal a priori error estimates for an elliptic problem with dirac right-hand side. *SIAM Journal on Numerical Analysis* **52**(4), 1753–1769 (2014)
- [7] Kuchta, M., Nordaas, M., Verschaeve, J., Mortensen, M., Mardal, K.A.: Preconditioners for saddle point systems with trace constraints coupling 2d and 1d domains. *SIAM Journal on Scientific Computing* **38**(6), B962–B987 (2016).
- [8] Nabil, M., Decuzzi, P., Zunino, P.: Modelling mass and heat transfer in nano-based cancer hyperthermia. *Royal Society Open Science* **2**(10) (2015).
- [9] Nabil, M., Zunino, P.: A computational study of cancer hyperthermia based on vascular magnetic nanoconstructs. *Royal Society Open Science* **3**(9) (2016).
- [10] Notaro, D., Cattaneo, L., Formaggia, L., Scotti, A., Zunino, P.: A Mixed Finite Element Method for Modeling the Fluid Exchange Between Microcirculation and Tissue Interstitium, pp. 3–25. Springer International Publishing (2016).

Fully-implicit solvers for coupled poromechanics of fractured reservoirs

NICOLA CASTELLETTO

(joint work with Massimiliano Ferronato, Andrea Franceschini, Randolph R. Settgast, Joshua A. White)

Accurate modeling of poromechanical effects in subsurface formations can play a significant role in making predictions, quantifying uncertainty, and assessing risk in many systems, such unconventional oil and gas reservoirs, hydraulic fracturing operations, and geologic carbon storage. The coupled behavior of this multiphysics

problem is notoriously difficult to model, primarily due to large time- and length-scale disparities, nonlinearities introduced as a result of the coupling between mechanics and flow, and nonlinear constitutive relationships.

From a mathematical standpoint, isothermal multiphase flow in a deforming reservoir is governed by a set of coupled partial differential equations (PDEs) enforcing mass and linear momentum conservation, possibly subject to appropriate constraint equations that govern the contact behavior whenever faults and/or fractures are present. Generally speaking, the discretization and linearization of coupled poromechanics PDEs produce sequences of challenging Jacobian linear systems, irrespective of the numerically discretization used. The simplest approach to seek the solution would consist of splitting the global multiphysics problem into single-physics sub-problems that are addressed exploiting one-way or staggered in-time coupling strategies. Although appealing, it is typically hard to determine *a priori* when such decoupling assumptions produce an accurate approximation. Therefore, a fundamental requirement to obtain reliable modeling predictions is the availability of tools allowing for robust two-way coupling. Two-way coupled algorithms can be grouped into two families, namely *sequential-implicit* (SI) and *fully-implicit* (FI) methods. Here, we focus on FI approaches, which can provide unconditionally stable schemes and good convergence properties.

The main objective of this work is to develop efficient preconditioning techniques for accelerating the fully-implicit solution by a Krylov solver of linear systems encountered in two relevant applications: (i) Lagrange multiplier-based fault mechanics simulations based on a mixed finite element approach, and (ii) multiphase poromechanics based on a mixed finite element-finite volume formulation. A unified preconditioning strategy is devised based on a block triangular factorization that exploits the inherent block structure of the Jacobian matrix, the focus being on the design of effective approximations for the Schur complement and its inverse. We propose novel Schur complement approximations that are designed using either physically-based or pure algebraic arguments. For the fault mechanics application we explored two strategies. The first option is based on a *Least Square Commutator* (LSC) strategy [2] and provides an explicit representation of the Schur complement inverse that can be applied via three matrix-by-vector products involving sparse and block-diagonal matrices. The second alternative makes use of a *Factorized Sparse Approximate Inverse* (FSAI) technique [3] that constructs an approximate Schur complement replacing the displacement stiffness matrix by an explicit sparse approximate inverse. As to multiphase poromechanics, the proposed approach builds upon the *Fixed-Stress* strategy [6, 4, 5, 7] to construct a reduced saturation-pressure Schur complement for which a two-stage *Constrained Pressure Residual* (CPR) preconditioning approach [8, 9, 1] is then used. Robustness and scalability of the proposed framework is investigated on numerical examples based on synthetic and realistic datasets.

Acknowledgement: Portions of this work were performed under the auspices of the U.S. Department of Energy by Lawrence Livermore National Laboratory under Contract DE-AC52-07NA27344.

REFERENCES

- [1] H. Cao, H. A. Tchelepi, J. R. Wallis, H. Yardumian, *Parallel scalable unstructured CPR-type linear solver for reservoir simulation*, Proceedings - SPE Annual Technical Conference and Exhibition, Society of Petroleum Engineers (2005), doi:10.2118/96809-MS.
- [2] H. Elman, V. E. Howle, J. Shadid, R. Shuttleworth, R. Tuminaro, R., *Block preconditioners based on approximate commutators*, SIAM J. Sci. Comput. **32**(5) (2006), 1651–1668.
- [3] C. Janna, M. Ferronato, F. Sartoretto, G. Gambolati, *FSAIPACK: A software package for high-performance factored sparse approximate inverse preconditioning*, ACM Trans. Math. Softw., **41**(2) (2015), Article No. 10.
- [4] J. Kim, H. A. Tchelepi, R. Juanes, R., *Stability, accuracy and efficiency of sequential methods for coupled flow and geomechanics*, SPE J., **16**(2) (2011), 249–262.
- [5] A. Mikelić, M. F. Wheeler, *Convergence of iterative coupling for coupled flow and geomechanics*, Comput. Geosci., **17**(3) (2013), 455–461.
- [6] A. Settari, F. M. Mourits, *A coupled reservoir and geomechanical simulation system*, SPE J., **3**(3) (1998), 219–226.
- [7] J. A. White, N. Castelletto, H. A. Tchelepi, *Block-partitioned solvers for coupled poromechanics: A unified framework*, Comput. Meth. Appl. Mech. Eng., **303** (2016), 55–74.
- [8] J. R. Wallis, *Incomplete Gaussian elimination as a preconditioning for generalized conjugate gradient acceleration*, Proceedings - 7th SPE Reservoir Simulation Symposium, Society of Petroleum Engineers (1983), doi:10.2118/12265-MS.
- [9] J. R. Wallis, R. P. Kendall, T. E. Little, *Constrained residual acceleration of conjugate residual methods*, Proceedings - 8th SPE Reservoir Simulation Symposium, Society of Petroleum Engineers (1985), doi:10.2118/13536-MS.

**Towards the fully dynamic system of poroelasticity: Efficient
variational space-time methods**

MARKUS BAUSE

(joint work with M. Anselmann, S. Becher, U. Köcher, G. Matthies, F. A. Radu,
F. Schieweck)

Information on flow in deformable porous media has become of increasing importance in various fields of natural sciences and technology. Consequently, quantitative methods, based on numerical simulations, are desirable in analyzing experimental data and designing theories based on mathematical concepts. Typically, the quasi-steady Biot system (cf. [7]) is used to model flow in deformable porous media. However, in the case of larger contrast coefficients that stand for the ratio between the intrinsic characteristic time and the characteristic domain time scale the full hyperbolic-parabolic Biot–Allard system with memory (cf. [5]) has to be considered. Such applications can be found in, for instance, noise protection, material science polymers for lightweight design and filter technology. In

dimensionless form the Biot–Allard system is given by

$$(1) \quad \kappa \partial_t^2 \mathbf{u} - \nabla \cdot (\mathbf{C} : \boldsymbol{\varepsilon}(\mathbf{u}) - \boldsymbol{\alpha} p) + \partial_t \int_0^t \mathcal{A}((t - \zeta)/\kappa_f) \\ \cdot (\psi_f \mathbf{F}(\mathbf{x}, \zeta) - \nabla p(\mathbf{x}, \zeta) - \kappa_f \partial_\zeta^2 \mathbf{u}(\mathbf{x}, \zeta)) \, d\zeta = \psi \mathbf{F},$$

$$(2) \quad M \partial_t p + \nabla \cdot (\boldsymbol{\alpha} \partial_t \mathbf{u}) + \nabla \cdot \int_0^t \mathcal{A}((t - \zeta)/\kappa_f) \\ \cdot \left(\frac{\psi_f}{\kappa_f} \mathbf{F}(\mathbf{x}, \zeta) - \frac{1}{\kappa_f} \nabla p(\mathbf{x}, \zeta) - \partial_\zeta^2 \mathbf{u}(\mathbf{x}, \zeta) \right) \, d\zeta = 0.$$

Here, the unknown \mathbf{u} is the effective solid phase displacement and the unknown p is the effective pressure. Moreover, $\boldsymbol{\varepsilon}(\cdot)$ denotes the symmetrized gradient or strain tensor and $\mathcal{A}(\cdot)$ the dynamic permeability (cf. [5]).

The numerical approximation of (1), (2) comprises several complexities:

- A.) A unified discretization technique in space and time for second-order hyperbolic and parabolic equations is required.
- B.) An efficient treatment of the convolution integrals within this discretization framework has to be developed.
- C.) A monolithic solver or an iterative splitting scheme with guaranteed stability properties needs to be provided for the fully-discrete system.

The first of these three requirements is particularly addressed here. We aim at approximating Eqs. (1), (2) by generalized space-time finite element methods that admit solutions of higher-order regularity in the time variable. They offer the potential that the convolution integrals involving second order time derivatives of the displacement variable can be approximated in a natural way. Here we introduce such schemes for the scalar-valued wave equation that can be studied as a prototype model for Eq. (1) if the convolution term is omitted. Variational space-time discretization schemes for parabolic problems and iterative coupling schemes for the quasi-static Biot system were recently investigated in, e.g., [2, 3, 6].

Prototype model (wave equation). Let $X := L^2(0, T; V) \times L^2(0, T; H)$, with $H = L^2(\Omega)$ and $V = H_0^1(\Omega)$. Further, let the right-hand side function $f \in L^2(0, T; H)$ and the initial values $u_0 \in V$ and $u_1 \in H$ be given. With $F = \{0, f\}$ and $U_0 = \{u_0, u_1\}$ we consider the scalar-valued wave problem rewritten as first-order in time evolution problem:

Find $u \in X$, with $U = \{u^0, u^1\}$, such that

$$(3) \quad \partial_t U + \mathcal{A}U = F \quad \text{for } t \in (0, T), \quad U(0) = U_0.$$

The operator $\mathcal{A} : V \times H \mapsto H \times V'$ is defined by $\mathcal{A} = \begin{pmatrix} 0 & -I \\ A & 0 \end{pmatrix}$ with the identity mapping $I : H \mapsto H$ and $A : V \mapsto V'$ is given by $\langle Au, v \rangle = \langle \nabla u, \nabla v \rangle$ for all $v \in V$.

Continuous Galerkin–Petrov approximation with C^1 -regular lifting. For a time mesh $\mathcal{M}_\tau := \{I_1, \dots, I_n\}$, with $I_n = (t_{n-1}, t_n]$ and $I = I_1 \cup \dots \cup I_n$, let

$$\mathbb{P}_k(I_n; V_h) := \left\{ w_\tau : I_n \mapsto V_h \mid w_\tau(t) = \sum_{j=0}^k W^j t^j, W^j \in V_h \right\},$$

with a conforming finite element space $V_h \subset V$, for brevity. Choosing a discontinuous discrete test basis with basis functions supported on a single subinterval I_n , our space-time discretization of Eq. (3) reads as follows (cf. [1] for details):

For $n = 1, \dots, N$ find $U_{\tau,h} \in (\mathbb{P}_k(I_n; V_h))^2$, with $U_{\tau,h}(t_{n-1}) = U_{\tau,h|_{I_{n-1}}}(t_{n-1})$ for $n > 1$ and $U_{\tau,h}(t_0) = U_{0,h}$, such that

$$(4) \quad \tilde{B}_h^n(U_{\tau,h}, V_{\tau,h}) = Q_n(\langle\langle F, V_{\tau,h} \rangle\rangle)$$

for all $V_{\tau,h} \in (\mathbb{P}_{k-1}(I_n; V_h))^2$ is satisfied.

In Eq. (4), the bilinear form $\tilde{B}_h^n(\cdot, \cdot)$ is defined by

$$\tilde{B}_h^n(W, V) := Q_n(\langle\langle \partial_t W, V \rangle\rangle) + Q_n(\langle\langle \mathcal{A}_h W, V \rangle\rangle),$$

with the inner product $\langle\langle \cdot, \cdot \rangle\rangle$ of $(L^2(\Omega))^2$ and the Gauß-Lobatto quadrature formula $Q_n(g) := \frac{\tau}{2} \sum_{\mu=0}^k \hat{\omega}_\mu g(t_{n,\mu}) \approx \int_{I_n} g(t) dt$.

To lift the approximation $U_{\tau,h} \in (X_{\tau,h}^k(V_h))^2$ of Eq. (4), where $X_{\tau,h}^k(V_h) := \{w_\tau \in C(\bar{I}; V_h) \mid w_\tau|_{I_n} \in \mathbb{P}_k(I_n; V_h)\}$, to a function that is C^1 -regular in time, we introduce an operator L_τ that is defined recursively by

$$L_\tau : X_\tau^k(B) \mapsto X_\tau^{k+1}(B) \cap C^1(\bar{I}, B), \quad L_\tau w_\tau(t) = w_\tau(t) - c_{n-1}(w_\tau) \vartheta_n(t),$$

$$c_{n-1}(w_\tau) := \begin{cases} \partial_t w_\tau|_{I_n}(t_{n-1}) - \partial_t L_\tau w_\tau(0), & \text{for } n = 1, \\ \partial_t w_\tau|_{I_n}(t_{n-1}) - \partial_t L_\tau w_\tau|_{I_{n-1}}(t_{n-1}), & \text{for } n > 1, \end{cases}$$

and with $\vartheta_n \in \mathbb{P}_{k+1}(I_n; \mathbb{R})$ such that $\vartheta_n(t_{n,\mu}) = 0$ for the Gauss-Lobatto quadrature points $t_{n,\mu}$, for $\mu = 0, \dots, k$ on I_n and $d_t \vartheta_n(t_{n-1}) = 1$.

In [1], for $k \geq 2$ and the discrete initial value $U_{0,h} := \{R_h u_0, R_h u_1\}$, with the Ritz projection $R_h : V \mapsto V_h$, the following estimates of optimal order are proved for the error $\tilde{E}(t) = \{\tilde{e}^0(t), \tilde{e}^1(t)\} = U(t) - L_\tau U_{\tau,h}(t)$ of the lifted approximation:

$$\|\tilde{e}^0(t)\| + \|\tilde{e}^1(t)\| \lesssim \tau^{k+2} + h^{r+1}, \quad \|\nabla \tilde{e}^0(t)\| \lesssim \tau^{k+2} + h^r, \quad t \in I,$$

$$\|\tilde{e}^0\|_{L^2(I;H)} + \|\tilde{e}^1\|_{L^2(I;H)} \lesssim \tau^{k+2} + h^{r+1}, \quad \|\nabla \tilde{e}^0\|_{L^2(I;H)} \lesssim \tau^{k+2} + h^r.$$

The first two estimates show superconvergence of the scheme (4) in the nodes t_n . Beyond the increased order of convergence in time, the computationally cheap lifting offers potential for a-posteriori error control and adaptive time stepping.

Generalized Galerkin–Petrov approximation with higher-order regularity in time. The previous framework can be exploited further to construct space-time finite element approximations of higher-order regularity in time. For this, we combine the concept of variational time discretization with the idea of collocation; cf. [4] for ode systems. This yields the following family of schemes:

Let $k \geq 3$. For $n = 1, \dots, N$ and given $U_{\tau,h|I_{n-1}}(t_{n-1})$ for $n > 1$ and $U_{\tau,h|I_1}(t_0) = U_{0,h}$ for $n = 1$, find $U_{\tau,h|I_n} \in (\mathbb{P}_k(I_n; V))^2$ such that

$$\begin{aligned} U_{\tau,h|I_n}(t_{n-1}) &= U_{\tau,h|I_{n-1}}(t_{n-1}), \\ \partial_t^s U_{\tau,h|I_n}(t_{n-1}) &= -\mathcal{A}_h \partial_t^{s-1} U_{\tau,h|I_n}(t_{n-1}) + \mathcal{P}_h \partial_t^{s-1} F(t_{n-1}), \\ \partial_t^p U_{\tau,h|I_n}(t_n) &= -\mathcal{A}_h \partial_t^{p-1} U_{\tau,h|I_n}(t_n) + \mathcal{P}_h \partial_t^{p-1} F(t_n), \end{aligned}$$

for $1 \leq s \leq \lfloor \frac{k-1}{2} \rfloor =: S$ and $1 \leq p \leq \lfloor \frac{k}{2} \rfloor$ and

$$\int_{I_n} (\langle \partial_t U_{\tau,h}, V_{\tau,h} \rangle + \langle \mathcal{A}_h U_{\tau,h}, V_{\tau,h} \rangle) dt = Q_n^H(\langle F, V_{\tau,h} \rangle)$$

for all $V_{\tau,h} \in (\mathbb{P}_0(I_n; V_h))^2$.

The discrete solution satisfies $U_{\tau,h} \in (C^S(\bar{T}; V_h))^2$. Our first numerical experiments yielded very promising results with respect to accuracy and efficiency for this family of generalized variational space-time approximation schemes. For a challenging test problem, its superiority over the C^0 -regular scheme of Eq. (4) is observed.

REFERENCES

- [1] M. Bause, U. Köcher, F. A. Radu, F. Schieweck, *Post-processed Galerkin approximation of improved order for wave equations*, Math. Comp., **submitted** (2018), pp. 1–34; arXiv:1803.03005
- [2] M. Bause, F. A. Radu, U. Köcher, *Space-time finite element approximation of the Biot poroelasticity system with iterative coupling*, Comput. Methods Appl. Mech. Engrg., **320** (2017), pp. 745–768.
- [3] M. Bause, F. A. Radu, U. Köcher, *Error analysis for discretizations of parabolic problems using continuous finite elements in time and mixed finite elements in space*, Numer. Math., **137** (2017), pp. 773–818.
- [4] S. Becher, G. Matthies, D. Wenzel, *Variational methods for stable time discretization of first-order differential equations*, Preprint TU Dresden (2017), pp. 1–13.
- [5] A. Mikelić, M. F. Wheeler, *Theory of the dynamic Biot–Allard equations and their link to the quasi-static Biot system*, J. Math. Phys., **53** (2012), pp. 123702:1–15.
- [6] A. Mikelić, M. F. Wheeler, *Convergence of iterative coupling for coupled flow and geomechanics*, Comput. Geosci., **17** (2013), 479–496.
- [7] R. Showalter, *Diffusion in poro-elastic media*, J. Math. Anal. Appl., **251** (2000), 310–340.

Pore Scale Simulation — Potential and Limitations

ULRICH RÜDE

(joint work with Dominik Bartuschat, Martin Bauer, Simon Bogner, Sebastian Eibl, Ehsan Fattahi, Christian Godenschwager, Harald Köstler, Christoph Rettinger, Florian Schornbaum, Christoph Schwarzmeier)

By definition exa-scale computers, as they will soon become available, will perform 10^{18} operations per second. Thus, if a porous medium consisted of 10^9 grains, we can perform a Gigaflop, i.e. 10^9 operations per particle and in each second. Furthermore, if the pore space were to be resolved by 10^3 cells for each of the 10^9 particles, then the flow domain were resolved by 10^{12} cells. Even

then an exascale system would deliver a MegaFlop—that is the a performance of a high end PC in 1990—for each of these cells. This simple argument shows that technological progress in computer technology may open the door to new approaches end will enable simulations of quite large systems on the particle or pore scale.

This, however, requires novel mathematical models, fundamentally new methods, and ultra scalable algorithms that can be implemented for modern super-computer architectures. This is necessary since computer technology will in the foreseeable future not be able to produce processing units operating at much more than one GHz, i.e. each stream of operands will produce results at a rate of approximately 10^9 per second. Exascale can thus only be reached when at any time 10^9 such operand streams are executed concurrently.

The dominating constraint is that the algorithms must be massively parallel. Therefore models and modeling approaches must be carefully chosen to permit a scalable implementation. Additionally, we must expect that the models must have significant size for being suitable for exascale systems. E.g. we may expect that a finite element or finite volume model will only be able to exploit a degree of concurrency of 10^9 when it has significantly more than 10^9 degrees of freedom.

As an alternative and as a complement to macroscopic and homogenized models for porous media processes, we present here parallel algorithms for coupling multi-body systems with hydrodynamics as a way to model multiphase flows in 3D that have a fluid carrier phase and a suspended solid phase. Specifically, we study a fully resolved approach where each particle is represented as an individual geometric entity. Moving particles are represented with a Lagrangian approach and are treated as rigid objects that can interact through frictional collisions. The fluid is simulated by the Lattice Boltzmann method (LBM) and interacts with the particulate phase via fluid-structure interaction techniques. The simulations rely critically on parallel algorithms and their efficient implementation.

For the massively parallel granular dynamics simulations on distributed memory architectures [25, 21] a domain partitioning approach is proposed [34]. Special algorithms for massively parallel granular dynamics simulations [2, 20] with fully resolved rigid particles on distributed memory architectures are developed, where collisions are geometrically detected [8, 12] and the physical response is modelled with hard contacts [24, 27] using the paradigm of measure differential inclusions.

The global frictional multi-contact problem leads to a complementarity problem [2] that is solved using a parallel non-linear block Gauss-Seidel method. Excellent strong and weak scaling has been demonstrated [26]. The robustness and scalability is assessed on peta-scale supercomputers with up to 458 752 processor cores. Such granular media simulations can reach an unprecedented resolution of up to ten billion (10^{10}) non-spherical particles and contacts [26]. This approach has shown promising results when used to set up virtual porous media [32] and can thus be used as a basis for porous media flow simulations, such as in [10, 11].

For modeling the fluid phase, the LBM is employed [7, 23, 13, 1]. Many implementations of the LBM [18, 19, 16] are specifically designed for parallel computers. A carefully crafted architecture-aware implementation is realized in the WALBERLA framework [14] that achieves excellent absolute performance so that complex flow computations with more than a trillion (10^{12}) lattice cells can be performed [17]. These methods can be extended with adaptive mesh refinement techniques (AMR). [30, 31] demonstrate the scalability to the range beyond a million parallel processes for AMR methods including load balancing.

Coupled simulations with particles embedded in the fluid add additional complexity. Here it is essential that the coupling mechanism is designed so that both the Lagrangian particle simulation and the Eulerian flow simulation can be parallelized together without excessive communication. The simulation model developed here and its implementation allows fluid simulations in 3D with millions of interacting particles [15] suspended in the flow. The fluid-structure-interaction relies on explicit time stepping [29, 28]. This simulation framework can model particles of arbitrary shape [4], includes the so-called lubrication correction [22, 9] and can be extended to include electrostatic effects [3, 5]. A thorough analysis demonstrates that these techniques achieve excellent computational performance [3, 28]. Future research will also address multiphase flows involving a particulate phase combined with a liquid and a gaseous phase [6].

This work illuminates the potential of pore scale resolved models on supercomputers. However, many aspects of the methods are still poorly understood and thus significant further research will be needed to better understand their properties and to develop them into reliable predictive tools.

REFERENCES

- [1] Aidun C, Clausen J (2010) Lattice-Boltzmann method for complex flows, *Annual Review of Fluid Mechanics*, 42, pp. 439–472.
- [2] Anitescu M, Potra F (1997) Formulating dynamic multi-rigid-body contact problems with friction as solvable linear complementarity problems. *Nonlinear Dynamics* 14(3), pp. 231–247.
- [3] Bartuschat, D and Rde U (2015) Parallel multiphysics simulations of charged particles in microfluidic flows, *Journal of Computational Science* 8, pp. 1–19.
- [4] Bartuschat D, Fischermeier, E., Gustavsson, K., Rde, U. (2016) Two Computational Models for Simulating the Tumbling Motion of Elongated Particles in Fluids. *Computers and Fluids*, 127, pp. 17–35.
- [5] Bartuschat, D., Rde, U. (2018). A scalable multiphysics algorithm for massively parallel direct numerical simulations of electrophoretic motion. *Journal of Computational Science*, 27, pp. 147–167.
- [6] Bogner, S., Harting, J., Rde, U. (2017). Direct simulation of liquid-gas-solid flow with a free surface lattice Boltzmann method. *International Journal of Computational Fluid Dynamics*, 31(10), pp. 463–475.
- [7] Shiyi Chen and Doolen, G (1998) Lattice Boltzmann method for fluid flows, *Annual Review of Fluid Mechanics* 30, pp. 329–364.

- [8] Cohen J, Lin M, Manocha D, Ponamgi M (1995) I-COLLIDE: An interactive and exact collision detection system for large-scale environments. In: Proceedings of the 1995 symposium on Interactive 3D graphics, ACM, pp. 189–ff.
- [9] E. J. Ding, C. K. Aidun (2003) Extension of the lattice-Boltzmann method for direct simulation of suspended particles near contact, *J. Stat. Phys.* 112 (3), pp. 685–708.
- [10] Fattahi, E., Waluga, C., Wohlmuth, B., Rude, U. (2015). Large scale lattice Boltzmann simulation for the coupling of free and porous media flow. In International Conference on High Performance Computing in Science and Engineering (pp. 1–18). Springer, Cham.
- [11] Fattahi, E., Waluga, C., Wohlmuth, B., Rude, U., Manhart, M., Helmig, R. (2016). Lattice Boltzmann methods in porous media simulations: From laminar to turbulent flow. *Computers and Fluids*, 140, 247–259.
- [12] Gilbert E, Johnson D, Keerthi S (1988) A fast procedure for computing the distance between complex objects in three-dimensional space. *IEEE Journal of Robotics and Automation* 4(2), pp. 193–203
- [13] I. Ginzburg, F. Verhaeghe, D. d’Humieres (2008) Study of simple hydrodynamic solutions with the two-relaxation-times lattice Boltzmann scheme, *Commun. Comput. Phys.* 3 (3), pp. 519–581.
- [14] Getz, J., Feichtinger, C., Iglberger, K., Donath, S., Rude, U. (2008). Large scale simulation of fluid structure interaction using Lattice Boltzmann methods and the physics engine. *ANZIAM Journal*, 50, pp. 166–188.
- [15] Getz J., Iglberger K., Feichtinger C., Donath S., Rude U (2010) Coupling multibody dynamics and computational fluid dynamics on 8192 processor cores, *Parallel Comput.* 36 (2) pp. 142–141.
- [16] Groen D, Hetherington J, Carver H, Nash R, Bernabeu M, Coveney P (2013) Analysing and modelling the performance of the HemeLB lattice-Boltzmann simulation environment, *Journal of Computational Science*, 4 pp. 412–422.
- [17] Godenschwager C, Schornbaum F, Bauer M, Kostler H, Rude U (2013), A framework for hybrid parallel flow simulations with a trillion cells in complex geometries, in: Proceedings of the International Conference on High Performance Computing, Networking, Storage and Analysis, SC ’13, IEEE, pp. 35:1–35:12.
- [18] Hasert M, Masilamani K, Zimny S, Klimach H, Qi J, Bernsdorf J, Roller S (2014) Complex fluid simulations with the parallel tree-based lattice boltzmann solver musubi, *Journal of Computational Science*, pp. 784 – 794.
- [19] Heuveline V, Latt J (2007) The OpenLB Project: An Open Source and Object Oriented Implementation of Lattice Boltzmann Methods, *International Journal of Modern Physics C*, 18, pp. 627–634.
- [20] Iglberger K, Rude U (2009) Massively parallel rigid body dynamics simulations. *Computer Science-Research and Development* 23(3-4), pp. 159–167
- [21] Koziara T, Biani N (2011) A distributed memory parallel multibody contact dynamics code. *International Journal for Numerical Methods in Engineering* 87(1–5), pp. 437–456
- [22] A. J. C. Ladd, R. Verberg (2001) Lattice-Boltzmann Simulations of Particle-Fluid Suspensions, *J. Stat. Phys.* 104 (5), pp. 1191–1251.
- [23] L.-S. Luo (1998) Unified Theory of Lattice Boltzmann Models for Nonideal Gases, *Phys. Rev. Lett.* 81 (8), pp. 1618–1621.
- [24] Moreau J, Panagiotopoulos P (1988) *Nonsmooth Mechanics and Applications*, vol 302. Springer.
- [25] Negrut D, Tasora A, Mazhar H, Heyn T, Hahn P (2012) Leveraging parallel computing in multibody dynamics. *Multibody System Dynamics* 27(1), pp. 95–117.
- [26] Preklik, T., Rude, U (2015) Ultrascale simulations of non-smooth granular dynamics. *Computational Particle Mechanics*, pp. 1–24.
- [27] Preklik, T., Eibl, S., Rude, U (2018) The maximum dissipation principle in rigid-body dynamics with inelastic impacts. *Computational Mechanics*, 62, pp. 81–96.

- [28] Rettinger, C., Godenschwager, C., Eibl, S., Preclik, T., Schruff, T., Frings, R., Rüde, U. (2017). Fully resolved simulations of dune formation in riverbeds. In *International Supercomputing Conference* (pp. 3–21). Springer, Cham.
- [29] Rettinger, C., Rüde, U. (2017). A comparative study of fluid-particle coupling methods for fully resolved lattice Boltzmann simulations. *Computers and Fluids*, 154, pp. 74–89.
- [30] Schornbaum, F., Rüde, U. (2016) Massively parallel algorithms for the lattice Boltzmann method on nonuniform grids. *SIAM Journal on Scientific Computing*, 38(2), pp. C96–C126.
- [31] Schornbaum, F., Rüde, U. (2018). Extreme-scale block-structured adaptive mesh refinement. *SIAM Journal on Scientific Computing*, 40(3), pp. C358–C387.
- [32] Schruff, T., Liang, R., Rüde, U., Schüttrumpf, H., Frings, R. M. (2018). Generation of dense granular deposits for porosity analysis: assessment and application of large-scale non-smooth granular dynamics. *Computational Particle Mechanics*, 5(1), 59-70.
- [33] Tasora A, Anitescu M (2011) A matrix-free cone complementarity approach for solving large-scale, nonsmooth, rigid body dynamics. *Computer Methods in Applied Mechanics and Engineering* 200(5), pp. 439–453.
- [34] Visseq V, Martin A, Dureisseix D, Dubois F, Alart P (2012) Distributed nonsmooth contact domain decomposition (NSCDD): Algorithmic structure and scalability. In: *Proceedings of the International Conference on Domain Decomposition Methods*.

Steps towards lattice Boltzmann methods for deformable media

EHSAN FATTAHI

(joint work with Ivan Pribec, Thomas Becker)

In the past three decades, the lattice Boltzmann method (LBM) has been developed into a powerful simulation tool for generalized hydrodynamics, covering diverse fields [1]. These capabilities make LBM an attractive option also for deformable systems arising in the life sciences such as biological tissues or food products and their intermediates (e.g., bread and pasta dough). In both of these applications mass (and heat) transfer is intricately coupled with fluid flow and mechanical deformation.

Existing approaches to simulate deformable media with LBM include diffuse-interface methods (in connection with a multiphase description), level-set methods, immersed boundary methods, and coordinate transformations. All of these methods build upon the rigid (Eulerian) lattice structure of LBM. For specific deformable systems, however, a Lagrangian perspective, where the computational nodes follow the material, might be preferred. This requires significant changes in the lattice Boltzmann method, either by modifying the lattice velocities and equilibria or, by switching to an off-lattice Boltzmann method (OLBM). For the latter case, we have developed a new meshfree lattice Boltzmann method.

Our first example comes from the pasta industry. If pasta is dried too fast, excessive internal moisture gradients will result in stresses and ultimately a failure in the form of cracks. The drying-induced stresses can be avoided by appropriate temperature and humidity control. This requires an understanding of the internal moisture movement. Mathematically, this process can be described by

$$(1) \quad \frac{\partial m}{\partial t} + \mathbf{u}_s \cdot \nabla m = \nabla \cdot (D(m) \nabla m),$$

where $m(\mathbf{x}, t)$ is the moisture concentration, $D(m(\mathbf{x}, t))$ is the moisture diffusivity that depends on the local moisture content, and $\mathbf{u}_s(\mathbf{x}, t)$ is the shrinkage velocity of the solid matrix. The drying air acts on the surface of the pasta and can be abstracted to a Robin boundary condition:

$$(2) \quad -D(m) \frac{\partial m}{\partial \mathbf{n}} = k(y(m) - y_\infty).$$

Here, \mathbf{n} is the normal vector at the boundary, k is the convective mass transfer coefficient, y_∞ is the specific humidity of the bulk air and $y = y(m)$ is a suitable moisture desorption isotherm. Equations similar to (1) and (2) can also be written for the transport of heat. Finally, a link is needed between the solids velocity \mathbf{u}_s and the changes in moisture content. In general, this missing link can be obtained from a momentum balance along with a model of the rheological behavior of pasta. In the one-dimensional case, the shrinkage velocity can be determined using some simplifying assumptions on the dough and moisture incompressibility.

To solve Eq. (1) we have used the deformable-lattice Boltzmann method developed in Ref. [2]. This method uses a non-equidistant spatial grid and changing lattice velocities in order to allow for shrinkage. Furthermore, the collision step is performed in moment space in order to subtract the convective term associated with shrinkage from the local moisture diffusion. Instead of a first-order finite difference at the boundary, we apply a quadratic polynomial (or cubic spline) extrapolation method [3].

The deformable-lattice Boltzmann method does not generalize directly to the multi-dimensional case of Eq. (1). A workaround is to preserve the static velocity lattice and use an off-lattice Boltzmann method where time and space are discretized separately instead. Since we would like to move the nodes dynamically, a flexible spatial discretization method is needed. Meshless methods, based upon scattered point interpolation techniques such as moving least squares or radial basis functions, can fulfill this requirement. As a first step towards a meshless lattice Boltzmann method, we have implemented an incompressible flow solver for a static domain. The solver is based upon Strang splitting of the discrete Boltzmann equation [3] combined with a Lax-Wendroff method for the simple convection equation. As a first test case we have solved the lid-driven cavity flow (see Fig. 2) using a weighted least squares approach and monomial basis functions. These allow us to use non-uniform point sets, non-integer velocity lattices.

Future work will focus on merging the deformable-lattice collision step with the meshless discretization for a multi-dimensional deformable-lattice Boltzmann method.

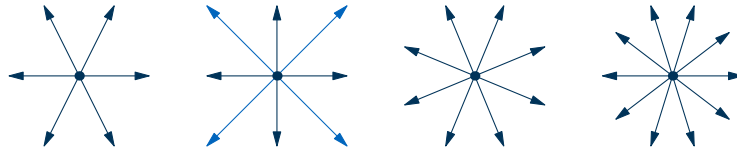


FIGURE 1. The D2Q7, D2Q9, D2S9, and D2Q11 velocity sets.

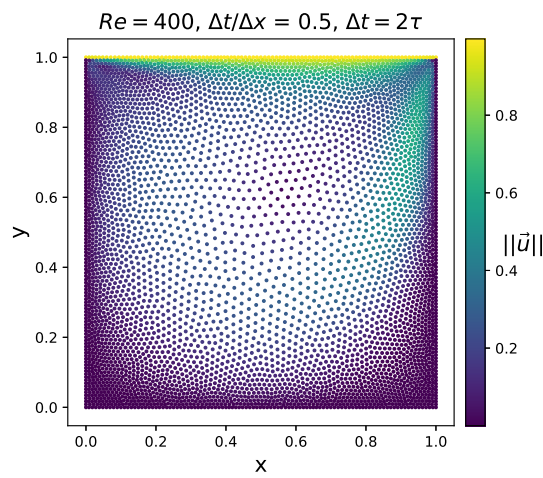


FIGURE 2. Lid-driven cavity flow with a non-uniform point set calculated by the meshless LBM algorithm.

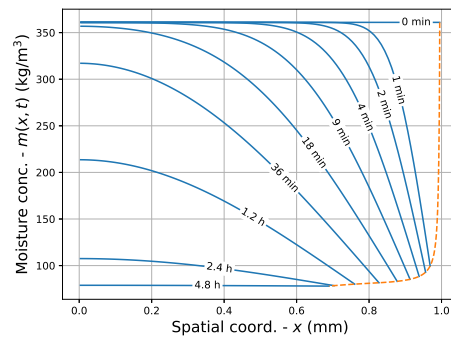


FIGURE 3. One-dimensional drying with a deforming-lattice Boltzmann method. The orange line indicates the shrinkage of the domain.

REFERENCES

- [1] E. Fattahi, C. Waluga, B. Wohlmuth, U. Rde, M. Manhart, R. Helmig, *Lattice Boltzmann methods in porous media simulations: From laminar to turbulent flow*, Computers and Fluids **140** (2016), 247–259.
- [2] R.G.M. Van der Sman, *Moisture transport in swelling media modelled with a lattice Boltzmann scheme having a deforming lattice*, Journal of Food Engineering **124** (2014), 54–63.
- [3] P.J. Dellar, *An interpretation and derivation of the lattice Boltzmann method using Strang splitting*, Computers & Mathematics with Applications **65** (2013), 129–141.
- [4] T. Lee, C.-L. Lin, *An Eulerian description of the streaming process in the lattice Boltzmann equation*, Journal of Computational Physics **185** (2003), 445–471.
- [5] B. Fornberg, N. Flyer, *A primer on radial basis functions with applications to the geosciences*. Society for Industrial and Applied Mathematics (2015).

Upscaling of a phase field formulation for reactive transport

CARINA BRINGEDAL

(joint work with Iuliu Sorin Pop)

Reactive flow with changing pore geometry includes a free boundary at the pore scale. Chemical reactions as mineral precipitation and dissolution can alter the pore structure, where the fluid-grain interface evolves according to a reaction rate. Problems with evolving interfaces are usually formulated through the location of the sharp interfaces, but we here propose a phase field formulation that allows formulating the relevant processes on a larger, stationary domain with the evolving interface appearing as a diffuse transition of non-zero width. In the limit as the diffuse interface width approaches zero, the usual sharp interface formulation is obtained. The pore scale phase field formulation is upscaled to the Darcy scale using homogenization. For the momentum equation, Darcy’s law is obtained where the permeability depends on the evolving phase field.

We consider a simple reactive transport problem, where a fluid of constant density ρ_f and viscosity μ flow through a domain, transporting a solute which can precipitate and become a mineral, and where the mineral also can dissolve. Extending the phase field models for mineral precipitation and dissolution found in [4, 6] to include fluid flow, we can formulate the phase field model

$$(1a) \quad \alpha \xi^2 \partial_t \phi + 6P'(\phi) = \frac{3}{4} \xi^2 \nabla^2 \phi - 4\alpha \xi \phi(1 - \phi)f(u),$$

$$(1b) \quad \partial_t(\phi(u - u^*)) + \nabla \cdot (\phi \mathbf{q} u) = D \nabla \cdot (\phi \nabla u),$$

$$(1c) \quad \nabla \cdot (\phi \mathbf{q}) = 0,$$

$$(1d) \quad \rho_f \partial_t(\phi \mathbf{q}) + \rho_f \nabla \cdot (\phi \mathbf{q} \otimes \mathbf{q}) = -\phi \nabla p + \mu \nabla^2(\phi \mathbf{q}) - (1 - \phi) \mathbf{q},$$

where \mathbf{q} is the fluid velocity, p fluid pressure, u solute concentration, D is ion diffusivity, and u^* is the mineral concentration. The reaction rate $f(u)$ depicts precipitation minus dissolution rate and can be as in [1, 5]. Further, ϕ is a phase field having the value 1 in the fluid and 0 in the mineral, with a smooth transition of width $O(\xi)$ between them. The double well potential $P(\phi) = \phi^2(1 - \phi)^2$ ensures that ϕ is attracted to these two values. The constant α is connected to the strength

of the surface tension [4]. Note that the phase field model is formulated for both fluid and mineral, and is hence on a stationary domain. Using matched asymptotic expansions with suitable matching conditions, as outlined in [3], and following similar steps as in [4], one can show that the phase field formulation (1) reduces to the expected sharp interface model (similar as those found in e.g. [1, 5, 6]) when ξ approaches zero.

We formulate the phase field model equations (1) on a domain Ω^ε with small, periodically distributed perforations, mimicking a porous medium, as sketched in Figure . The perforations are non-reactive grains which the phase field equations are not defined on. Hence, the perforations do not change with time.

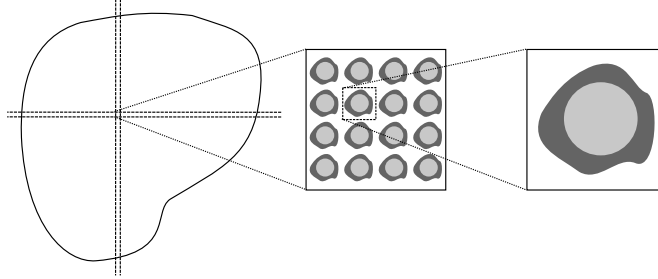


FIGURE 1. Structure of porous medium.

We identify the scale separator as $\varepsilon = l/L$, where l is a typical length scale at the pore (e.g., the width of the right-most box in Figure) and L is a typical length scale at the larger domain scale (e.g., the width of the domain seen to the left in Figure). We reformulate the phase field model slightly to incorporate dependence on ε . Since the volume of a grain is proportional to ε^d , d being the spatial dimension, so is the volume of the surrounding phases. Hence, the width ξ should be proportional to ε . The relaxation parameter α is scaled so that $\alpha\xi^2$ remains constant. To ensure we are in the viscosity dominated regime where Darcy law is valid, ρ_f and μ is scaled using $\rho_f = \varepsilon^2\rho_{f0}$ and $\mu_f = \varepsilon^2\mu_{f0}$. Hence,

$$(2a) \quad \alpha_1 \partial_t \phi^\varepsilon + 6P'(\phi^\varepsilon) = \alpha_2 \varepsilon^2 \nabla^2 \phi^\varepsilon - \alpha_3 \phi^\varepsilon (1 - \phi^\varepsilon) f(u^\varepsilon) \quad \text{in } \Omega^\varepsilon,$$

$$(2b) \quad \partial_t (\phi^\varepsilon (u^\varepsilon - u^*)) + \nabla \cdot (\phi^\varepsilon \mathbf{q}^\varepsilon u^\varepsilon) = D \nabla (\phi^\varepsilon \nabla u^\varepsilon) \quad \text{in } \Omega^\varepsilon,$$

$$(2c) \quad \nabla \cdot (\phi^\varepsilon \mathbf{q}^\varepsilon) = 0 \quad \text{in } \Omega^\varepsilon,$$

$$(2d) \quad \rho_{f0} \varepsilon^2 (\partial_t (\phi^\varepsilon \mathbf{q}^\varepsilon) + \nabla \cdot (\phi^\varepsilon \mathbf{q}^\varepsilon \otimes \mathbf{q}^\varepsilon)) = -\phi^\varepsilon \nabla p^\varepsilon + \mu_{f0} \varepsilon^2 \nabla^2 (\phi^\varepsilon \mathbf{q}^\varepsilon) - (1 - \phi^\varepsilon) \mathbf{q}^\varepsilon \quad \text{in } \Omega^\varepsilon,$$

$$(2e) \quad \nabla \phi^\varepsilon \cdot \mathbf{n}^\varepsilon = 0 \quad \text{on } \Gamma^\varepsilon,$$

$$(2f) \quad \phi^\varepsilon \nabla u^\varepsilon \cdot \mathbf{n}^\varepsilon = 0 \quad \text{on } \Gamma^\varepsilon,$$

$$(2g) \quad \mathbf{q}^\varepsilon = \mathbf{0} \quad \text{on } \Gamma^\varepsilon.$$

In the phase field equation, $\alpha_1 = \alpha_0 \xi_0^2$, $\alpha_2 = 3\xi_0^2/4$, $\alpha_3 = 4\alpha_0 \xi_0$. We have used superscript ε in the unknowns to indicate dependence on the highly oscillatory behavior. Further, Γ^ε is the union of all the internal boundaries for the perforations.

We apply the homogenization ansatz, namely that the unknowns can be written as a series expansion in terms of ε with explicit dependence on the microscopic variable;

$$\phi^\varepsilon(t, \mathbf{x}) = \phi_0(t, \mathbf{x}, \mathbf{y}) + \varepsilon\phi_1(t, \mathbf{x}, \mathbf{y}) + \varepsilon^2\phi_2(t, \mathbf{x}, \mathbf{y}) + \dots,$$

where a local variable \mathbf{y} is introduced to describe the highly oscillatory dependence, and where \mathbf{x} will see the effective behavior. Hence, \mathbf{y} is only defined for single pores P , as seen in the right-most part in Figure . Following steps similar as in [2, 5], an upscaled, effective model for (2) is obtained: For macroscopic \mathbf{x} ,

$$\begin{aligned} \partial_t(\overline{\phi_0}(u_0 - u^*)) + \nabla_{\mathbf{x}} \cdot (\overline{\phi_0 \mathbf{q}_0} u_0) &= D \nabla_{\mathbf{x}} (\mathcal{A} \nabla_{\mathbf{x}} u_0) && \text{in } \Omega, \\ \nabla_{\mathbf{x}} \cdot (\overline{\phi_0 \mathbf{q}_0}) &= 0 && \text{in } \Omega, \\ \overline{\phi_0 \mathbf{q}_0} &= -\mathcal{K} \nabla_{\mathbf{x}} p_0 && \text{in } \Omega, \end{aligned}$$

where the fluid geometry ϕ_0 is updated by solving

$$\begin{aligned} \alpha_1 \partial_t \phi_0 + 6p'(\phi_0) &= \alpha_2 \nabla_{\mathbf{y}}^2 \phi_0 - \alpha_3 \phi_0 (1 - \phi_0) f_0(u_0) && \text{in } P, \\ \nabla_{\mathbf{y}} \phi_0 \cdot \mathbf{n}_P &= 0 && \text{on } \Gamma_P, \end{aligned}$$

and effective matrices \mathcal{A} and \mathcal{K} are found through

$$\begin{aligned} a_{ij}(t, \mathbf{x}) &= \frac{1}{|P|} \int_P \phi_0 (\delta_{ij} + \partial_{y_i} v^j) d\mathbf{y}, \text{ where} \\ \nabla_{\mathbf{y}} \cdot (\phi_0 \nabla_{\mathbf{y}} v^j + \phi_0 \mathbf{e}_j) &= 0 && \text{in } P, \\ \phi_0 (\nabla_{\mathbf{y}} v^j + \mathbf{e}_j) \cdot \mathbf{n}_P &= 0 && \text{on } \Gamma_P, \end{aligned}$$

and

$$\begin{aligned} k_{ij}(t, \mathbf{x}) &= \frac{1}{|P|} \int_P \phi_0 w_i^j d\mathbf{y}, \text{ where} \\ \phi_0 (\mathbf{e}_j + \nabla_{\mathbf{y}} \Pi^j) + \nabla_{\mathbf{y}}^2 (\phi_0 \mathbf{w}^j) - (1 - \phi_0) \mathbf{w}^j &= 0 && \text{in } P, \\ \nabla_{\mathbf{y}} \cdot (\phi_0 \mathbf{w}^j) &= 0 && \text{in } P, \\ \mathbf{w}^j &= 0 && \text{on } \Gamma_P, \end{aligned}$$

together with periodicity requirements in \mathbf{y} across ∂P . Note that u_0 and p do not depend on \mathbf{y} , while the macroscopic phase field $\overline{\phi_0}$ is defined as $\overline{\phi_0}(t, \mathbf{x}) = \frac{1}{|P|} \int_P \phi_0(t, \mathbf{x}, \mathbf{y}) d\mathbf{y}$.

Due to the periodicity, the cell problems are decoupled. Each cell problem must be solved for every macroscopic point \mathbf{x} , but due to the decoupling they can be solved in parallel. Hence, from an implementation point of view, the separation between \mathbf{x} and \mathbf{y} can speed up a numerical simulation. However, the micro scale \mathbf{y} still needs to resolve the evolution of the phase field. This usually requires a fine enough grid to resolve the interface width.

REFERENCES

- [1] C. Bringedal, I. Berre, I. S. Pop, and F. A. Radu. A model for non-isothermal flow and mineral precipitation and dissolution in a thin strip. *Journal of Computational and Applied Mathematics*, 289:346 – 355, 2015. Sixth International Conference on Advanced Computational Methods in Engineering (ACOMEN 2014).
- [2] C. Bringedal, I. Berre, I. S. Pop, and F. A. Radu. Upscaling of non-isothermal reactive porous media flow with changing porosity. *Transport in Porous Media*, 114(2):371–393, 2016.
- [3] G. Caginalp and P. Fife. Dynamics of layered interfaces arising from phase boundaries. *SIAM Journal on Applied Mathematics*, 48(3):506–518, 1988.
- [4] M. Redeker, C. Rohde, and I. S. Pop. Upscaling of a tri-phase phase-field model for precipitation in porous media. *IMA Journal of Applied Mathematics*, 81(5):898–939, 2016.
- [5] T. van Noorden. Crystal precipitation and dissolution in a porous medium: Effective equations and numerical experiments. *Multiscale Modeling & Simulation*, 7(3):1220–1236, 2009.
- [6] T. L. van Noorden and C. Eck. Phase field approximation of a kinetic moving-boundary problem modelling dissolution and precipitation. *Interfaces and Free Boundaries*, 13(1):29–55, 2011.

Model reduction for parameterized systems and inverse problems

MARIO OHLBERGER

(joint work with Stephan Rave, Felix Schindler, Tobias Wedemeier)

The numerical approximation of mathematical models for reactive flow in deformable complex structures naturally leads to large scale (non-)linear systems that have to be solved repeatedly for many time steps and parameter variations. Modern model order reduction methods are able to reduce the computational complexity of such problems drastically by taking advantage of the smoothness and approximation properties of the solution manifold of the underlying parameterized systems, where time is also considered as a parameter. Particular instances of projection based model order reduction methods are Reduced Basis Methods (RBM) or Balanced Truncation (BT). We refer e.g. to [1] for tutorials on these methods. As a particular application we consider mathematical modeling and simulation of degradation processes in batteries. In order to capture detailed dynamics of the underlying electrochemical processes, we consider simulation in spatially resolved porous electrodes. The charge rate is considered as a parameter and a full charging or discharging sweep is simulated. Model reduction of the resulting non-linear advection-diffusion-reaction system is obtained by the POD(-Greedy) RBM, where the nonlinearities are interpolated using our framework of empirical operator interpolation [2]. With these reduction techniques, the CPU time of a resolved Finite Volume approximation could be reduced from about 7.5 hours to 1.5 minutes [8]. As there is no robust and efficient rigorous a posteriori error estimate for this system, we have used the hierarchical error indicator from [7] for a detailed degradation model with lithium plating in [6].

While the online efficiency of these model reduction methods is very convincing, there are still major drawbacks and limitations. Most importantly, the construction of the reduced system in the offline phase is extremely CPU-time and memory

consuming. For practical applications, it is thus necessary to derive model reduction techniques that do not rely on a classical offline/online splitting but allow for more flexibility in the usage of computational resources. A promising approach with this respect is localized model reduction with adaptive enrichment [12, 3], which can also be combined with local randomized training as recently investigated in [4]. Efficient a posteriori error estimates for parabolic problems were derived in [10] and a first proof of concept for the application to a nonlinear Finite Volume battery model with resolved electrode geometry is given in [9].

As a next step, we investigate the benefits of localized model reduction with adaptive enrichment for the solution of large scale inverse problems or PDE constrained optimization [13, 11], i.e.

$$(1) \quad \left. \begin{aligned} &\text{Find } \mu^* = \arg \min J(u(\mu), \mu) \\ &\text{subject to } C_j(u(\mu), \mu) \leq 0 \quad \forall j = 1, \dots, m, \\ &\mu \in \mathcal{P} \end{aligned} \right\}$$

with a compact *parameter set* $\mathcal{P} \subset \mathbb{R}^P$ for $P \in \mathbb{N}$. In (1), the *state variable* $u(\mu)$ is given as the weak solution of the following parameterized problem

$$(2) \quad \left. \begin{aligned} -\nabla \cdot (A(\mu)\nabla u(\mu)) &= f(\mu) && (\text{in } \Omega) \\ u(\mu) &= 0 && (\text{on } \partial\Omega) \end{aligned} \right\}$$

In (2), $\Omega \subset \mathbb{R}^d$ for $d = 1, 2, 3$ is a bounded domain and A denotes a diffusion tensor.

To this end, we derive rigorous a posteriori error estimations for the state variable $u(\mu)$ and its first and second derivatives with respect to the parameters. As the derivatives are solutions of variational problems that are very similar to that of the state equation itself, we adopt the locally conservative flux reconstruction technique from [12] to obtain suitable error estimates for the derivatives. Under certain regularity assumptions on the objective functional J , we can then also control the first and second order derivatives of the objective functional with respect to the parameters, i.e. for a localized reduced basis approximation $u_N(\mu)$ of $u(\mu)$ we have computable upper bounds $\eta_J(\mu)$, $\eta_{\nabla J}(\mu)$ and $\eta_{\nabla^2 J}(\mu)$ such that

$$\begin{aligned} |J(u(\mu)) - J(u_N(\mu))| &\leq \eta_J(\mu), \\ \|\nabla_{\mu} J(u(\mu)) - \nabla_{\mu} J(u_N(\mu))\|_2 &\leq \eta_{\nabla J}(\mu), \\ \|\nabla_{\mu}^2 J(u(\mu)) - \nabla_{\mu}^2 J(u_N(\mu))\|_2 &\leq \eta_{\nabla^2 J}(\mu). \end{aligned}$$

Following the ideas in [5], we finally derive the following a posteriori error estimate for the approximation of the optimization problem.

Theorem 1. *Let μ^* denote the exact solution of (1) and μ_N^* the solution of the PDE constrained optimization, where the exact weak solution $u(\mu)$ of the state equation (2) is replaced by a localized reduced basis approximation $u_N(\mu)$. Let the*

condition $\|(\nabla_{\mu}^2 J(u_N(\mu_N^*)))^{-1}\| \eta_{\nabla^2 J}(\mu_N^*) < 1$ be satisfied and let us define

$$\begin{aligned}\zeta_N &:= \|\nabla J(u_N(\mu_N^*))\|_2 + \eta_{\nabla^2 J}(\mu_N^*), \\ \rho_N &:= \frac{\|\nabla^2 J(u_N(\mu_N^*))^{-1}\|_2}{1 - \|\nabla^2 J(u_N(\mu_N^*))^{-1}\|_2 \eta_{\nabla^2 J}(\mu_N^*)}, \\ L_N(r) &:= \sup_{\mu \in B_r(\mu_N^*)} \|\nabla^2 J(u_N(\mu_N^*)) - \nabla^2 J(u_N(\mu))\|_2 + \eta_{\nabla^2 J}(\mu) + \eta_{\nabla^2 J}(\mu_N^*).\end{aligned}$$

If the saturation condition $2\rho_N L_N(2\rho_N \zeta_N) \leq 1$ is satisfied, we have the following a posteriori error bound on the optimal parameter:

$$\|\mu^* - \mu_N^*\|_2 \leq 2\rho_N \zeta_N.$$

REFERENCES

- [1] P. Benner, A. Cohen, M. Ohlberger, K. Willcox. Model Reduction and Approximation: Theory and Algorithms. Computational Science & Engineering, 15. SIAM, Philadelphia, PA, 2017. xx+412 pp. doi: 10.1137/1.9781611974829.
- [2] M. Drohmann, B. Haasdonk, and M. Ohlberger. Reduced basis approximation for nonlinear parametrized evolution equations based on empirical operator interpolation. *SIAM J. Sci. Comput.*, 34:A937-A969, 2012.
- [3] A. Buhr, C. Engwer, M. Ohlberger, S. Rave. ArbiLoMod, a Simulation Technique Designed for Arbitrary Local Modifications. *SIAM J. Sci. Comput.* 39(4):A1435–A1465, 2017. doi: 10.1137/15M1054213.
- [4] A. Buhr, K. Smetana. Randomized Local Model Order Reduction. *SIAM J. Sci. Comput.* 40(4):A2120-A2151, 2018. doi: 10.1137/17M1138480.
- [5] M. Dihlmann, B. Haasdonk. Certified PDE-constrained parameter optimization using reduced basis surrogate models for evolution problems. *Comput. Optim. Appl.* 60(3):753787, 2015.
- [6] J. Feinauer, S. Hein, S. Rave, S. Schmidt, D. Westhoff, J. Zausch, O. Iliev, A. Latz, M. Ohlberger, V. Schmidt. MULTIBAT: Unified workflow for fast electrochemical 3D simulations of lithium-ion cells combining virtual stochastic microstructures, electrochemical degradation models and model order reduction. *Journal of Computational Science*, 2018 (in press). doi: 10.1016/j.jocs.2018.03.006.
- [7] S. Hain, M. Ohlberger, M. Radic, K. Urban. A Hierarchical A-Posteriori Error Estimator for the Reduced Basis Method. ArXiv e-prints arXiv:1802.03298 [math.NA], Preprint (Submitted) - 2018.
- [8] M. Ohlberger, S. Rave, F. Schindler. Model Reduction for Multiscale Lithium-Ion Battery Simulation. In Numerical Mathematics and Advanced Applications ENUMATH 2015, edited by Karasözen B, Manguoglu M, Teuer-Sezgin M, Göktepe S, Ugur Ö, 317–331, Springer, 2016. doi: 10.1007/978-3-319-39929-4_31.
- [9] M. Ohlberger, S. Rave. Localized Reduced Basis Approximation of a Nonlinear Finite Volume Battery Model with Resolved Electrode Geometry. In Model Reduction of Parametrized Systems, edited by Benner P., Ohlberger M., Patera A., Rozza G., Urban K., 201–212. Cham: Springer International Publishing, 2017. doi: 10.1007/978-3-319-58786-8_13.
- [10] M. Ohlberger, S. Rave, F. Schindler. True Error Control for the Localized Reduced Basis Method for Parabolic Problems. In Model Reduction of Parametrized Systems, edited by Benner P., Ohlberger M., Patera A., Rozza G., Urban K., 169–182. Cham: Springer International Publishing, 2017. doi: 10.1007/978-3-319-58786-8_11.
- [11] M. Ohlberger, M. Schaefer, F. Schindler. Localized Model Reduction in PDE Constrained Optimization. In Shape Optimization, Homogenization and Optimal Control DFG-AIMS

- workshop held at the AIMS Center Senegal, March 13-16, 2017, edited by Schulz V, Seck D., 143-163, Basel: Birkhäuser, 2018. doi: 10.1007/978-3-319-90469-6_8.
- [12] M. Ohlberger, F. Schindler. Error control for the localized reduced basis multi-scale method with adaptive on-line enrichment. *SIAM J. Sci. Comput.* 37(6):A2865–A2895, 2015. doi: 10.1137/151003660.
- [13] M. Ohlberger, F. Schindler. Non-Conforming Localized Model Reduction with Online Enrichment: Towards Optimal Complexity in PDE constrained Optimization. In *Finite Volumes for Complex Applications VIII - Hyperbolic, Elliptic and Parabolic Problems: FVCA 8*, Lille, France, June 2017, edited by Cances C, Omnes P, 357-365. Cham: Springer International Publishing, 2017. doi: 10.1007/978-3-319-57394-6_38.

A simple a posteriori estimate on general polytopal meshes with applications to complex porous media flows

MARTIN VOHRALÍK

(joint work with Soleiman Yousef)

The present contribution shows how to derive simple *a posteriori error estimates* applicable on general *polytopal meshes*. For the model steady linear single-phase Darcy porous media flow, they take the form

$$\|\mathbf{K}^{-1/2}(\mathbf{u} - \mathbf{u}_h)\|_{L^2(\Omega)} \leq \left\{ \sum_{K \in \mathcal{T}_H} \eta_K^2 \right\}^{1/2},$$

where \mathbf{K} is the diffusion tensor, \mathbf{u} is the unknown exact Darcy velocity, \mathbf{u}_h is its available numerical approximation, \mathcal{T}_H is a mesh of the computational domain Ω where each element K is a polygon (in two space dimensions), polyhedron (in three space dimensions), or a polytope in general, and η_K can be completely calculated from \mathbf{u}_h .

We develop a framework including *any lowest-order locally conservative method* like the mimetic finite difference [3], multi-point finite volume [1], hybrid and mixed finite volume [4], multipoint flux mixed finite element [10], mixed virtual element [2], or mixed finite element [7, 8] ones. Our focus is to derive estimates that can be *easily coded, cheaply evaluated, and efficiently used in practical simulations*. In particular, we want to avoid the physical construction and coding of any simplicial submesh as well as solution of local problems that are sometimes used in a posteriori error estimation. The evaluation of our estimates is fully explicit and merely consists in a matrix-vector multiplication of the form

$$(1) \quad \eta_K^2 := (\mathbf{U}_K^{\text{ext}})^t \widehat{\mathbf{A}}_{\text{MFE},K} \mathbf{U}_K^{\text{ext}} + \mathbf{S}_K^t \widehat{\mathbf{S}}_{\text{FE},K} \mathbf{S}_K + 2(\mathbf{U}_K^{\text{ext}})^t \mathbf{S}_K^{\text{ext}} - 2\mathbf{F}_K |K|^{-1} \mathbf{1}^t \widehat{\mathbf{M}}_{\text{FE},K} \mathbf{S}_K.$$

Here $\mathbf{U}_K^{\text{ext}}$ is an algebraic vector collecting the degrees of freedom corresponding to normal fluxes of \mathbf{u}_h over the faces of the mesh element K , $\mathbf{S}_K^{\text{ext}}$ and \mathbf{S}_K are respectively algebraic vectors collecting the degrees of freedom corresponding to pressure values in element faces/vertices, \mathbf{F}_K expresses the element sources, $|K|$ is

the measure of the element K , and $\widehat{\mathbf{A}}_{\text{MFE},K}$, $\widehat{\mathbf{S}}_{\text{FE},K}$, and $\widehat{\mathbf{M}}_{\text{FE},K}$ are three small matrices immediately constructed from the element geometry (respectively the mixed finite element mass matrix, the finite element stiffness matrix, and the finite element mass matrix). This probably gives the easiest and most practically accessible application to polytopal meshes of the general methodology of H^1 -conforming potential reconstruction and $\mathbf{H}(\text{div}, \Omega)$ -conforming flux reconstruction, see [6] and the references therein, as all the ingredients are readily available. A numerical illustration can be found in Figure 1.

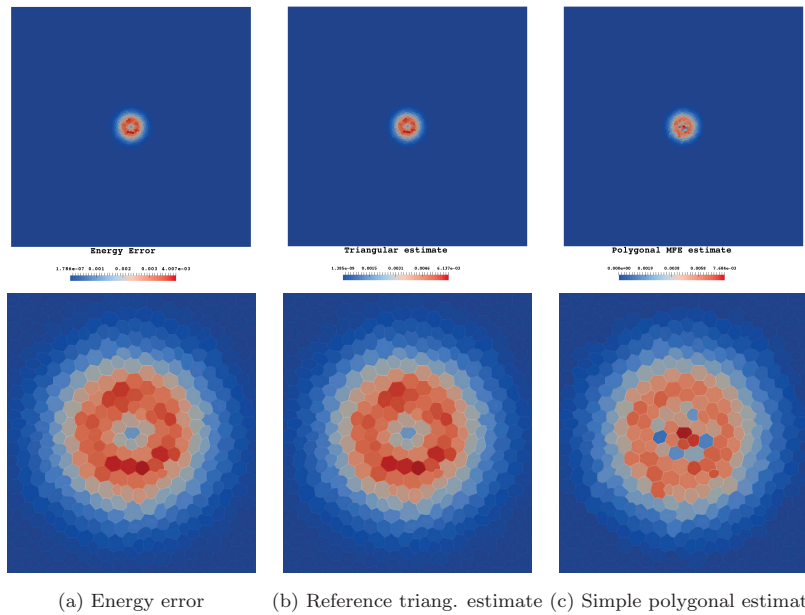


FIGURE 1. Actual and estimated error distributions, entire domain (top) and zoom (bottom), single-phase Darcy flow, 2D

We next show that, in extension of [5] and the references therein, structurally the same results can also be obtained for a model nonlinear steady diffusion problem, where the *guaranteed* a posteriori error estimate takes the form

$$c_{\mathbf{K}}^{1/2} \|\mathbf{u} - \mathbf{u}_h^{k,i}\|_{L^2(\Omega)} \leq \eta_{\text{sp}}^{k,i} + \eta_{\text{lin}}^{k,i} + \eta_{\text{alg}}^{k,i} + \eta_{\text{rem}}^{k,i}.$$

Here $c_{\mathbf{K}}$ is a monotonicity constant, $\mathbf{u}_h^{k,i}$ is a numerical approximation available on the current mesh \mathcal{T}_H , the current step $k \geq 1$ of an iterative linearization, and the current step $i \geq 1$ of an iterative algebraic solver, and $\eta_{\text{sp}}^{k,i}$, $\eta_{\text{lin}}^{k,i}$, and $\eta_{\text{alg}}^{k,i}$ respectively correspond to the three arising *error components* because of discretization, linearization, and algebraic solver; $\eta_{\text{rem}}^{k,i}$ is a small adaptively-controlled remainder term. Importantly, all the estimators still take the form of the *simple matrix-vector multiplication* (1), with the *same local matrices* as in the *linear case*.

Finally, we apply the entire methodology to the context of numerical approximations of unsteady nonlinear systems of partial differential equations describing multiphase compositional porous media Darcy flows. The estimates are still fully computable and feature no unknown generic constant. They are crucially valid at each stage of the overall solution algorithm: on *each time step* $n \geq 1$, each *linearization step* $k \geq 1$, and each *linear solver step* $i \geq 1$. They also allow to distinguish different error components and design *adaptive stopping criteria* for the involved iterative solvers, as well as *adaptive choice* of *space* and *time meshes*; an example of evolution of the total and algebraic estimates in function of algebraic solver iterations can be found in Figure 2, left, whereas the benefits of the adaptive algebraic solver stopping criterion can be appreciated in Figure 2, right.

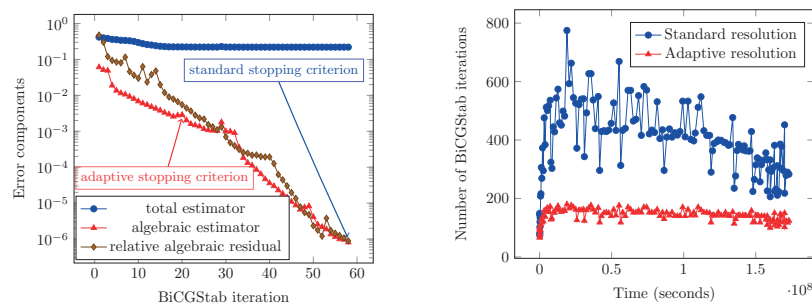


FIGURE 2. Standard resolution vs. resolution with adaptive stopping criterion of the algebraic solver: total estimator and its algebraic component (*left*) and number of BiCGStab iterations per time step (*right*), black-oil model, 3D

On the practical level, this contribution presents a posteriori error estimates that can be readily implemented into (reservoir engineering) production codes on general polytopal meshes with a minimal overhead, yet give fully computable, unknown-constant-free, and theoretically justified error bounds. All the details can be found in [9].

REFERENCES

- [1] I. Aavatsmark, T. Barkve, Ø Bøe, T. Mannseth, *Discretization on unstructured grids for inhomogeneous, anisotropic media. I. Derivation of the methods*, SIAM J. Sci. Comput. **19** (1998), 1700–1716.
- [2] L. Beirão da Veiga, F. Brezzi, L. D. Marini, A. Russo, *Mixed virtual element methods for general second order elliptic problems on polygonal meshes*, ESAIM Math. Model. Numer. Anal. **50** (2016), 727–747.
- [3] F. Brezzi, K. Lipnikov, M. Shashkov., *Convergence of the mimetic finite difference method for diffusion problems on polyhedral meshes*, SIAM J. Numer. Anal. **43** (2005), 1872–1896.
- [4] J. Droniou, R. Eymard, T. Gallouët, R. Herbin, *A unified approach to mimetic finite difference, hybrid finite volume and mixed finite volume methods*, Math. Models Methods Appl. Sci. **20** (2010), 265–295.

- [5] A. Ern, M. Vohralik, *Adaptive inexact Newton methods with a posteriori stopping criteria for nonlinear diffusion PDEs*, SIAM J. Sci. Comput. **35** (2013), A1761–A1791.
- [6] A. Ern, M. Vohralik, *Polynomial-degree-robust a posteriori estimates in a unified setting for conforming, nonconforming, discontinuous Galerkin, and mixed discretizations*, SIAM J. Numer. Anal. **53** (2015), 1058–1081.
- [7] Y. Kuznetsov, S. Repin, S., *New mixed finite element method on polygonal and polyhedral meshes*, Russian J. Numer. Anal. Math. Modelling **18** (2003), 261–278.
- [8] M. Vohralik, B. I. Wohlmuth, *Mixed finite element methods: implementation with one unknown per element, local flux expressions, positivity, polygonal meshes, and relations to other methods*, Math. Models Methods Appl. Sci. **23** (2013), 803–838.
- [9] M. Vohralik, S. Yousef, *A simple a posteriori estimate on general polytopal meshes with applications to complex porous media flows*, Comput. Methods Appl. Mech. Engrg. **331** (2018), 728–760.
- [10] M. F. Wheeler, I. Yotov, *A multipoint flux mixed finite element method*, SIAM J. Numer. Anal. **44** (2006), 2082–2106.

Effective interface transmission conditions for transport processes through thin heterogeneous membranes

MARKUS GAHN

(joint work with Maria Neuss-Radu and Peter Knabner)

Introduction: We deal with the mathematical modeling of nonlinear transport processes through a thin heterogeneous membrane. The aim is the rigorous derivation of homogenized models, where the thin layer is replaced by a lower dimensional interface, and the transport processes through the membrane are described by effective interface transmission conditions.

More precisely, in the microscopic model, we consider a system of nonlinear reaction–diffusion equations in a domain consisting of two bulk regions separated by a thin layer Ω_ϵ^M with a periodic heterogeneous structure. The thickness of the layer and the period within the layer are of order ϵ . Additionally, the equations within the layer depend on the scaling parameter ϵ . The aim is the derivation of a homogenized model for $\epsilon \rightarrow 0$, the solution of which approximates the solution of the microscopic model. For $\epsilon \rightarrow 0$ the thin layer reduces to an interface Σ separating the two bulk-regions. The limit equations in the bulk-regions carry the same structure as in the microscopic model. However, the crucial point is the derivation of the effective transmission conditions across the interface Σ . In fact, one has to deal with the coupling between the bulk-domains and the thin layer, the heterogeneous structure within the thin layer and the periodic coefficients in the microscopic equations, the singular limit, when the thin layer reduces to an interface, and the nonlinear reaction-kinetics. To overcome these difficulties, we used the method of two-scale convergence and the unfolding operator in thin domains.

The microscopic model: We consider a domain $\Omega = \Sigma \times (-H, H) \subset \mathbb{R}^n$, where Σ is a rectangle in \mathbb{R}^{n-1} , which consists of two bulk-domains Ω_ϵ^+ and Ω_ϵ^- separated by the thin layer $\Omega_\epsilon^M = \Sigma \times (-\epsilon, \epsilon)$ with a periodic heterogeneous structure. The

interface between Ω_ϵ^\pm and Ω_ϵ^M is denoted by S_ϵ^\pm , i. e., we have

$$\Omega = \Omega_\epsilon^+ \cup \Omega_\epsilon^M \cup \Omega_\epsilon^- \cup S_\epsilon^+ \cup S_\epsilon^-.$$

We consider the following problem: Find $u_\epsilon^\pm : (0, T) \times \Omega_\epsilon^\pm \rightarrow \mathbb{R}^m$ and $u_\epsilon^M : (0, T) \times \Omega_\epsilon^M \rightarrow \mathbb{R}^m$, such that

$$\begin{aligned} \partial_t u_{i,\epsilon}^\pm - D_i^\pm \Delta u_{i,\epsilon}^\pm &= f_i^\pm(t, x, u_\epsilon^\pm) && \text{in } (0, T) \times \Omega_\epsilon^\pm, \\ \frac{1}{\epsilon} \partial_t u_{i,\epsilon}^M - \epsilon^\gamma \nabla \cdot (D_i^M \left(\frac{x}{\epsilon}\right) \nabla u_{i,\epsilon}^M) &= \frac{1}{\epsilon} g_i \left(\frac{x}{\epsilon}, u_\epsilon^M\right) && \text{in } (0, T) \times \Omega_\epsilon^M, \end{aligned}$$

with $\gamma \in [-1, 1]$ and Neumann-zero boundary condition on the outer boundary $\partial\Omega$ together with suitable initial conditions. The parameter γ describes the strength of the diffusion within the thin layer and we distinguish three different cases: $\gamma = -1$, $\gamma \in (-1, 1)$, and $\gamma = 1$. A crucial point, is the transmission condition across the interfaces S_ϵ^\pm between the layer and the bulk-domains. We consider two different types of transmission conditions:

Continuity of the solutions and the normal fluxes:

$$\begin{aligned} u_\epsilon^\pm &= u_\epsilon^M && \text{on } (0, T) \times S_\epsilon^\pm, \\ -D_i^\pm \nabla u_{i,\epsilon}^\pm \cdot \nu &= -\epsilon^\gamma D_i^M \left(\frac{x}{\epsilon}\right) \nabla u_{i,\epsilon}^M \cdot \nu && \text{on } (0, T) \times S_\epsilon^\pm. \end{aligned}$$

Nonlinear Neumann-transmission conditions:

$$\begin{aligned} -D_i^\pm \nabla u_{i,\epsilon}^\pm \cdot \nu &= -h_i^\pm(u_\epsilon^\pm, u_\epsilon^M) && \text{on } (0, T) \times S_\epsilon^\pm, \\ -\epsilon^\gamma D_i^M \left(\frac{x}{\epsilon}\right) \nabla u_{i,\epsilon}^M \cdot \nu &= -h_i^{M,\pm} \left(\frac{x}{\epsilon}, u_\epsilon^\pm, u_\epsilon^M\right) && \text{on } (0, T) \times S_\epsilon^\pm. \end{aligned}$$

The nonlinear functions on the right-hand sides describe reaction and transport processes and are assumed to be uniformly Lipschitz continuous. We proved existence and uniqueness of a microscopic solution $u_\epsilon = (u_\epsilon^+, u_\epsilon^M, u_\epsilon^-)$.

The macroscopic model: Our aim is to pass to the limit $\epsilon \rightarrow 0$ when the thin layer reduces to an interface Σ between the bulk-domains Ω^+ and Ω^- . Then, the microscopic solutions $u_\epsilon = (u_\epsilon^+, u_\epsilon^M, u_\epsilon^-)$ converge in a suitable sense to a limit function $u_0 = (u_0^+, u_0^M, u_0^-)$ which is the solution of a macroscopic model. The limits in the bulk-domains u_0^+ and u_0^- are solutions of the equation

$$\partial_t u_{i,0}^\pm - D_i^\pm \Delta u_{i,0}^\pm = f_i^\pm(t, x, u_0^\pm) \quad \text{in } (0, T) \times \Omega^\pm.$$

The challenge is the derivation of the interface conditions across Σ . These conditions are coupled to cell or local problems on $Z = Y \times (-1, 1) = (0, 1)^{n-1} \times (-1, 1)$. The case $\gamma = 1$ (low diffusion) with continuous transmission conditions in was treated in [3]. In [1], we considered the case $\gamma \in [-1, 1)$ for continuous transmission conditions across S_ϵ^\pm , and in [2] the case $\gamma \in [-1, 1]$ for the nonlinear Neumann-transmission conditions. In the following, we state some of our results for the critical cases $\gamma = \pm 1$.

Theorem 1. For $\gamma = -1$ and continuous transmission conditions across S_ϵ^\pm , the limit function $u_0 = (u_0^+, u_0^M, u_0^-)$ with

$$u_0^M \in L^2((0, T), H^1(\Sigma))^m \cap H^1((0, T), L^2(\Sigma))^m$$

is the unique weak solution of

$$\begin{aligned} \partial_t u_{i,0}^\pm - D_i^\pm \Delta u_{i,0}^\pm &= f_i^\pm(t, x, u_0^\pm) && \text{in } (0, T) \times \Omega^\pm, \\ u_0^+ &= u_0^- = u_0^M && \text{on } (0, T) \times \Sigma, \\ |Z| \partial_t u_{i,0}^M - \nabla_{\bar{x}} \cdot (D_i^{M,*} \nabla_{\bar{x}} u_{i,0}^M) &= -[D_i \nabla u_{i,0} \cdot \nu]_\Sigma \\ &+ \int_Z g_i(y, u_0^M) dy && \text{on } (0, T) \times \Sigma, \end{aligned}$$

together with suitable initial conditions and Neumann-zero boundary conditions on $\partial\Omega$ and $\partial\Sigma$. The homogenized diffusion-coefficient $D_i^{M,*} \in \mathbb{R}^{(n-1) \times (n-1)}$ is given by

$$(D_i^{M,*})_{kl} = \int_Z D_i^M(y) (\nabla w_{i,k} + e_k) \cdot (\nabla w_{i,l} + e_l) dy,$$

and the $w_{i,k}$ are the solutions of the cell-problems

$$\begin{aligned} -\nabla \cdot (D_i^M (\nabla w_{i,j} + e_j)) &= 0 \text{ in } Z, \\ -D_i^M (\nabla w_{i,j} + e_j) \cdot \nu &= 0 \text{ on } S^+ \cup S^-, \\ w_{i,j} &\text{ is } Y\text{-periodic with } \int_Z w_{i,j} dy = 0, \end{aligned}$$

with $S^\pm = Y \times \{\pm 1\}$.

The concentrations are continuous at Σ . However, the jump of the normal fluxes across Σ is described by a reaction-diffusion equation i.e., a dynamic Wentzell-boundary condition. For $\gamma \in (-1, 1)$ the diffusion term in the equation on Σ vanishes.

Theorem 2. For $\gamma = 1$ and nonlinear Neumann-transmission conditions across S_ϵ^\pm , the limit function $u_0 = (u_0^+, u_0^M, u_0^-)$ with

$$u_0^M \in L^2((0, T), L^2(\Sigma, \mathcal{H}_{\text{per}}))^m \cap H^1((0, T), L^2(\Sigma, \mathcal{H}_{\text{per}})')^m,$$

where $\mathcal{H}_{\text{per}} = \{u \in H^1(Z) : u \text{ is } Y\text{-periodic}\}$, is the unique weak solution of

$$\begin{aligned} \partial_t u_{i,0}^\pm - D_i^\pm \Delta u_{i,0}^\pm &= f_i^\pm(u_0^\pm) && \text{in } (0, T) \times \Omega^\pm, \\ -D_i^\pm \nabla u_{i,0}^\pm \cdot \nu &= - \int_Y h_i^\pm(u_0^\pm, u_0^M(\cdot, t, \cdot, \bar{x}, \cdot, \bar{y}, \pm 1)) d\bar{y} && \text{on } (0, T) \times \Sigma, \\ \partial_t u_{i,0}^M - \nabla_y \cdot (D_i^M \nabla_y u_{i,0}^M) &= g_i(\cdot, y, u_0^M) && \text{in } (0, T) \times \Sigma \times Z, \\ -D_i^M \nabla_y u_{i,0}^M \cdot \nu &= -h_i^{M,\pm}(\cdot, \bar{y}, u_0^\pm(\cdot, t, \cdot, \bar{x}, 0), u_0^M(\cdot, t, \cdot, \bar{x}, \cdot, \bar{y}, \pm 1)) && \text{on } (0, T) \times \Sigma \times S^\pm, \\ u_0^M &\text{ is } Y\text{-periodic with respect to the last variable.} \end{aligned}$$

The system is completed by suitable initial conditions and Neumann-zero boundary conditions at the lateral boundary.

We see that the limit function u_0^M of the membrane concentration u_c^M is described by a local problem with respect to the microscopic variable $y \in Z$, depending on an additional parameter $\bar{x} \in \Sigma$. Hence, in every macroscopic point $\bar{x} \in \Sigma$, we have to solve a local problem on Z .

REFERENCES

- [1] M. Gahn, M. Neuss-Radu, and P. Knabner. Derivation of effective transmission conditions for domains separated by a membrane for different scaling of membrane diffusivity. *Discrete & Continuous Dynamical Systems-Series S*, 10(4):773–797, 2017.
- [2] M. Gahn, M. Neuss-Radu, and P. Knabner. Effective interface conditions for processes through thin heterogeneous layers with nonlinear transmission at the microscopic bulk-layer interface. *Accepted in Networks and Heterogeneous Media*.
- [3] M. Neuss-Radu and W. Jäger. Effective transmission conditions for reaction-diffusion processes in domains separated by an interface. *SIAM J. Math. Anal.*, 39:687–720, 2007.

Upscaling reactive transport in an evolving porous medium

NADJA RAY

(joint work with Jens Oberlander, Peter Frolovic)

We consider porous media applications that contain evolving solid phases. Deriving models that describe such structural changes at a variety of scales is essential to understanding the intimate link between structure and function. With reference to the soil's heterogeneity, we aim to develop a mathematical model at the pore scale, perform its upscaling to transfer our model from the pore scale to the macroscale and investigate the resulting model numerically.

At the pore scale, we consider a coupled system of partial differential equations. It consists of transport equations for the species' concentrations while taking the processes of convection and diffusion into account. In our model, structural changes in the porous medium's composition may occur due to heterogeneous reactions in- or decreasing the ratio of the solid phase. The interface between an attached layer of immobile chemical species and the fluid is characterized by means of a level-set.

We determine a macroscopic model description based on the pore-scale model applying two-scale asymptotic expansion in a level set framework as introduced in [1]. A micro-macro model emerges that is comprised of several levels of couplings: Macroscopic equations describing transport at the scale of the porous medium (macro scale) include averaged time- and space-dependent coefficient functions. These functions may explicitly be computed by means of auxiliary cell problems (micro scale). Finally, the pore space in which the cell problems are defined is time- and space dependent. For the fully continuum description, the pore space's geometry is determined by means of the level-set equation and information from the transport equation's solutions is used to determine the explicit geometric structure (micro-macro scale).

For evaluation purposes, we complement our theoretical results with numerical computations. For the level set equation an upwind scheme described by Rouy

and Tourin in [2] is applied. (Extended) Finite Element Methods [3] are used for the evaluation of the cell problems and the transport equation. Ultimately, we investigate the dissolution of an array of calcite grains in the micro-macro context.

REFERENCES

- [1] T. van Noorden, *Crystal precipitation and dissolution in a porous medium: effective equations and numerical experiments*, Multiscale Model. Simul. **7**, (2009).
- [2] E. Rouy, A. Tourin, *A viscosity solution approach to shape from shading*, SIAM J. Numer. Anal. **29(3)**, (1992).
- [3] T.-P. Fries, T. Belytschko, *The extended/generalized finite element method: An overview of the method and its applications*, International Journal for Numerical Methods in Engineering, Wiley-Blackwell, 2010.

Numerical models for fault reactivation based on Nitsche method and XFEM

LUCA FORMAGGIA

(joint work with Anna Scotti)

The exploitation of subsoil by human activities, like oil and gas exploitation, geothermal storage and CO₂ sequestration, may alter the stress field and cause nearby faults to activate and trigger (micro)seismicity. It is a matter of great concern and several techniques have been developed in the last years to simulate this phenomenon.

We are currently investigating numerical techniques based on the following assumptions and modeling choices:

- A poro-elasticity model where the effect of fault in the flow and pore pressure field is taken into account by a hybrid dimensional technique, following [12, 7];
- Quasi-static assumption: the time scale of mechanical response is sufficiently small compared to the evolution of the flow so that it is possible to consider the material in mechanical equilibrium at every time;
- Frictional contact only, since typically the fault is subject to a strongly compressing stress field. The frictional contact is modeled by Coulomb's law;
- Use of Nitsche's penalization approach to express the contact conditions. This allows to employ standard functional spaces. The presence of discontinuities in the effective stress field and fluid velocity at the internal interface that represents the fault is accounted for by employing eXtended Finite Elements (XFEM), as in [7, 4] (where however the coupled poro-elasticity problem is not considered);
- Operator splitting techniques based on the so-called fixed-stress splitting [13, 2] to be able to treat the mechanical problem separately from the fluid problem.

We assume that the domain $\Omega \subset \mathbb{R}^2$ is completely cut by a fault Γ , modeled as a planar interface that subdivides Ω into Ω^+ and Ω^- . Thus $\Gamma = \text{int}(\partial\Omega^+ \cap \partial\Omega^-)$. We can identify a normal \mathbf{n}_Γ to Γ and we use the notation $\llbracket f \rrbracket$ and $\{f\}$ for the jump and average of f across Γ , respectively. We set $\Omega_\Gamma = \Omega \setminus \bar{\Gamma}$.

In this short note it is not possible to give the full derivation of the model, we just give the description of the final differential problem. We indicate with \mathbf{q} and p the Darcy’s velocity and pressure in Ω_Γ , respectively, and by \mathbf{u} the displacement of the rock matrix. While, \mathbf{q}_Γ and p_Γ are Darcy’s flux and pressure in the fault Γ , respectively. The total Cauchy stress $\boldsymbol{\sigma} = \boldsymbol{\sigma}(\mathbf{u}, p)$ takes into account of the combined action of the solid and fluid that compose the rock. According to Biot’s theory it is expressed as

$$(1) \quad \boldsymbol{\sigma} = \boldsymbol{\sigma}'(\mathbf{u}) - bp\mathbf{I},$$

where \mathbf{I} is the identity tensor and $\boldsymbol{\sigma}'$ the effective stress that accounts for the action of the solid part, and b the Biot’s coefficient. We assume small deformations and elastic behaviour, so we define the strain tensor as $\boldsymbol{\varepsilon}(\mathbf{u}) = \frac{1}{2}(\nabla\mathbf{u} + \nabla^T\mathbf{u})$ and we have

$$\boldsymbol{\sigma}'(\mathbf{u}) = \lambda \text{tr}(\boldsymbol{\varepsilon}(\mathbf{u})) + 2\mu\boldsymbol{\varepsilon}(\mathbf{u}),$$

λ and μ being the Lamè parameters, which we assume to be both strictly positive and bounded in Ω_Γ . We assume that the fluid viscosity is constant throughout the domain, and in the following \mathbf{K} indicates the permeability scaled with viscosity, which, in general, is a symmetric positive definite tensor with bounded components in Ω_Γ . As detailed in [9], we assume that the permeability in the fracture can be decomposed into a normal, \hat{K}_n and a tangential component \hat{K}_τ , to take into account that fault resistance to flow may be different in the normal and tangential direction. The reduced model for the fracture makes use of effective permeabilities, which scale with fracture aperture. In particular, we define

$$K_\Gamma = l_\Gamma \hat{K}_\tau, \quad \eta = \frac{l_\Gamma}{\hat{K}_n}.$$

We assume that $0 < \underline{K}_\Gamma \leq K_\Gamma(\mathbf{x}) \leq \overline{K}_\Gamma$ and $0 < \underline{\eta} \leq \eta(\mathbf{x}) \leq \overline{\eta}$, for almost all $\mathbf{x} \in \Gamma$.

With this definitions, the differential model in the bulk and in the fracture reads:

$$(2) \quad \begin{cases} \frac{\partial}{\partial t} \left(\frac{1}{M} p + b \text{div } \mathbf{u} \right) + \text{div } \mathbf{q} = \mathbf{f} \\ \mathbf{K}^{-1} \mathbf{q} + \nabla p = \rho_f \mathbf{g} \\ - \text{div } \boldsymbol{\sigma}(\mathbf{u}, p) = -\rho \mathbf{g} \end{cases} \quad \text{in } \Omega_\Gamma \quad t > 0,$$

$$(3) \quad \begin{cases} l_\Gamma \frac{\partial}{\partial t} \left(\frac{1}{M} p_\Gamma \right) + \text{div}_\tau \mathbf{q}_\Gamma - \llbracket \mathbf{q} \cdot \mathbf{n}_\Gamma \rrbracket = f_\Gamma \\ K_\Gamma^{-1} \mathbf{q}_\Gamma + \nabla_\tau p_\Gamma = \rho_f \mathbf{g} \end{cases} \quad \text{in } \Gamma \quad t > 0.$$

Here, M is the rock compressibility, \mathbf{f} and \mathbf{f}_Γ source terms representing possible injection/extraction of fluids, \mathbf{g} the gravity acceleration, ρ_f is the (constant) fluid

density, while ρ is the density of the rock, which is related to that of the fluid, ρ_f , and that of the solid matrix, ρ_s , by $\rho = \phi\rho_f + (1 - \phi)\rho_s$, ϕ being the fluid porosity (which for simplicity we assume constant). Finally, $\operatorname{div}_{\boldsymbol{\tau}}$ and $\nabla_{\boldsymbol{\tau}}$ are the divergence and gradient operator on the fracture plane.

The problem is completed by appropriate boundary and initial conditions, which we not detail here for the sake of space, and *coupling* conditions on Γ , which can be written for the fluid problem as

$$(4) \quad \begin{cases} \eta\{\mathbf{q} \cdot \mathbf{n}_{\Gamma}\} = \llbracket p \cdot \mathbf{n}_{\Gamma} \rrbracket, \\ \eta_0 \llbracket \mathbf{q} \cdot \mathbf{n}_{\Gamma} \rrbracket = \{p \cdot \mathbf{n}_{\Gamma}\} - p_{\Gamma}, \end{cases}$$

where $\eta_0 = \xi_0\eta$ and $\xi_0 > 0$ is a closure parameter of the model, usually taken equal to 1/12, while for the mechanical model we have a Coulomb friction condition since we assume that the fault may only act as a potentially sliding surface: at each time $t > 0$ and on Γ ,

$$(5) \quad \begin{cases} \llbracket u_{n_{\Gamma}} \rrbracket = 0, \\ \llbracket \boldsymbol{\sigma}_{n_{\Gamma}} \rrbracket = \mathbf{0}, \\ \llbracket \boldsymbol{\tau} \rrbracket = \mathbf{0}, \\ \mathcal{G} \leq 0, \\ \exists \beta \leq 0 \text{ s.t. } \llbracket \dot{\mathbf{u}}_{t_{\Gamma}} \rrbracket = \beta\{\boldsymbol{\tau}\} \\ \beta\mathcal{G} = 0. \end{cases}$$

We have used the following notation for the tangential and normal components of the Cauchy stress and displacement on Γ :

$$\sigma_{n_{\Gamma}} = (\boldsymbol{\sigma} \cdot \mathbf{n}_{\Gamma}) \cdot \mathbf{n}_{\Gamma}, \quad \sigma'_{n_{\Gamma}} = (\boldsymbol{\sigma}' \cdot \mathbf{n}_{\Gamma}) \cdot \mathbf{n}_{\Gamma},$$

$$\boldsymbol{\sigma}_{n_{\Gamma}} = \boldsymbol{\sigma}_{n_{\Gamma}} \cdot \mathbf{n}_{\Gamma}, \quad \boldsymbol{\sigma}'_{n_{\Gamma}} = \boldsymbol{\sigma}'_{n_{\Gamma}} \cdot \mathbf{n}_{\Gamma}, \quad \boldsymbol{\tau} = \boldsymbol{\sigma} \cdot \mathbf{n}_{\Gamma} - \boldsymbol{\sigma}_{n_{\Gamma}}, \quad \boldsymbol{\tau}' = \boldsymbol{\sigma}' \cdot \mathbf{n}_{\Gamma} - \boldsymbol{\sigma}'_{n_{\Gamma}},$$

and $\mathbf{u}_{n_{\Gamma}} = u_{n_{\Gamma}} \cdot \mathbf{n}_{\Gamma} = (\mathbf{u} \cdot \mathbf{n}_{\Gamma}) \mathbf{n}_{\Gamma}$, $\mathbf{u}_{t_{\Gamma}} = \mathbf{u} - \mathbf{u}_{n_{\Gamma}}$. The quantity \mathcal{G} is defined as

$$\mathcal{G} = |\{\boldsymbol{\tau}\}| + \mu_f \bar{\sigma}'_{n_{\Gamma}},$$

where μ_f is the friction coefficient and $\bar{\sigma}'_{n_{\Gamma}}$ is a reference value of the compressive part of the normal component of the effective stress on the fault, which may be taken as $\bar{\sigma}'_{n_{\Gamma}} = \min(0, \{\sigma'_{n_{\Gamma}}\})$. Thus, the friction condition states that slip may occur only if the modulus of the tangential stress reaches the critical value $-\mu_f \bar{\sigma}'_{n_{\Gamma}}$.

The problem is tackled by resorting to a particular operator-splitting technique, called fixed-stress splitting, which provides an unconditionally stable time advancing procedure, and whose details may be found in the cited literature. An advantage of this type of splitting for the problem at hand, is that it decouples the fluid equations from the mechanical one. In particular, for the latter we have that within each time step $t^n \leq t \leq t^{n+1}$, we need to solve an iterative procedure of the type

$$(6) \quad -\operatorname{div} \boldsymbol{\sigma}'(\mathbf{u}^{(k+1)}) = \rho \mathbf{g} - b \nabla p^{(k)} \quad \text{in } \Omega_{\Gamma},$$

where $p^{(k)}$ comes from the solution of a modified problem for the fluid, coupled with suitably rewritten friction conditions on Γ , namely

$$\begin{cases} \llbracket u_{n_\Gamma}^{(k+1)} \rrbracket = 0, \\ \llbracket \boldsymbol{\sigma}_{n_\Gamma}^{(k+1)} \rrbracket = \mathbf{0}, \\ \llbracket \boldsymbol{\tau}^{(k+1)} \rrbracket = \mathbf{0}, \\ \mathcal{G}^{(k+1)} \leq 0, \\ \exists \beta^{(k+1)} \leq 0 \text{ s.t. } \llbracket \mathbf{u}_{t_\Gamma}^{(k+1)} - \mathbf{u}_{t_\Gamma}^n \rrbracket = \beta^{(k+1)} \{ \boldsymbol{\tau}^{(k+1)} \}, \\ \mathcal{G}^{(k+1)} \beta^{(k+1)} = 0. \end{cases}$$

We can then focus for the solution of a “standard” Coulomb friction problem. Several techniques may be adopted, for instance treating the related variational inequality by Lagrange multipliers, as in [10, 11, 8]. In our work we want to exploit the flexibility of a Nitsche treatment of the interface conditions, a technique already exploited for similar problems in [6, 3, 1, 5]. The main original idea in our research is to reinterpret the problem as a control problem.

Indeed, given a slip displacement $\boldsymbol{\beta} = \llbracket \mathbf{u}_{t_\Gamma} - \mathbf{u}_{t_\Gamma}^n \rrbracket \in \mathcal{B} \subset \mathbf{H}_{00}^{1/2}(\Gamma)$, (we are omitting the suffix $(k + 1)$) the use of Nitsche approach allows us to write the finite element discretization of (6) in the form: find $\mathbf{u} = \mathbf{u}(\boldsymbol{\beta}) \in \mathbf{V}_h \subset \mathbf{H}^1(\Omega_\gamma)$ s.t.

$$(7) \quad a(\mathbf{u}, \mathbf{v}) = F(\mathbf{v}) + h(\boldsymbol{\beta}, \mathbf{v}), \quad \forall \mathbf{v} \in \mathbf{V}_h,$$

where $a(\cdot, \cdot)$ is a symmetric and coercive bilinear form on \mathbf{V}_h , F is a linear functional that incorporates the effect of forcing terms and boundary conditions, while

$$h(\boldsymbol{\beta}, \mathbf{v}) = \int_\Gamma \alpha_t \boldsymbol{\beta} \cdot \llbracket \mathbf{v}_{t_\Gamma} \rrbracket - \int_\Gamma \{ \boldsymbol{\tau}(\mathbf{v}) \} \cdot \boldsymbol{\beta},$$

enforces the given slip, $\alpha_t > 0$ being the Nitsche penalization parameter. In operator form, we may write

$$A\mathbf{u}(\boldsymbol{\beta}) = F + H\boldsymbol{\beta}.$$

which identifies $\boldsymbol{\beta}$ as the control parameter. The observed quantity is $\{ \boldsymbol{\tau}(\mathbf{u}) \}$, which will be written as $C\mathbf{u}$. The key is then to find a suitable functional $J(\boldsymbol{\gamma}) = J(C\mathbf{u}(\boldsymbol{\gamma}), \boldsymbol{\gamma})$ whose minimum coincides with an approximation of the Coulomb friction conditions.

In this setting the problem may be set as: Find $\boldsymbol{\beta}$ such that

$$\boldsymbol{\beta} = \operatorname{argmin}_{\boldsymbol{\gamma} \in \mathcal{B}} J(C\mathbf{u}(\boldsymbol{\gamma}), \boldsymbol{\gamma}),$$

under the constraint

$$A\mathbf{u}(\boldsymbol{\gamma}) = F + H\boldsymbol{\gamma}.$$

At the time being we are trying different functionals J and different strategies for the solution of the control problem. The preliminary results are rather encouraging.

The advantage of the technique is that it can readily be implemented in a non-conforming discretization setting, like eXtended Finite Elements, and it does not require to add new degrees of freedom for the Lagrange multipliers. It gives

also freedom in the choice of the functional, which may be extended to take into account other possible constraints.

REFERENCES

- [1] Chandrasekhar Annavarapu, Martin Hautefeuille, and John E. Dolbow, *A Nitsche stabilized finite element method for frictional sliding on embedded interfaces. Part I: Single interface*, Computer Methods in Applied Mechanics and Engineering **268** (2014), 417–436.
- [2] Jakub Wiktor Both, Manuel Borregales, Jan Martin Nordbotten, Kundan Kumar, and Florin Adrian Radu, *Robust fixed stress splitting for Biot 's equations in heterogeneous media*, Applied Mathematics Letters **68** (2017), 101–108.
- [3] Franz Chouly and Patrick Hild, *A Nitsche-Based Method for Unilateral Contact Problems: Numerical Analysis*, SIAM Journal on Numerical Analysis **51** (2013), 1295–1307.
- [4] Franz Chouly, Patrick Hild, Vanessa Lleras, and Yves Renard, *Nitsche-based finite element method for contact with Coulomb friction*, HAL archive ouvertes **hal-016544** (2017).
- [5] Franz Chouly, Patrick Hild, and Yves Renard, *A Nitsche finite element method for dynamic contact: 1. Space semi-discretization and time-marching schemes*, ESAIM. Mathematical Modelling and Numerical Analysis **49** (2015), no. 2, 481–502.
- [6] E. T. Coon, B. E. Shaw, and M. Spiegelman, *A Nitsche-extended finite element method for earthquake rupture on complex fault systems*, Computer Methods in Applied Mechanics and Engineering **200** (2011), 2859–2870.
- [7] Carlo D'Angelo and Anna Scotti, *A mixed finite element method for Darcy flow in fractured porous media with non-matching grids*, ESAIM: Mathematical Modelling and Numerical Analysis **46** (2012), 465–489.
- [8] Andrea Franceschini, Massimiliano Ferronato, Carlo Janna, and Pietro Teatini, *A novel Lagrangian approach for the stable numerical simulation of fault and fracture mechanics*, Journal of Computational Physics **314** (2016), 503–521.
- [9] Alessio Fumagalli and Anna Scotti, *A numerical method for two-phase flow in fractured porous media with non-matching grids*, Advances in Water Resources **62** (2013), Part C, 454–464, Computational Methods in Geologic CO2 Sequestration.
- [10] S. Hübner and B. Wohlmuth, *Equilibration techniques for solving contact problems with Coulomb friction*, Computer Methods in Applied Mechanics and Engineering **205-208** (2012), 29–45.
- [11] Birendra Jha and Ruben Juanes, *Coupled multiphase flow and poromechanics: a computational model of pore pressure effects on fault slip and earthquake triggering*, Water Resources Research **50** (2014), no. 5, 3776–3808.
- [12] Vincent Martin, Jérôme Jaffré, and Jean E Roberts, *Modeling fractures and barriers as interfaces for flow in porous media*, SIAM Journal on Scientific Computing **26** (2005), 1667–1691.
- [13] Joshua A. White, Nicola Castelletto, and Hamdi A. Tchelepi, *Block-partitioned solvers for coupled poromechanics: A unified framework*, Computer Methods in Applied Mechanics and Engineering **303** (2016), 55–74.

Participants

Dr. Elyes Ahmed

Department of Mathematics
University of Bergen
Allegaten 41
5008 Bergen
NORWAY

Prof. Dr. Todd Arbogast

Department of Mathematics
The University of Texas at Austin
1 University Station C1200
Austin, TX 78712-1082
UNITED STATES

Manuela Bastidas Olivares

Department WNI
Hasselt University
Gebouw D
Agoralaan
3590 Diepenbeek
BELGIUM

Dr. Ilenia Battiato

Department of Energy Resources
Engineering
Stanford University
367 Panama Street
Stanford, CA 94305-2220
UNITED STATES

Prof. Dr. Markus Bause

Fakultät für Maschinenbau
Helmut-Schmidt-Universität
Universität der Bundeswehr Hamburg
Holstenhofweg 85
22043 Hamburg
GERMANY

Runar Berge

Department of Mathematics
University of Bergen
Allegaten 41
5008 Bergen
NORWAY

Prof. Dr. Inga Berre

Matematisk Institutt
Universitetet i Bergen
P.O. Box 7800
5020 Bergen
NORWAY

Dr. Wietse Boon

Fachbereich Mathematik
Universität Stuttgart
Pfaffenwaldring 57
70569 Stuttgart
GERMANY

Jakub Both

Department of Mathematics
University of Bergen
Allegaten 41
5008 Bergen
NORWAY

Dr. Carina Bringedal

Department WNI, Faculty of Sciences
Hasselt University
Campus Diepenbeek, Building D
Agoralaan
3590 Diepenbeek
BELGIUM

Dr. Nicola Castelletto

Atmospheric, Earth and Energy Division
Lawrence Livermore National
Laboratory
7000 East Avenue
Livermore, CA 94550
UNITED STATES

Prof. Dr. Björn Engquist

Department of Mathematics
The University of Texas at Austin
1 University Station C1200
Austin, TX 78712-0257
UNITED STATES

Prof. Dr. Robert Eymard

Faculté de Mathématiques
Université Paris-Est Marne-la-Vallée
Champs-sur-Marne
5, Boulevard Descartes
77454 Marne-la-Vallée Cedex 2
FRANCE

Dr. Ehsan Fattahi Evati

AG BioPat und Digitalisierung
Lehrstuhl für Brau- und
Getränketechnologie
Gregor-Mendel-Strasse 4
85354 Freising -Weihenstephan
GERMANY

Prof. Dr. Luca Formaggia

Dipartimento di Matematica
Politecnico di Milano
Piazza Leonardo da Vinci, 32
20133 Milano
ITALY

Dr. Markus Gahn

Interdisziplinäres Zentrum für
wissenschaftliches Rechnen (IWR)
Universität Heidelberg
Im Neuenheimer Feld 205
69120 Heidelberg
GERMANY

Prof. Dr. Francisco J. Gaspar

Departamento de Matemáticas
Universidad de Zaragoza
Facultad de Ciencias
Campus Plza. San Francisco
50009 Zaragoza
SPAIN

Ingeborg Gjerde

Department of Mathematics
University of Bergen
Postboks 7803
5020 Bergen
NORWAY

Dr. Shubhangi Gupta

Helmholtz Centre for Ocean Research
Kiel
Division of Marine Geosystems Germany
Wischhofstraße 1-3
24148 Kiel
GERMANY

Prof. Dr. Rainer Helmig

Institut für Wasser- und
Umweltsystemmodellierung
Universität Stuttgart
Pfaffenwaldring 61
70569 Stuttgart
GERMANY

**Prof. Dr. Dr. h.c. mult. Willi
Jäger**

Interdisziplinäres Zentrum für
Wissenschaftliches Rechnen (IWR)
c/o Gabriela Schocke
Im Neuenheimer Feld 368
69120 Heidelberg
GERMANY

Prof. Dr. Peter Knabner

Department Mathematik
Universität Erlangen
Cauerstrasse 11
91058 Erlangen
GERMANY

Dr. Johannes Kraus

Fakultät für Mathematik
Universität Duisburg-Essen
45117 Essen
GERMANY

Prof. Dr. Kundan Kumar

Department of Mathematics
University of Bergen
P.O. Box 7800
5020 Bergen
NORWAY

Prof. Dr. Dmitri Kuzmin

Institut für Angewandte Mathematik
Universität Dortmund, LS III
Vogelpothsweg 87
44227 Dortmund
GERMANY

Prof. Dr. Stephan Luckhaus

Mathematisches Institut
Universität Leipzig
Postfach 10 09 20
04109 Leipzig
GERMANY

Dr. Steven Mattis

Zentrum für Mathematik
Technische Universität München
Boltzmannstrasse 3
85748 Garching bei München
GERMANY

Prof. Dr. Andro Mikelic

Département de Mathématiques
Université Claude Bernard Lyon I
43, Bd. du 11 Novembre 1918
69622 Villeurbanne Cedex
FRANCE

Koondanibha Mitra

Department of Mathematics
Eindhoven University of Technology
P.O.Box 513
5600 MB Eindhoven
NETHERLANDS

Prof. Dr. Adrian Muntean

Department of Mathematics
Karlstad University
65188 Karlstad
SWEDEN

PD Dr. Maria Neuss-Radu

Department Mathematik
Universität Erlangen-Nürnberg
Cauerstrasse 11
91058 Erlangen
GERMANY

Prof. Dr. Jan Martin Nordbotten

Department of Mathematics
University of Bergen
Johs. Brunsgate 12
5008 Bergen
NORWAY

Prof. Dr. J. Tinsley Oden

ICES
The University of Texas at Austin
1 University Station (CO200)
201 E. 24th Street
Austin, TX 78712-1229
UNITED STATES

Prof. Dr. Mario Ohlberger

Institut für Analysis und Numerik
Universität Münster
Einsteinstrasse 62
48149 Münster
GERMANY

Dr. Géraldine Pichot

INRIA Paris
Equipe SERENA
CS 42112
2, Rue Simone Iff
75589 Paris Cedex 12
FRANCE

Prof. Dr. Iuliu Sorin Pop

Faculty of Sciences
Hasselt University
Building D
Agoralaan
3590 Diepenbeek
BELGIUM

Prof. Dr. Mario Putti

Department of Mathematics
University of Padova
via Trieste 63
35121 Padova
ITALY

Prof. Dr. Florin Adrian Radu

Department of Mathematics
University of Bergen
Postboks 7803
5020 Bergen
NORWAY

Dr. Nadja Ray

Department Mathematik
Universität Erlangen
Cauerstrasse 11
91058 Erlangen
GERMANY

Dr. Carmen Rodrigo Cardiel

Departamento de Matematicas
Universidad de Zaragoza
Edificio de Matemáticas, planta 1
Pedro Cerbuna, 12
50009 Zaragoza
SPAIN

Prof. Dr. Christian Rohde

Institut für Angewandte Analysis und
Numerische Simulation
Universität Stuttgart
Pfaffenwaldring 57
70569 Stuttgart
GERMANY

Prof. Dr. Ulrich Rüde

Lehrstuhl für Informatik 10
(Systemsimulation)
Universität Erlangen-Nürnberg
Cauerstraße 11
91058 Erlangen
GERMANY

Prof. Dr. Ben Schweizer

Fakultät für Mathematik
Technische Universität Dortmund
Vogelthoßweg 87
44227 Dortmund
GERMANY

Sohely Sharmin

Faculty of Sciences
Hasselt University
Building D
Agoralaan
3590 Diepenbeek
BELGIUM

Prof. Dr. Angela Stevens

Institut für Analysis und Numerik
Universität Münster
Einsteinstrasse 62
48149 Münster
GERMANY

Prof. Dr. Martin Vohralik

INRIA Paris, Equipe SERENA
2, Rue Simone Iff
75589 Paris Cedex 12
FRANCE

Prof. Dr. Mary Fanett Wheeler

ICES
The University of Texas at Austin
1 University Station (CO200)
201 East 24th Street
Austin, TX 78712-1229
UNITED STATES

Prof. Dr. Thomas Wick
Institut für Angewandte Mathematik
Leibniz Universität Hannover
Welfengarten 1
30167 Hannover
GERMANY

Prof. Dr. Barbara Wohlmuth
Zentrum für Mathematik
Technische Universität München
Boltzmannstrasse 3
85748 Garching bei München
GERMANY

Prof. Dr. Ivan Yotov
Department of Mathematics
University of Pittsburgh
301 Thackeray Hall
Pittsburgh, PA 15260
UNITED STATES

Prof. Dr. Ludmil Zikatanov
Department of Mathematics
Pennsylvania State University
University Park, PA 16802
UNITED STATES

Prof. Dr. Paolo Zunino
Dipartimento di Matematica
Politecnico di Milano
Via Bonardi 9
20133 Milano
ITALY

